Pipe-Soil Interaction Test Database Study

API TECHNICAL REPORT 2TRPSI
FIRST EDITION, APRIL 2025

Table of Contents

Tables

Figures

Special Notes

API publications necessarily address problems of a general nature. With respect to particular circumstances, local, state, and federal laws and regulations should be reviewed. Neither API nor any of API's employees, subcontractors, consultants, committees, or other assignees make any warranty or representation, either express or implied, with respect to the accuracy, completeness, or usefulness of the information contained herein, or assume any liability or responsibility for any use, or the results of such use, of any information or process disclosed in this publication. Neither API nor any of API's employees, subcontractors, consultants, or other assignees represent that use of this publication would not infringe upon privately owned rights.

API publications may be used by anyone desiring to do so. Every effort has been made by the Institute to assure the accuracy and reliability of the data contained in them; however, the Institute makes no representation, warranty, or guarantee in connection with this publication and hereby expressly disclaims any liability or responsibility for loss or damage resulting from its use or for the violation of any authorities having jurisdiction with which this publication may conflict. API publications are published to facilitate the broad availability of proven, sound engineering and operating practices. These publications are not intended to obviate the need for applying sound engineering judgment regarding when and where these publications should be utilized. The formulation and publication of API publications is not intended in any way to inhibit anyone from using any other practices.

Foreword

Nothing contained in any API publication is to be construed as granting any right, by implication or otherwise, for the manufacture, sale, or use of any method, apparatus, or product covered by letters patent. Neither should anything contained in the publication be construed as insuring anyone against liability for infringement of letters patent.

Suggested revisions are invited and should be submitted to the Standards Department, API, 200 Massachusetts Avenue NW, Suite 1100, Washington, DC 20001, standards@api.org.

Executive Summary

The American Petroleum Institute (API) Sub-committee 2 (SC2) Research Group 7 (RG7) identified a knowledge gap in the current API Recommended Practice 2GEO (RP 2GEO) related to axial pipe-soil interaction (PSI) testing, interpretation, and analysis. From this, API SR3 was initiated by contracting the Norwegian Geotechnical Institute (NGI) to address these knowledge deficiencies through a project titled "Design Guidelines for Axial Pipe-Soil Interaction Analysis". This report presents the work completed as part of these efforts, culminating in an updated interface shear test database, recalibrations of relevant model parameters, as well as guidance for best practice applications of testing and interpretation.

The scope of work comprised four tasks: (1) collecting and cataloging project-specific low normal stress shear test data from various laboratories to establish an updated database of fine-grained interface shear test data and supplementary soil parameters, (2) review of the updated test database to establish a framework for dataset definition, (3) recalibration and refinement of existing models using the updated datasets, and (4) development of best practice guidance.

As part of the database interpretation and analysis, four datasets (A, B, C, and D) were identified and characterized including development of statistically derived descriptive parameters and judgement-based selection of model parameters to account for effects of (i) normal stress, (ii) overconsolidation, (iii) interface surface roughness, and (iv) drainage during shear. Each dataset was sequentially filtered for specific categories of soil types and surface materials from the database to narrow the statistical range of derived model parameters. This generally achieved coefficient of variation values as low as 0.15 but began to reach a point of diminishing returns due to the small sample sizes in the most restrictive dataset. While it is the most restrictive and filtered dataset, it is recommended that Dataset D is used for all high plasticity, fine-grained, non-carbonate soils, which are typical of deepwater Gulf of Mexico sites. For all datasets, parameters were developed for smooth, intermediate, and rough surfaces sheared under undrained and drained conditions. Limitations of the database and interpretation of design values are described.

Best practice guidance is presented for test planning, execution, and interpretation, largely based on previous guidance provided in the public domain including technical publications developed as part of the SAFEBUCK Joint Industry Project. New insights are included based on more recent testing performed over the past several years. Collectively, these comprise:

- **Sampling and supplementary testing**: Box coring is recommended to obtain surficial soils for interface shear testing. Batch samples are recommended to be created using sub-samples from individual box cores. Separate batch samples on surficial layers may be warranted, particularly if the expected pipe embedment range extends into both layers. Batch samples are remolded to a (salt) water content value at or slightly higher than the liquid limit, accounting for effects of salt water on measured liquid limits. Supplementary laboratory testing performed on the batch samples is recommended to include water content, unit weight, particle size distribution, specific gravity, and Atterberg limits tests.

- **Test program design:** Normal stress values are recommended to cover the full range of empty through flooded pipeline submerged bearing pressures including wedging effects where appropriate. A minimum of three normal stress values is needed to capture the curvature of the stress effect. For projects where changes in pipe weight during pre-commissioning are significant, it may be useful to perform tests at overconsolidation ratios (OCR) > 1 on the same sample material and the same interface to derive the OCR *m* parameter to apply the SHANSEP approach for undrained strength derivation. A minimum of three OCR values is recommended, using the best estimate (BE) normal stress during shear for all three tests.

- **Interface surfaces selection and characterization:** Testing is ideally performed on representative pipeline coatings provided by the coating supplier. In the absence of actual coatings, plastic surfaces provide a practical substitute, selected to match the planned coating roughness. Sandpaper may be used as a proxy for a roughened surface, but for roughness significantly greater than 10 μm, soil-soil shear (i.e. direct shear) tests generally show less scatter compared to rough interface testing. Bare steel coatings create potential physicochemical interactions between the soil and the steel. Extremely smooth surfaces may induce bonding variations for high plasticity soils. It may be necessary to resurface interface plates throughout the testing program to avoid variations in roughness from test to test. Surface roughness measurements are recommended to be taken parallel to the direction of shearing before and after each test, or at a sufficient frequency to ensure consistency across the test program.

- **Test procedure:** Monitoring sample settlement during the consolidation phase, which may be performed in multiple increments of stress, allows estimation of the coefficient of consolidation of the soil. To measure the residual undrained shear resistance, fast shearing rates (no less than 0.1 mm/s) are recommended. Monotonic testing and cyclic testing with short displacement limits may overestimate the residual value due to lack of sufficient strain accumulation. It is recommended to maximize shearing displacement as much as practical within the constraints of the equipment and consideration of potential soil loss during shear. For cyclic testing, episodic consolidation periods between cycles or pairs of cycles allows for calibration of drainage models that capture the effects of pipeline startup and shutdown events. However, episodic consolidation may prohibit measurement of the minimum undrained residual strength. Gapping between the shear box/ring may promote soil loss and development of additional machine friction. Machine friction correction tests are recommended using an empty shear ring for each interface tested, which is then subtracted from the measured soil-interface resistance. To measure the drained shear resistance, tilt table testing is recommended, performing multiple shearing episodes to ensure the residual shear strength is attained. In the absence of tilt table testing, ISB testing can be performed at slow shearing rates (no greater than 0.001 mm/s). Repeat tests performed for a given set of project conditions allow assessment of how consistent (or inconsistent) the results are.

- **Test interpretation and design parameter derivation:** The residual resistance is selected from portions of the tests where a stable value is observed, averaging across enough data points to eliminate noise. For cyclic tests, the absolute values of shear resistance in each direction are averaged to remove any asymmetry in the data. Machine friction corrections in both forward and backward directions may be appropriate depending on the nature of the surface tested. Epistemic uncertainty and aleatoric variability influence quantification of low estimate (LE) and high estimate (HE) shear resistance from shear test programs. In the absence of explicit assessments of epistemic uncertainties, the coefficient of variation for a given dataset in this study may be used to derive LE and HE shear resistance values using the local mean value of a given parameter from site-specific testing on a batch sample.

Suggested future studies to reduce interface shear resistance uncertainty could include (i) comparisons of cyclic testing with and without episodic consolidation periods to determine the number of cycles required to attain minimum undrained shear strength, (ii) modifications/development of low normal stress ring shear devices to achieve true undrained residual shear resistance and avoid cyclic effects of machine friction and berm development, and (iii) investigations using a single soil sample and surface type to refine model calibrations.

1 Introduction

1.1 General

NGI in Houston (hereafter, NGI) has been contracted to the American Petroleum Institute (API) to perform a review of low normal stress interface shear tests performed over the past two decades as part of an effort to update industry guidance on pipe-soil interaction (PSI) testing, interpretation, and analysis. The work builds on efforts by laboratories to develop standardized approaches to PSI testing in relation to quantifying parameters used in calculations of axial resistance of seabed pipelines. This report presents the updated database and recalibrations of relevant model parameters, as well as guidance for best practice applications of testing and interpretation.

1.2 Motivation

The interface frictional response of subsea pipelines subject to cycles of expansion and contraction has gained considerable interest over the past two decades as developments are increasingly utilizing subsea tie-back pipelines to existing infrastructure. Energy developers are now routinely testing shallow seabed soils in a variety of custom-built modified direct interface shear box (ISB) devices and tilt table devices designed to apply low normal stresses to fine-grained or coarse-grained soils sheared against a structural surface representing the pipeline coating. The range of interface shear strength measured for a given soil type and interface surface combination is influenced by several factors, for which there is no standardized investigation approach. As a result, ranges in interface shear strength derived from site-specific testing can vary by a factor of 3 (or more) and may be only marginally narrower or even wider than published trends from large databases of both fine-grained soils (Westgate et al. 2018) and coarse-grained soils (Westgate et al. 2021).

The scatter in data is due to sensitivity in measured shear resistance to specimen preparation, testing procedure and equipment, variability of surface seabed soils, and surface roughness effects. These factors affect selection of design interface shear strength values. As a result, shear test program outcomes often present operators and their pipeline contractors with wide ranges of axial PSI inputs to pipeline design, leading to expensive solutions to mitigate pipeline expansion and associated lateral buckling. The lack of guidance means that the application of axial PSI in design will continue to vary based on operator experience. This may increase future risk of unplanned axial pipeline behavior including rogue buckle formation, excessive buckle feed-in, end expansion and through-life walking, resulting in potential buckle pullout and compromising the reliability of a project's controlled lateral buckling strategy. Current approaches to mitigate these issues utilizing strategies such as rock dumping, concrete mattresses, and hold-back anchoring are expensive, but can be used to avoid the significant environmental and financial consequences of excessive axial pipeline movements and their impact on structural pipeline system integrity.

1.3 Objectives

This research focuses on addressing gaps in current practice and improving the recommended practice for PSI under axial loading. The outcome is a set of design and assessment guidelines related to safe operation of new and existing pipelines as well as input to inspection, maintenance, and evaluation for life-extension/continued-service to support. Recent updates to ISO 19901-4 (ISO 2025) include discussion on testing and analysis methods for derivation of axial friction parameters for subsea pipelines in fine-grained soil, inspired by work performed within the SAFEBUCK Joint Industry Project (Atkins 2015). Much of the SAFEBUCK output is now included in the DNV Recommended Practice F114 (DNV, 2021); however, it is referred to as an 'alternative method'. An axial PSI testing database used to calibrate SAFEBUCK PSI models has been published (Westgate et al. 2018). The objective is to update current guidance to include guidance on axial PSI testing and analysis, including the statistical database presented in Westgate et al. (2018) and recently re-examined in Westgate (2022). Reducing uncertainty in the axial PSI inputs through improved code-based guidance can accelerate

deployment of resilient hydrocarbon development. The proposed project aims to utilize the wealth of project-specific data collected primarily by the Norwegian Geotechnical Institute (NGI) over the past several years to expand and refine the established database of Westgate et al. (2018) related to predictive models for low stress interface shear resistance.

1.4 Scope of work

The scope of work is divided into four tasks:

- Collect and catalogue project-specific interface shear test data from various laboratories to establish an updated database of fine-grained interface shear test data and supplementary soil parameters;
- Review of the updated test database to establish a framework for dataset definition and refinement;
- Recalibrate and refine existing design models to the updated datasets, and
- Develop guidance for best practice.

2 Axial pipe-soil interaction model

Axial PSI models used in subsea pipeline design generally follow the approach outlined in DNV (2021). The model utilizes a piecewise tri-linear or bi-linear model, depending on whether it is required and fully justified to include an initial breakout peak (Figure 1). The peak value (τ_{peak}) may not occur simultaneously for long sections of pipeline, and therefore adopted axial model parameters most often consist of a limiting (or 'residual') axial resistance (τ_{res}) and its associated mobilization displacement (x_{res}).

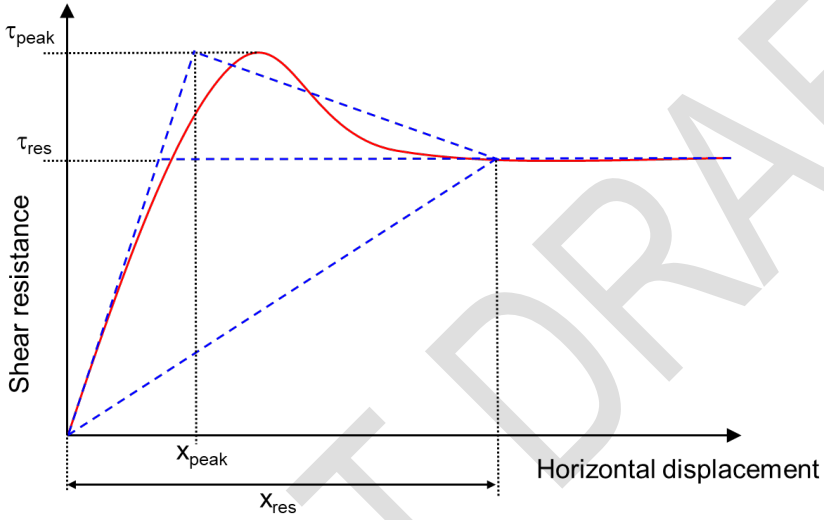

Figure 1 – Shear resistance model for axial pipe-soil interaction

The model utilizes the theoretical SHANSEP stress history framework (Ladd and Foott, 1974) to calculate undrained axial resistance associated with changes in pipe weight during the pre-commissioning phase, and a stress-dependent Mohr-Coulomb frictional response to calculate the drained axial resistance. Both models incorporate the effects of enhanced normal stress around the embedded perimeter of the pipeline via a wedging factor z (White and Randolph, 2007).

2.1 Undrained strength

The residual undrained shear resistance is calculated as:

$$\left(\frac{\tau_{res,u}}{\sigma'_{n0}}\right) = \left(\frac{\tau_{res,u}}{\sigma'_{n0}}\right)_{nc} OCR^m \qquad \text{Eq. (1a)}$$

where:

$\tau_{res,u}$ is residual undrained shear strength; calculated as:

$$\left(\frac{\tau_{res,u}}{p_a}\right)_{nc} = a_u \left(\frac{\sigma'_{n0}}{p_a}\right)^{b_u} \qquad \text{Eq. (1b)}$$

where:

$\left(\frac{\tau_{res,u}}{p_a}\right)_{nc}$ is the normally-consolidated, normalized undrained shear resistance;

σ'_{n0} is the initial effective normal stress;

p_a is atmospheric pressure (1 atm, or 101.3 kPa);

a_u and b_u are dimensionless power law fitting coefficients;

OCR is overconsolidation ratio, here taken as the ratio of the consolidation stress relative to the initial effective normal stress during shearing; and

m is equivalent to the SHANSEP index or the plastic volumetric strain ratio.

Alternatively, Equations 1a and 1b can be combined into a single Equation 1c as follows:

$$\left(\frac{\tau_{res,u}}{\sigma'_{n0}}\right) = a_u \left(\frac{\sigma'_{n0}}{p_a}\right)^{b_u-1} OCR^m \quad \text{Eq. (1c)}$$

2.2 Drained strength

The residual drained shear resistance is calculated as:

$$\left(\frac{\tau_{res,d}}{p_a}\right) = a_d \left(\frac{\sigma'_{n0}}{p_a}\right)^{b_d} \quad \text{Eq. (2a)}$$

or

$$\left(\frac{\tau_{res,d}}{\sigma'_{n0}}\right) = a_d \left(\frac{\sigma'_{n0}}{p_a}\right)^{b_d-1} \quad \text{Eq. (2b)}$$

where:

$\tau_{res,d}$ is residual drained shear strength;

σ'_{n0} is the initial effective normal stress;

p_a is atmospheric pressure (1 atm, or 101.3 kPa); and

a_d and b_d are dimensionless power law fitting coefficients.

2.3 Undrained to drained strength transition

The undrained to drained strength transition accounts for the consolidation of soil below the pipeline and its effect on increases in soil strength. Boukpeti and White (2017) describe approaches to calculating strength transitions, both during continuous shearing (i.e. while the pipeline is moving) and episodic shearing (i.e. while the pipeline remains stationary between startup and shutdown events). Interface shear testing can be designed to capture both aspects, e.g. by continuously shearing over large cumulative displacement either during cyclic movements in an interface shear box or monotonic rotation in a ring shear device. Brief pause periods can be incorporated into the test program between fast (notionally undrained) shearing to capture the episodic component of consolidation, which effectively speeds up the undrained to drained transition within the testing procedure.

3 Methodology

3.1 Data collection

The earliest axial PSI tests using modified direct shear box devices primarily comprised tests performed by the University of Western Australia (UWA) over two decades ago when pipeline expansion and walking became a key design concern among oil and gas field operators (e.g. Carr et al. 2006; Bruton et al. 2010). The energy company *bp* led much of these early studies, focusing on investigating normal stress, shearing rate, surface roughness, and overconsolidation effects on axial resistance. This led to development of a general framework for characterization of axial shear resistance (Figure 2). Data from some of these early tests were used to establish axial PSI guidance within the SAFEBUCK JIP (Atkins 2015), with selected test results provided in White et al. (2012), Hill et al. (2012), and Boukpeti and White (2017).

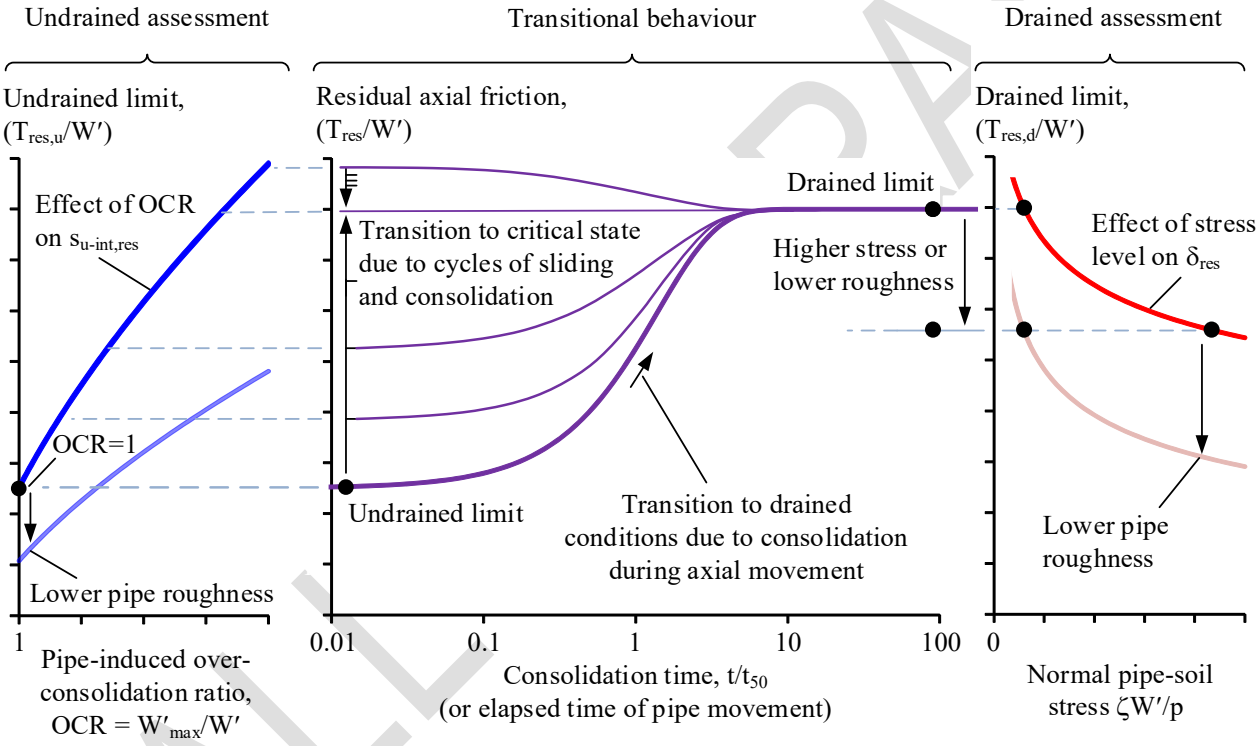

Figure 2 – Conceptual model for axial residual pipe-soil resistance (White 2014, Atkins 2015, DNV 2021)

During this period, separate developments were being investigated using a tilt table device, which gradually increases the inclination of a soil specimen below a lightly-loaded interface plate to determine its limiting drained shear strength at the angle of rotation when movement of the plate commences. This work was also led by *bp* and primarily conducted at the University of Texas at Austin, documented in the publications of Pedersen et al. (2003) and Najjar et al. (2003, 2007). Other developments in low normal stress interface shear testing as part of the SAFEBUCK JIP were led by Cambridge University, who describe the Cam-Tor device as detailed in Bolton et al. (2007), Ganesan et al. (2013), and Kuo et al. (2015). Various model testing approaches also exist to measure axial PSI behavior (see e.g. White et al. 2015).

These pioneering university-based studies led to developments by commercial testing facilities who developed approaches for axial PSI testing and analysis as described by White et al. (2015), Bransby et al. (2015), and

White et al. (2017). Westgate et al. (2018) published a large dataset of low normal stress interface shear testing on fine-grained soils, covering over 400 element tests from various operators and developing statistical values of relevant axial PSI model parameters for use in design, as well as guidance on test planning, execution, and interpretation. The database was revisited in Westgate (2022) which included surface roughness model fits to the fine-grained data (Westgate et al. 2018) as well as coarse-grained data originally presented in Westgate et al. (2021).

This report represents an update of the Westgate et al. (2018) database, which incorporates new data from tests performed by NGI as well as additional test data through donations by participating operators. All tests reported in the database are from project-specific datasets from offshore hydrocarbon field developments around the world. While some public domain research has also been conducted on low normal stress interface shear testing, these studies utilized either onshore soils or commercially-available soil such as kaolin (e.g. Pederson et al. 2003; Najjar et al. 2003, 2007), or used devices such as the ring shear apparatus which are known to produce lower values of residual shear resistance (e.g. Eid et al. 2015). No public domain data was included in the database update.

3.2 Database screening and dataset definition

The database described in the previous section spans over two decades of low normal stress interface shear testing across multiple testing facilities and devices, as well as an evolution in testing procedure and equipment functionality. A qualitative overview of the database metadata, soil, surface and testing descriptions is presented in Table 3-1, and is shown graphically in Figure 3 and Figure 4.

Table 3-1 – Qualitative database overview

Parameter	Range of values
Geographic regions:	North and South America; West, North, and East Africa; Northern and Eastern Europe; Southern Asia
Field operators:	12 energy companies
Years tested:	2002 through 2023
Testing facilities:	5 commercial labs and 2 university labs
Soil types and USCS classification:	High and low plasticity clays and silts (CH, CL, MH, ML)
Interface surface materials:	Aluminum, concrete, plastic (acetal, polypropylene, polyethylene, fusion-bonded epoxy), rubber, sandpaper, steel (bare and painted)
Testing devices:	Modified direct shear boxes, custom interface shear devices, tilt tables
Testing types:	Monotonic Cyclic (with and without intervening pause periods) using a range of fast and slow shearing cycles: Type A cyclic tests: N_{fast} = 18, N_{slow} = 2 Type B cyclic tests: N_{fast} = 2, N_{slow} = 2 Cyclic other: N = 1 to 25
Shearing displacement limits:	12 to 22 mm (monotonic) 5 to 12 mm (cyclic, per quarter cycle)

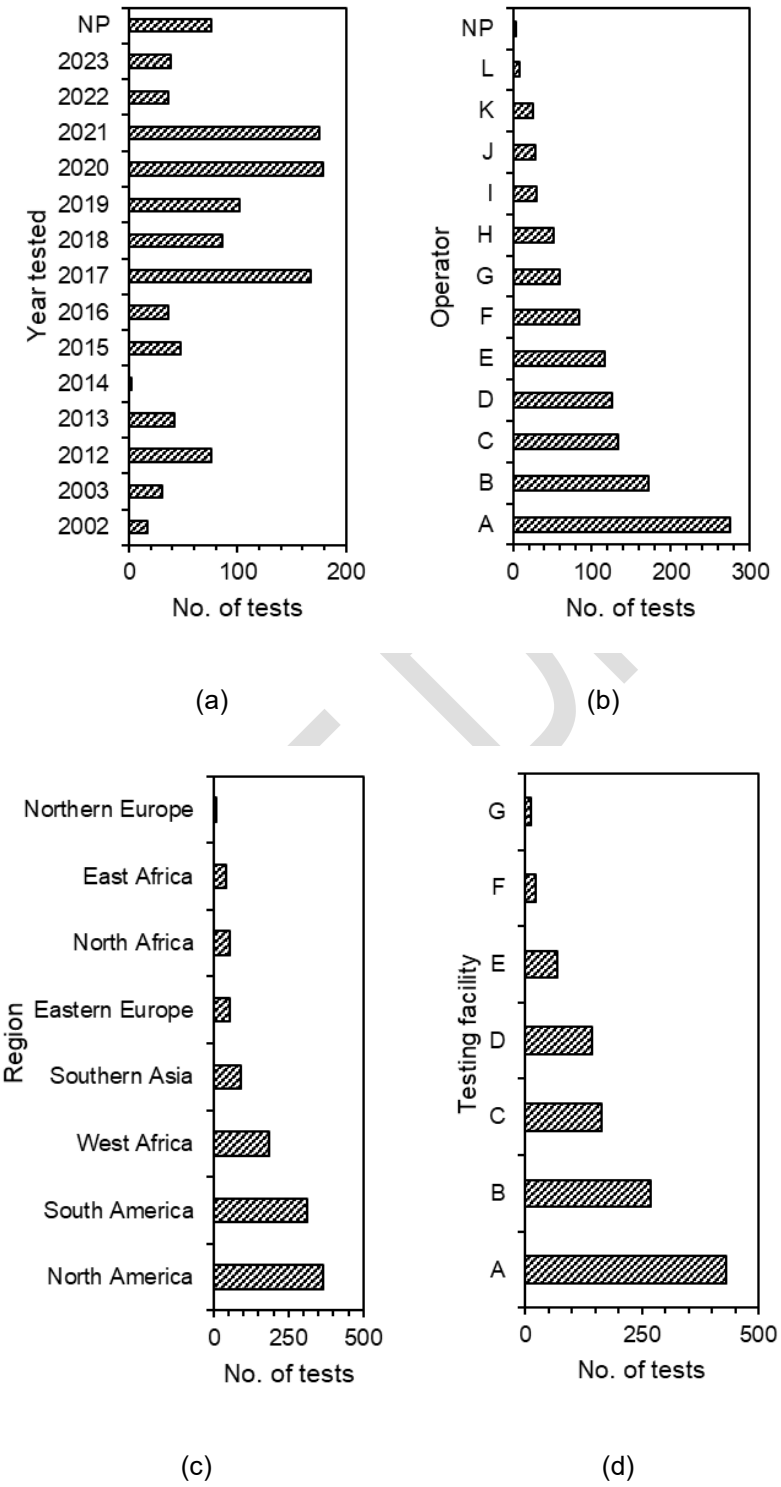

Figure 3 – Database metadata: (a) year tested, (b) field operator, (c) hydrocarbon region, and (d) testing laboratory (includes individual labs within the same company); NP = not provided

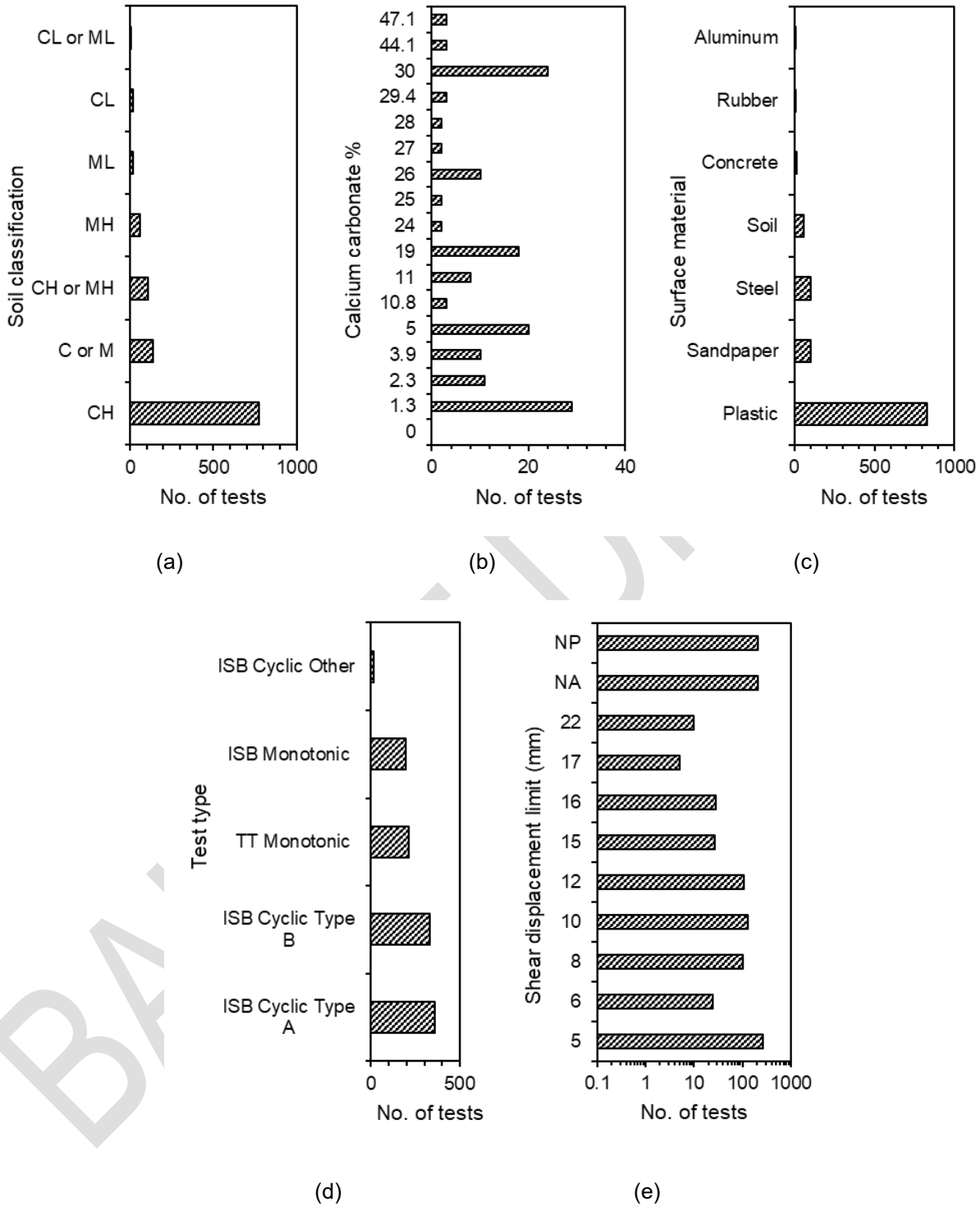

Figure 4 – Database soil, interface, and testing descriptions: (a) soil classification, (b) carbonate content, (c) surface material, (d) test type, and (e) shearing displacement limit; NP = not provided, NA = not applicable

Most of the devices utilized in the database were modified versions of commercial shear testing equipment; however, some devices were custom designed to address some of the limitations of the commercial equipment identified during testing. Examples of the devices used are shown in Figure 5. Most of these utilized dead weight systems of normal load application to improve control of target stress conditions, as well as modifications to test equipment and procedures. Several devices were modified from project to project; in general, the more recent test data provides more reliable values of axial resistance, with greater resolution of measured loads and displacements and lower corrections applied for machine friction. However, the year a test was performed was not used as a screening basis for dataset definition.

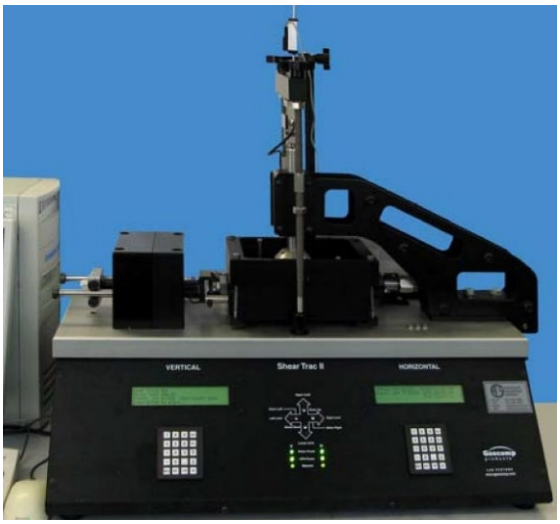

(a)

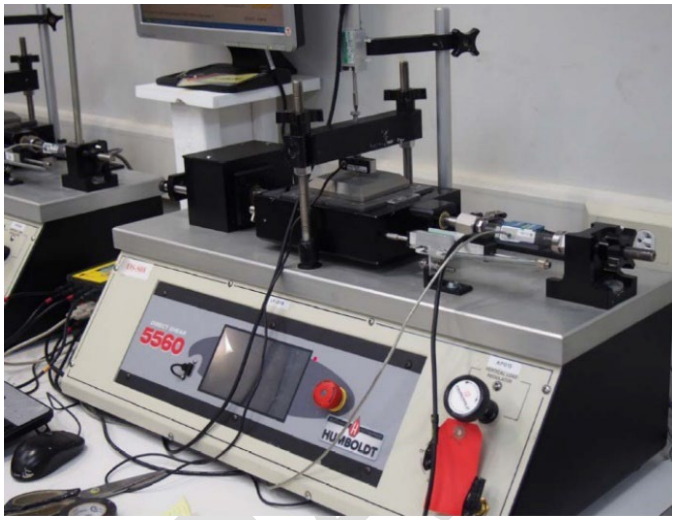

(b)

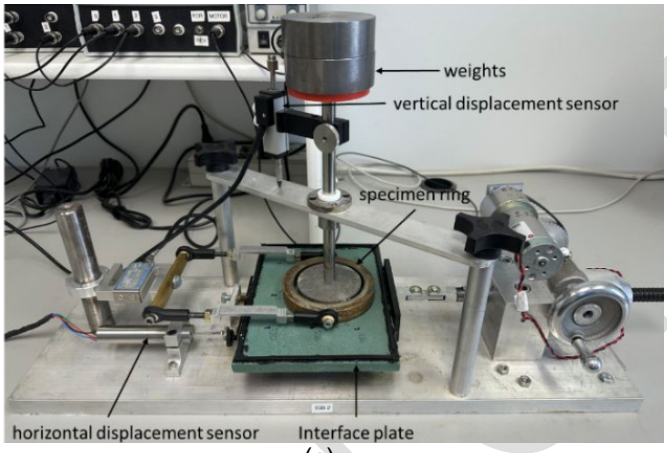

(c)

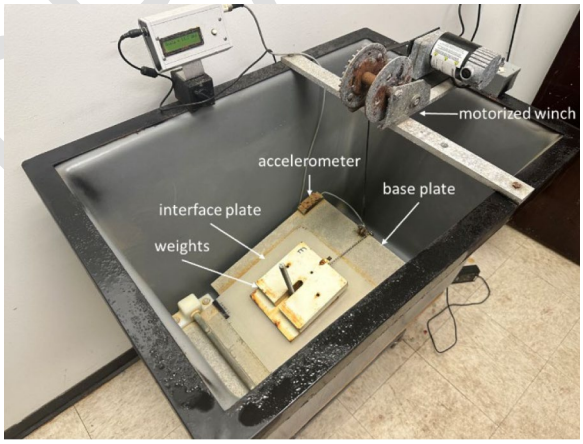

(d)

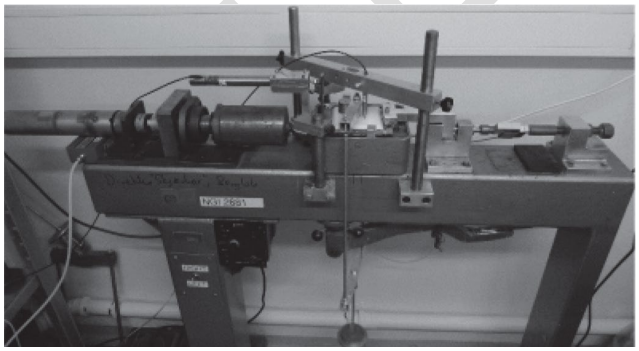

(e)

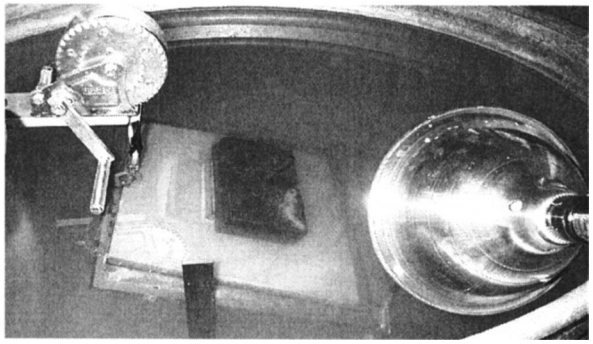

(f)

Figure 5 – Examples of devices utilized for testing: (a) Shear-Trac II (Westgate et al. 2018), (b) Humboldt (Westgate et al. 2018), (c) NGI custom-design interface shear (Das et al. 2023), (d) NGI tilt table (Das et al. 2023), (e) ELE International (Meyer et al. 2015), and (f) UT Austin tilt table (Najjar et al. 2007)

Specific parameters were used to define datasets to be characterized, detailed as follows:

- **Soil composition**: Fine-grained soils were identified using the Unified Soil Classification System (USCS), which defines fine-grained soils as those with more than 50% dry weight passing the No. 200 (75 mm) sieve. Atterberg limits were then used to classify the clay or silt as high or low plasticity. While undrained shear strength measurements were generally not reported, most of the reported values classify as 'soft' (i.e., undrained shear strength less than 20 kPa). Further, the vast majority (~99%) of tests used remolded specimens prepared at an initial water content close to or slightly greater than the liquid limit, and therefore typically had a mobilized undrained shear strength less than a few kPa at the start of testing.

- **Soil mineralogy**: The fine-grained database included non-carbonate soils ($CaCO_3$ < 10%) and calcareous soils ($CaCO_3$ between 10 and 50%), based on the framework of Clark and Walker (1977). Due to known effects of carbonate content on soil behavior (e.g. Watson et al. 2017), siliceous carbonate soils ($CaCO_3$ between 50 and 90%) and carbonate soils have not been considered. Note that much of the latter testing was performed on coarse-grained soil and therefore did not significantly detract from the overall size of the fine-grained database.

- **Normal stress**: Most of the database comprises tests performed at normal stresses less than 10 kPa, which represents most representative bearing pressures below subsea pipelines, after accounting for embedment and wedging effects. The fine-grained test data included higher stress values up to 18 kPa, which were retained in the database to provide a wider range of stresses for calibration of normal stress model parameters (i.e. the *a* and *b* parameters in Equations 1b, 1c, 2a, and 2b), calibrated for both drained conditions and undrained conditions following Westgate et al. (2018). While current guidelines (Atkins 2015; DNV 2021) do not recognize an undrained effective normal stress model, the data trends support an approach to applying the same stress-effect model across the drainage spectrum.

- **Overconsolidation**: Several tests were performed after preloading the specimen during the consolidation stage to induce a target overconsolidation ratio within the specimen to capture the effect of pipeline pre-commissioning events and associated changes in pipe weight on axial shear resistance. These were used to calibrate the OCR *m* parameter in Equations 1a and 1c.

- **Shearing rate**: Within the database, tests were generally performed at fast rates of 0.1 mm/s (notionally undrained conditions for fine-grained soils) or slow rates of 0.001 mm/s (notionally drained conditions in most soils), based on the approach of Gibson and Henkel (1954). Subsets of the database have been used to calibrate undrained and drained model parameters. Tilt table tests are considered to capture fully drained conditions. Due to the limited number of project datasets that investigated rate effects, no attempt has been made to recalibrate drainage transition models using the database.

- **Interface material and roughness**: Tests were performed across a wide range of interface material type (various plastics, rubber, steel, sandpaper, and concrete) and surface roughness (quantified using the average roughness R_a as defined by Ward (1999), and consistent with other PSI testing studies, e.g. Meyer et al. 2015). Subsets of the database have been used to calibrate smooth (notionally R_a < 1 μm) and rough (notionally R_a ≥ 10 μm) model parameters. Several tests were conducted on intermediate roughness values for various surface materials, predominantly bare steel and some plastics. Several direct shear tests were also conducted to assess soil-soil shearing to benchmark the fully rough interface condition. These are represented in the database using a roughness R_a = 99 μm for plotting purposes.

The quantitative range of database soil characteristics are listed in Table 3-2 below, with the database test conditions and associated model input provided in Table 3-3 below, which is also shown graphically in Figure 6.

Table 3-2 – Quantitative database soil characteristics

Parameter	Range of values
Fines content	> 50% passing 75 μm sieve
Mineralogy	Non-carbonate ($CaCO_3$ < 10%); Calcareous (10% < $CaCO_3$ < 50%)
Liquid limit, *LL*	29 to 212%
Liquidity index, *LI*	0.52 to 3.13
Plasticity index, *PI*	9 to 152%
Clay activity, *A*	0.56 to 1.75

Table 3-3 – Test input conditions

Parameter	Range of values	Model input
Initial normal effective stress, σ'_{n0}	1 to 18 kPa	Normal stress
Shearing rate, *v*	0.0001 to 0.67 mm/s	Drainage
Interface surface average roughness, R_a	0.1 to > 80 μm	Roughness
Overconsolidation ratio	1.0 to 11	OCR

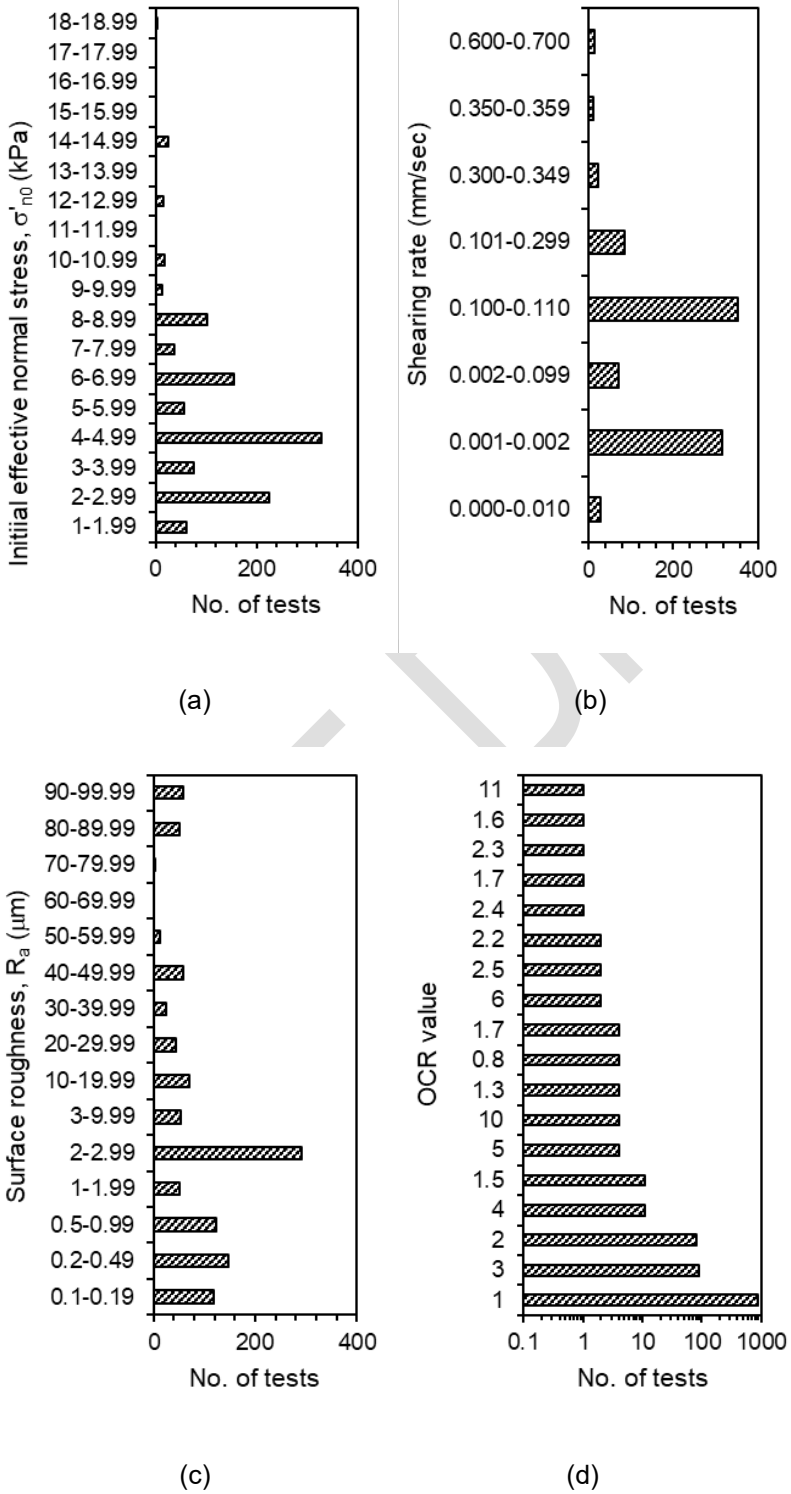

Figure 6 – Database test input conditions: (a) initial effective normal stress, (b) shearing rate, (c) surface average roughness, and (d) induced OCR

The overall database was categorized into subsets to narrow the statistical ranges of descriptive and model parameters. The following database subsets were considered:

- **Dataset A**: screened database as described in Table 3-2 (this was established to capture the widest range of soil, pipeline coating, and testing conditions within the database);
- **Dataset B**: subset of Dataset A excluding calcareous soil (found in several hydrocarbon-producing regions including the Gulf of Mexico and offshore South America, but generally not characteristic of most hydrocarbon field development regions);
- **Dataset C**: subset of Dataset B excluding low plasticity soil (to differentiate deepwater regions with predominantly high plasticity soils); and
- **Dataset D**: subset of Dataset C excluding bare steel (which can interact with salt water and create physicochemical reactions at the soil-steel interface, influencing the measured resistance) and all surfaces with R_a < 0.2 μm (observed to affect the bonding of the soil to the surface, leading to higher measured resistance due to creation of soil-soil shearing over portions of the sheared area).

While it is the most restrictive and filtered dataset, it is recommended that Dataset D is used for all high plasticity, fine-grained, non-carbonate soils, which are typical of deepwater Gulf of Mexico sites.

4 Results

4.1 Typical test results and interpretation basis

Examples of typical cyclic interface shear test results are presented in Figure 7, showing shear stress versus horizontal displacement (Figure 7a) and total horizontal displacement (Figure 7b) for a normally-consolidated soil sheared on a smooth surface, and shear stress versus horizontal displacement (Figure 7c) and total horizontal displacement (Figure 7d) for an overconsolidated soil sheared on an intermediate surface. The tests are considered Type A cyclic tests, where 18 cycles of fast shearing (v = 0.1 mm/s) were followed by 2 cycles of slow shearing (v = 0.001 mm/s). In these tests, no intervening periods of consolidation were employed.

For the normally-consolidated soil on the smooth surface, there is an initial peak shear stress of 2.3 kPa during the first half fast cycle, which strain softens to 1.8 kPa after 25 mm of monotonic shearing. This would effectively be the end of a monotonic test; however, a lower shear stress of 1.5 kPa is observed during the forward (positive) movement of the second fast cycle, while a higher value of 1.9 kPa is observed during backward movement. An advantage of the cyclic test approach is the ability to cancel this asymmetry in the data by averaging the forward and backward shearing data for each cycle, in this case resulting in a value of 1.7 kPa as the interpreted undrained residual shear stress before corrections for machine friction are applied. The residual shear stress values are straightforwardly interpreted from the data between shear displacement values of 20 to 25 mm in the forward direction and 0 to 5 mm in the backward direction, i.e. close to the arrows indicated on the plots. Where shorter displacement limits are employed, particularly with soils of high coarse-grained and/or very rough surfaces, selection of a steady residual value can be more challenging.

In some cases, a larger number of cycles is needed to reach the minimum undrained shear resistance for normally-consolidated soil, and this may have affected some of the undrained values interpreted in the database from Type B cyclic tests (limited to two fast cycles). After two cycles, there is a gradual increase in shear resistance through the remaining fast cycles due to continuous consolidation. During slow shearing, the shear resistance increases slightly as excess pore pressures are fully dissipated. The average value of the forward and backward shear stress in the final cycle would be taken as the interpreted drained residual shear stress, before corrections. Judgement is often applied in cases where there are significant differences between the first and second slow cycles, which can indicate excessive specimen loss and/or generation of additional machine friction.

For the overconsolidated soil on the intermediate surface (Figure 7c, Figure 7d), there is an initial peak shear stress of 5.8 kPa during the first half fast cycle, which strain softens to 5.3 kPa after 25 mm of monotonic shearing. The interpreted residual shear stress here would be taken as the average of the forward and backward shear stress in the first or second cycle to capture the overconsolidation effect. The resistance continues to reduce through the 9th cycle due to continuous swelling, before stabilizing during the remaining fast cycles. During slow shearing, the shear resistance increases slightly. Note that some of the slight increase in resistance through cycling can be due to soil loss below the shear ring and its effect on added friction.

Interpretation of tilt table test data is more straightforward, since the only output is a discrete value of table rotation where interface shearing commences, rather than a continuous stream of load and displacement data. Cyclic tilting can be employed to ensure a steady residual strength is attained, but this is not done consistently across all testing facilities. Only monotonic shearing was employed for the tilt table tests within the screened database, but these were repeated several times to achieve a consistent tilt angle that implies reaching critical state conditions.

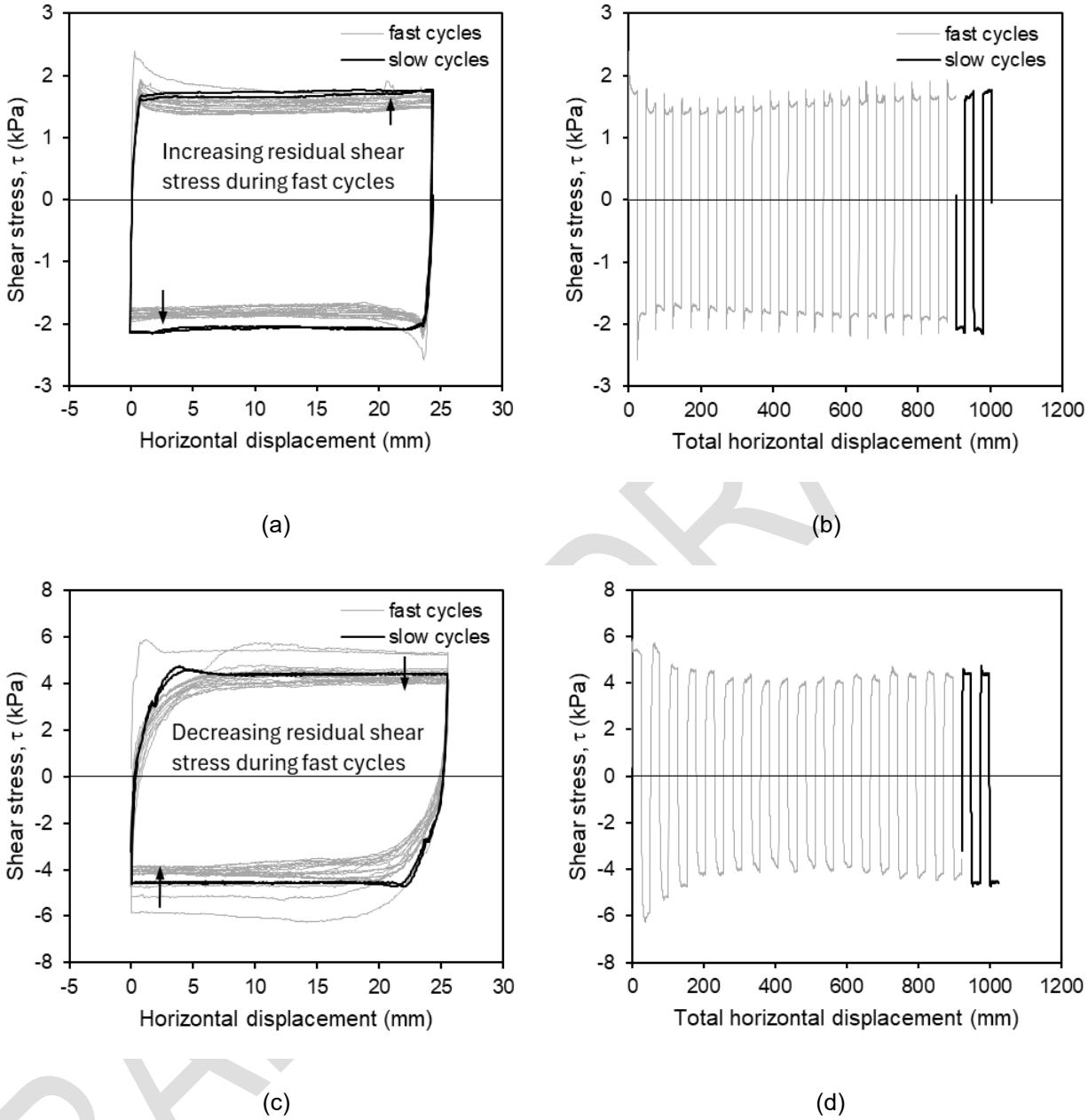

Figure 7 – Example cyclic interface shear box test results for showing: (a) and (b) shear stress versus horizontal displacement and total horizontal displacement, for normally-consolidated soil on a smooth surface (R_a < 1 μm), (c) and (d) shear stress versus horizontal displacement and total horizontal displacement for overconsolidated soil on an intermediate surface (1 μm ≤ R_a < 10 μm)

4.2 Results overview

An overview of database results is presented in Figure 8 and Figure 9 for Dataset A. The data shows extensive scatter since all variations in test conditions (normal stress, OCR, roughness and shearing rate) are included. Figure 8 illustrates the breadth of data and test conditions as well as which test input conditions dominate the database. Figure 9 illustrates the influence of soil properties on the test results; no clear trends can be discerned, again due to the wide range of input conditions.

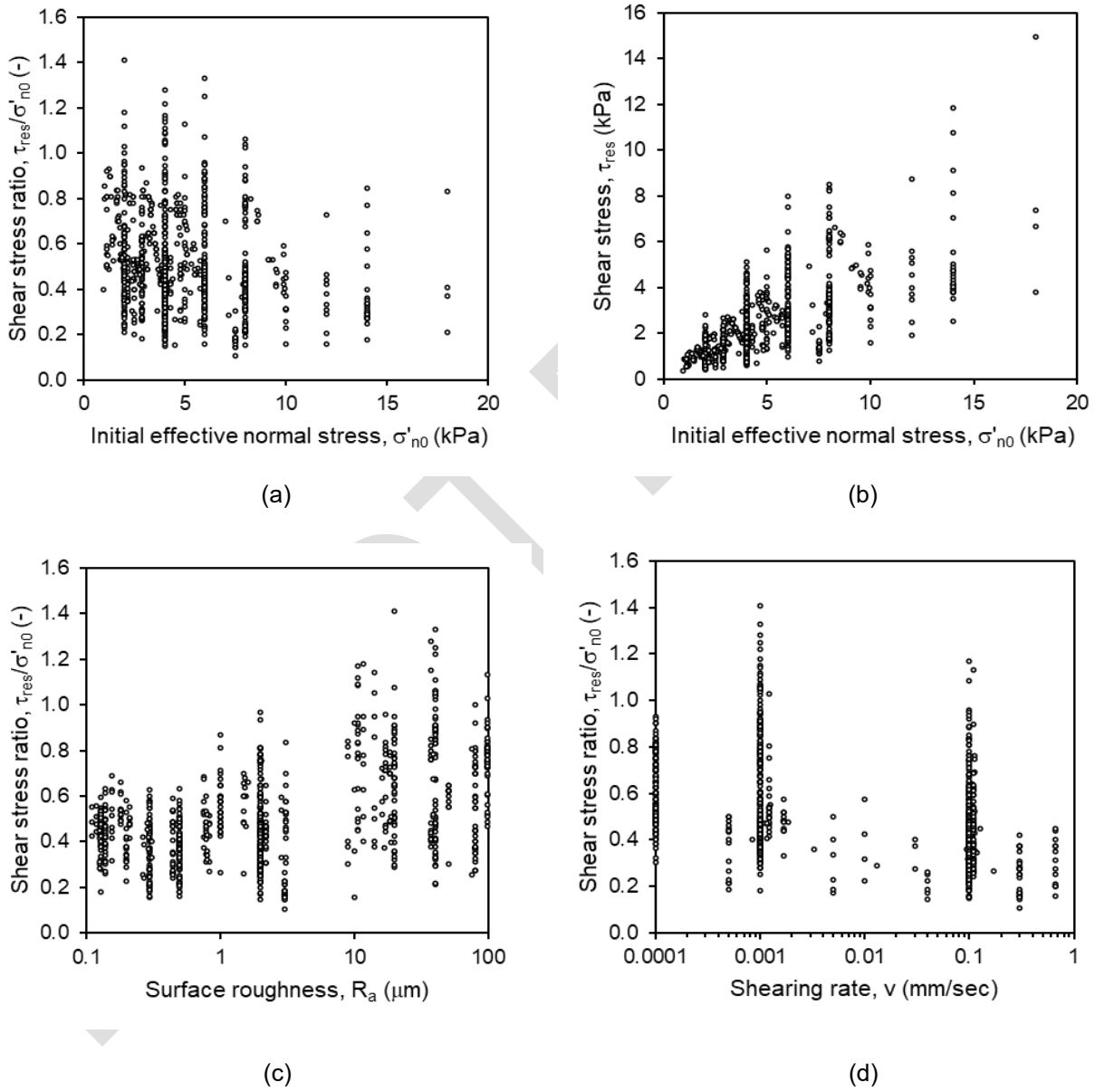

Figure 8 – Dataset A (all fine-grained, non-carbonate/calcareous): (a) shear stress ratio versus initial effective normal stress, (b) shear stress versus initial effective normal stress, (c) shear stress ratio versus surface roughness, and (d) shear stress ratio versus shearing rate (with tilt table results plotted at v = 0.0001 mm/s)

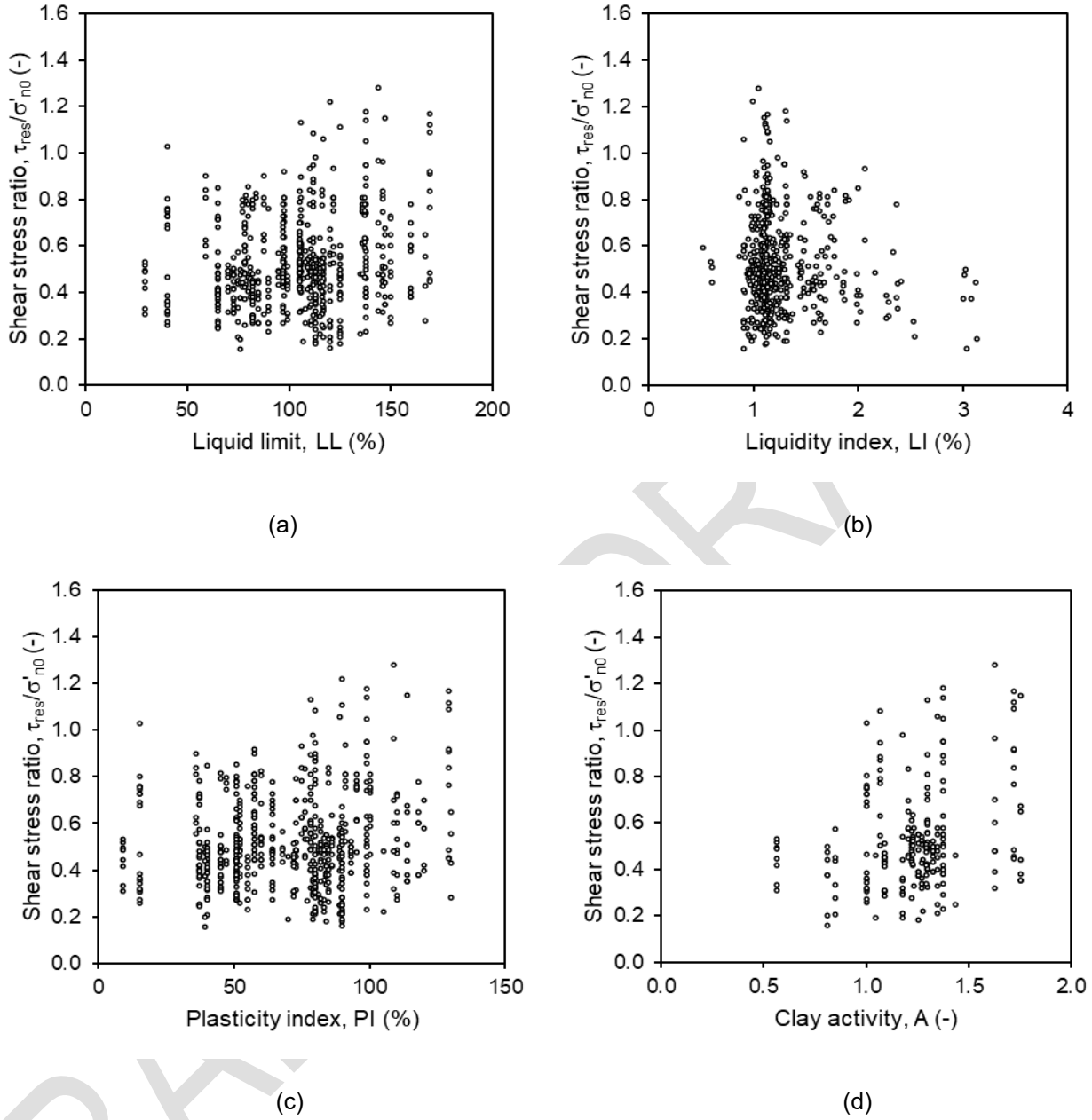

Figure 9 – Dataset A (all fine-grained, non-carbonate/calcareous): (a) shear stress ratio versus liquid limit, (b) shear stress ratio versus liquidity index, (c) shear stress ratio versus plasticity index, and (d) shear stress ratio versus clay activity

4.3 Dataset trends and model parameter calibrations

The database is presented for categorical subsets comprising (i) normally-consolidated, undrained test results and drained test results (all OCR values) and (ii) smooth, intermediate, and rough surface conditions following the classification presented in Table 4-1.

Table 4-1 – Surface roughness classification

Roughness Category	**R_a value**
Smooth	$R_a < 1$ μm
Intermediate	1 μm ≤ $R_a < 10$ μm
Rough	$R_a \geq 10$ μm

For each dataset, results are presented in the following sequence:

- A catalogue of figure references for each plot.
- Tables of all statistical descriptive values and model parameters.
- Histograms of normally-consolidated, undrained and drained shear strength ratios for all surface roughness conditions, including subsets for smooth, intermediate, and rough conditions; statistical parameter summaries are provided for each plot.
- Normal stress plots showing normalized shear stress versus normalized normal stress, with normal stress model fits for all surface roughness conditions, including subsets for smooth, intermediate, and rough conditions; statistical parameter summaries are provided for each plot.
- Surface roughness trends for normally-consolidated, undrained and drained shear strength ratios; statistical fits are provided for each plot for three categories of surface roughness: smooth, intermediate, and rough interface conditions.
- OCR parameter trends for undrained conditions, with OCR *m* parameter histograms for all surface roughness conditions, including subsets for smooth, intermediate, and rough conditions; statistical parameter summaries are provided for each plot.
- Soil property (*LL*, *LI*, *PI*, and *A*) trends for normally-consolidated, undrained and drained shear strength ratios for all surface roughness conditions, including subsets for smooth, intermediate, and rough conditions; statistical parameters are not provided due to the lack of any clear trends.

4.3.1 Dataset A

Results for Dataset A are presented in the following figures as noted in Table 4-2. A summary of statistics for Dataset A is presented in Table 4-3.

Table 4-2 – List of figures for Dataset A results

Plot description	Figure No.
Shear stress ratio histograms for undrained, normally-consolidated conditions	Figure 10
Shear stress ratio histograms for drained conditions (all OCR values)	Figure 11
Normal stress trends for undrained, normally-consolidated conditions	Figure 12
Normal stress trends for drained conditions (all OCR values)	Figure 13
Surface roughness trends for undrained, normally-consolidated conditions and drained conditions (all OCR values)	Figure 14
OCR m parameter histogram for all surfaces	Figure 15
Soil property trends for undrained, normally-consolidated conditions	Figure 16
Soil property trends for drained conditions (all OCR values)	Figure 17

Table 4-3 – Statistically-derived parameters for Dataset A: all fine-grained, non-carbonate/ calcareous data

Parameter		Und, all data	Und, smooth data	Und, interm data	Und, rough data	Und, NC data	Und, NC smooth data	Und, NC interm data	Und, NC rough data	Dr, all data	Dr, smooth data	Dr, interm data	Dr, rough data
	n	126	60	35	31	345	110	138	96	590	208	198	175
Shear stress ratio, τ_{res}/σ'_{n0}	μ	-	-	-	-	0.36	0.28	0.36	0.45	0.59	0.46	0.54	0.80
	σ	-	-	-	-	0.13	0.08	0.13	0.12	0.20	0.08	0.16	0.17
	cv	-	-	-	-	0.35	0.26	0.35	0.27	0.34	0.18	0.29	0.21
	P_5	-	-	-	-	0.19	0.18	0.16	0.29	0.34	0.32	0.30	0.54
	P_{50}	-	-	-	-	0.34	0.27	0.35	0.43	0.53	0.47	0.51	0.78
	P_{95}	-	-	-	-	0.61	0.43	0.61	0.68	0.93	0.58	0.81	1.11
Normal stress 'a' parameter	μ	-	-	-	-	0.23	0.15	0.27	0.22	0.41	0.28	0.27	0.72
	σ	-	-	-	-	0.08	0.04	0.09	0.05	0.14	0.04	0.07	0.15
	cv	-	-	-	-	0.34	0.25	0.34	0.23	0.34	0.16	0.27	0.21
	P_5	-	-	-	-	0.12	0.10	0.13	0.14	0.25	0.21	0.16	0.49
	P_{50}	-	-	-	-	0.22	0.14	0.26	0.21	0.36	0.28	0.26	0.71
	P_{95}	-	-	-	-	0.36	0.22	0.44	0.30	0.67	0.35	0.39	1.00
Normal stress 'b' parameter	b	-	-	-	-	0.86	0.80	0.91	0.77	0.89	0.85	0.78	0.97
OCR 'm' parameter	μ	0.48	0.43	0.53	0.51	-	-	-	-	-	-	-	-
	σ	0.23	0.20	0.25	0.23	-	-	-	-	-	-	-	-
	cv	0.47	0.47	0.47	0.45	-	-	-	-	-	-	-	-
	P_5	0.11	0.13	0.11	0.13	-	-	-	-	-	-	-	-
	P_{50}	0.46	0.39	0.54	0.52	-	-	-	-	-	-	-	-
	P_{95}	0.86	0.77	0.98	0.86	-	-	-	-	-	-	-	-

Notes: n = number of data points; cv = coefficient of variation; Und = undrained (fast shearing rate); Dr = drained (slow shearing rate)

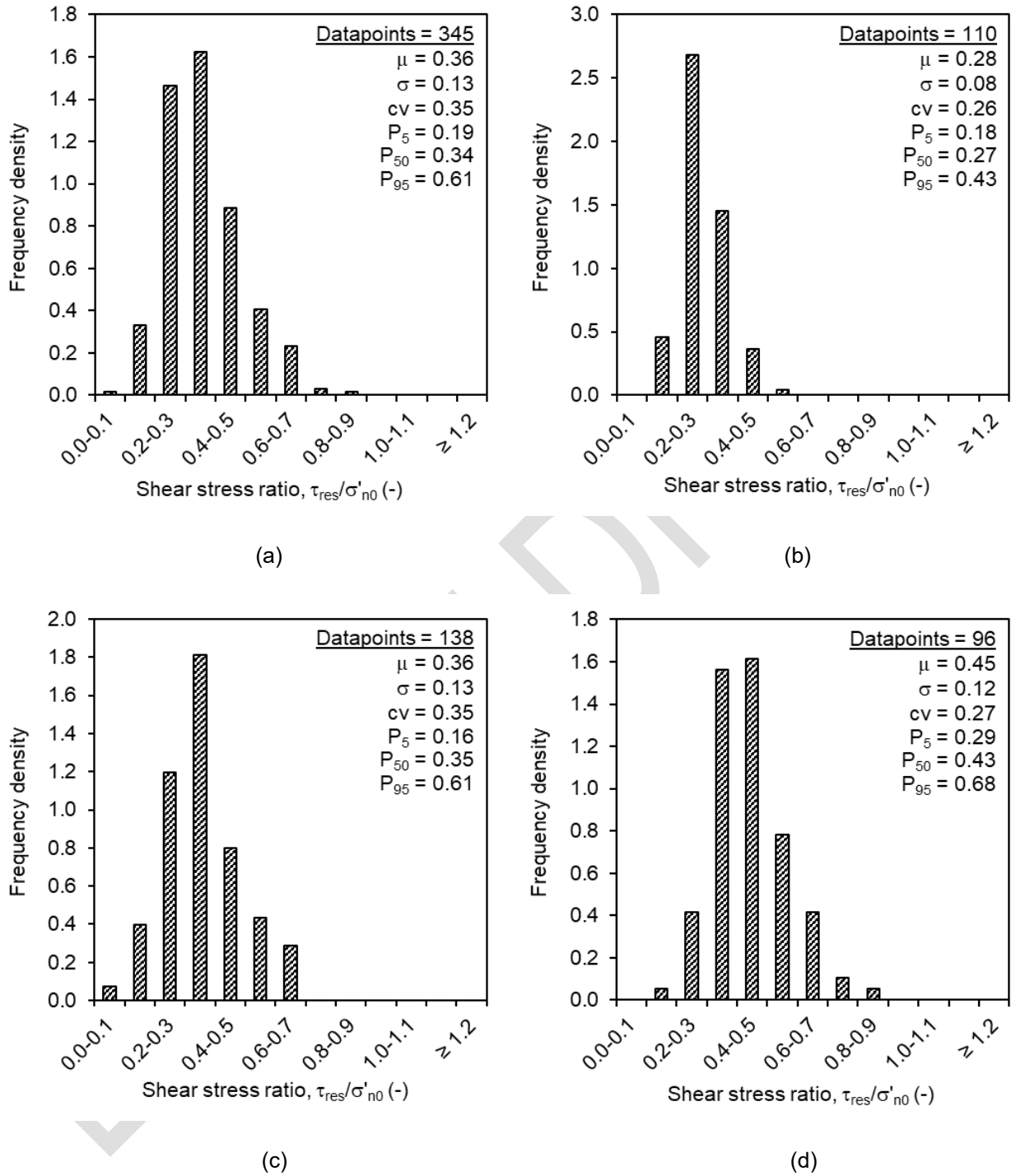

Figure 10 – Dataset A (all fine-grained, non-carbonate/calcareous): distributions of residual strength ratio for undrained normally-consolidated soils: (a) all surfaces (including one unknown roughness value), (b) smooth surfaces, (c) intermediate surfaces, and (d) rough surfaces

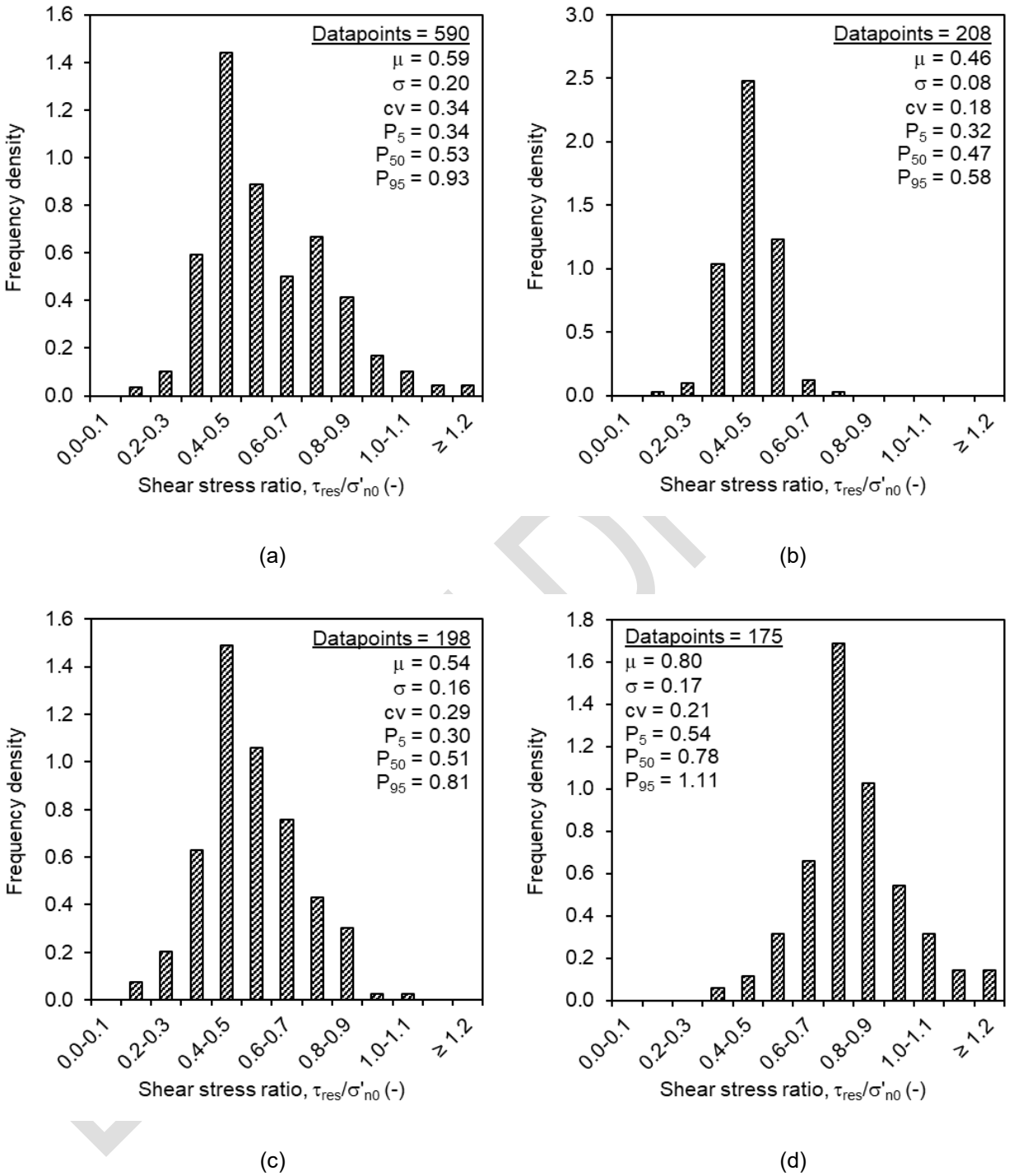

Figure 11 – Dataset A (all fine-grained, non-carbonate/calcareous): distributions of residual strength ratio for drained soils: (a) all surfaces (including nine unknown roughness values), (b) smooth surfaces, (c) intermediate surfaces, and (d) rough surfaces

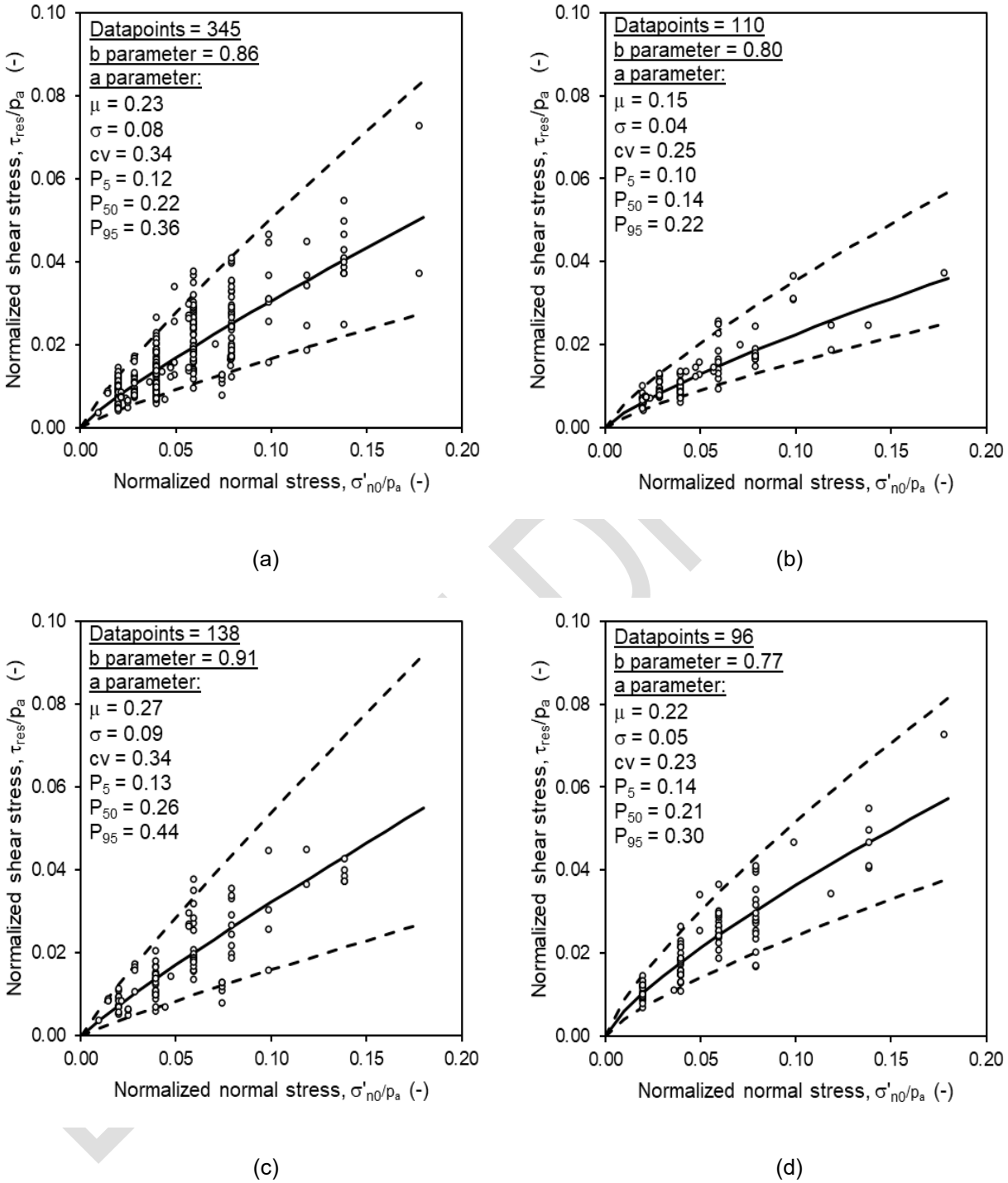

Figure 12 – Dataset A (all fine-grained, non-carbonate/calcareous): normal stress trends of residual strength ratio for undrained normally-consolidated soils: (a) all surfaces (including one unknown roughness value), (b) smooth surfaces, (c) intermediate surfaces, and (d) rough surfaces

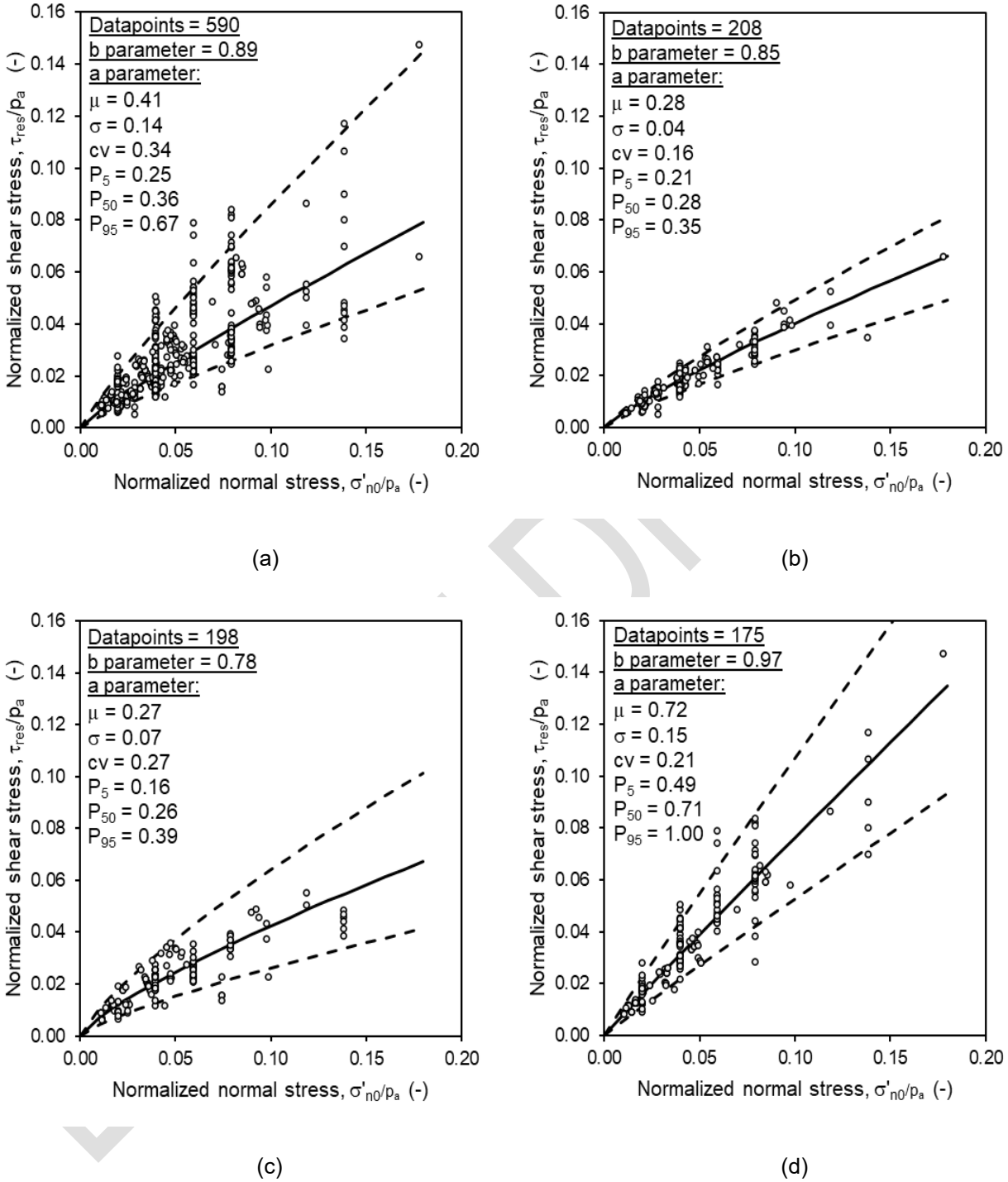

Figure 13 – Dataset A (all fine-grained, non-carbonate/calcareous): normal stress trends of residual strength ratio for drained soils: (a) all surfaces (including nine unknown roughness values), (b) smooth surfaces, (c) intermediate surfaces, and (d) rough surfaces

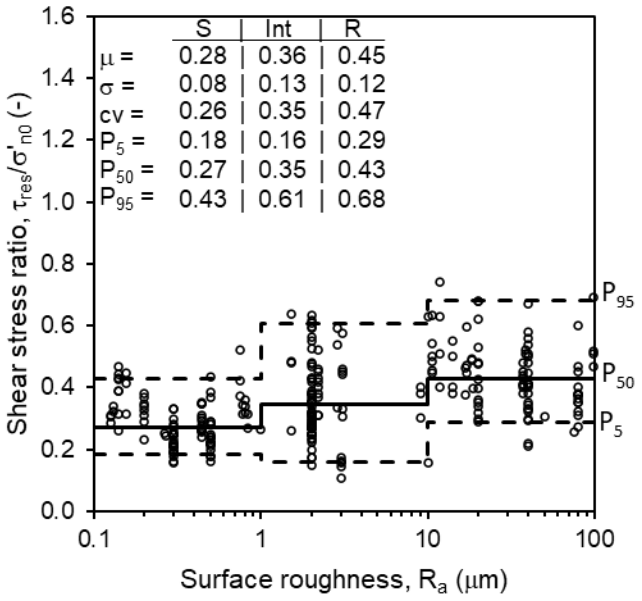

(a)

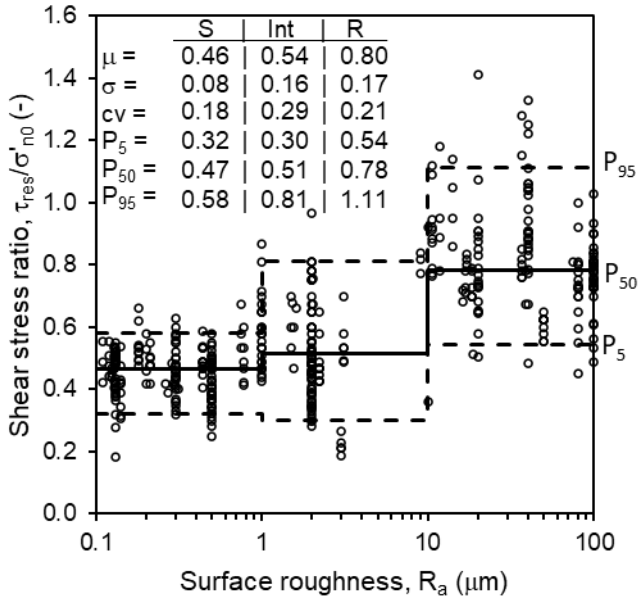

(b)

Figure 14 – Dataset A (all fine-grained, non-carbonate/calcareous): surface roughness trends of residual strength ratio for (a) undrained, normally-consolidated soils and (b) drained soils: S = smooth surfaces, Int = intermediate surfaces, and R = rough surfaces

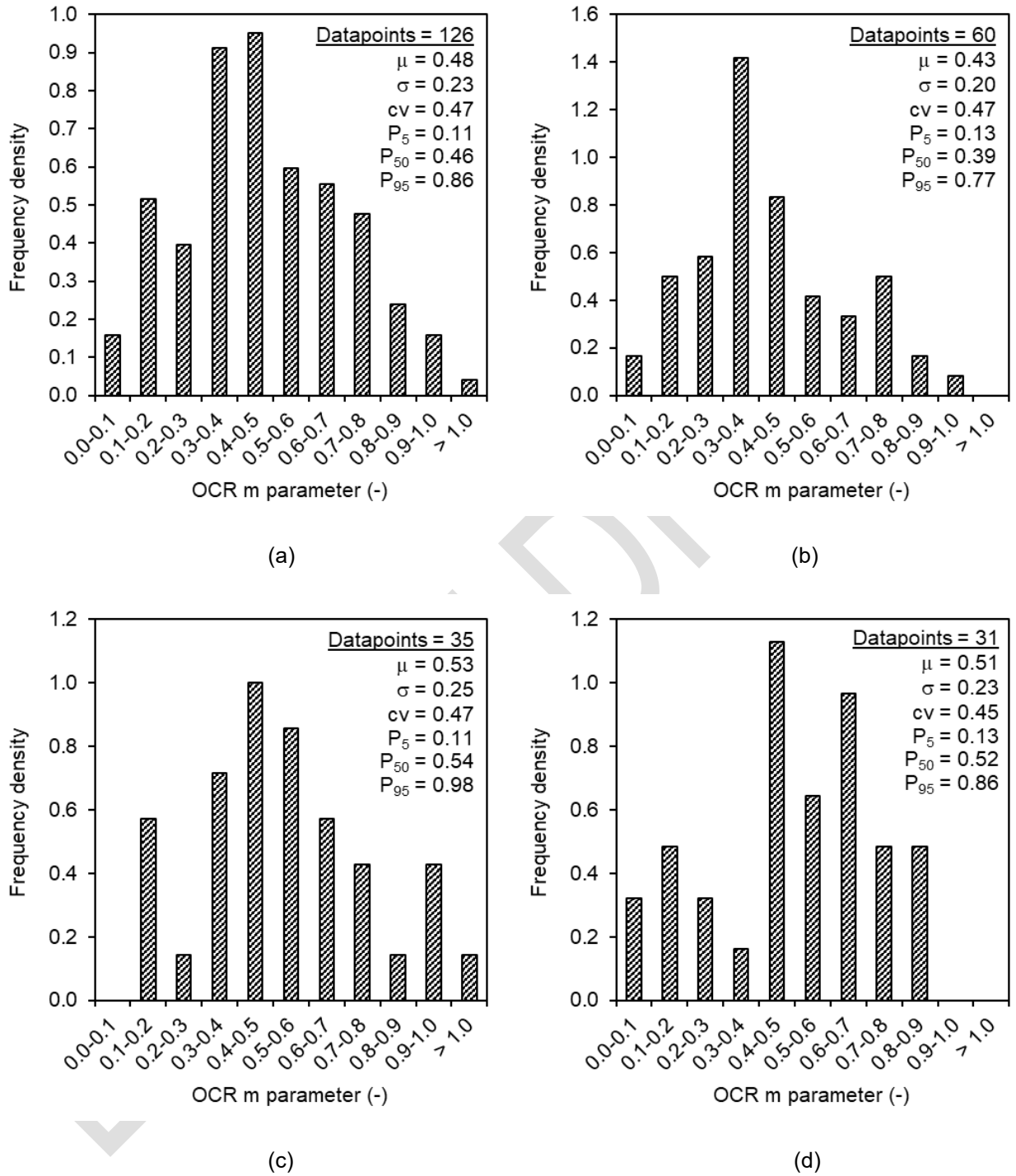

Figure 15 – Dataset A (all fine-grained, non-carbonate/calcareous): distributions of overconsolidation 'm' parameter for undrained soils: (a) all surfaces, (b) smooth surfaces, (c) intermediate surfaces, and (d) rough surfaces

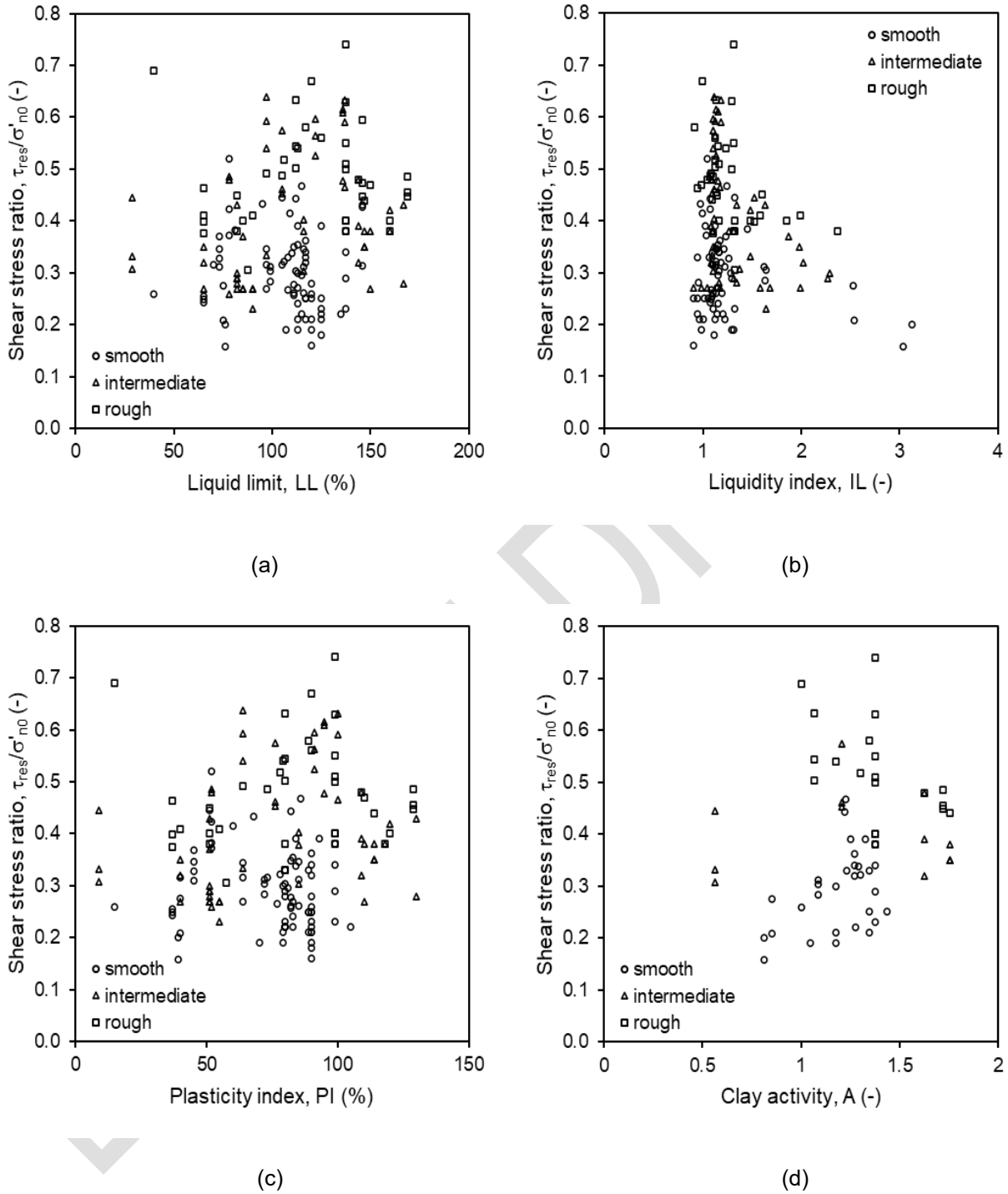

Figure 16 – Dataset A (all fine-grained, non-carbonate/calcareous): effect of index properties on residual shear strength trends for undrained, normally-consolidated soils (all surfaces and normal stress values): (a) liquid limit, (b) liquidity index, (c) plasticity index, and (d) clay activity

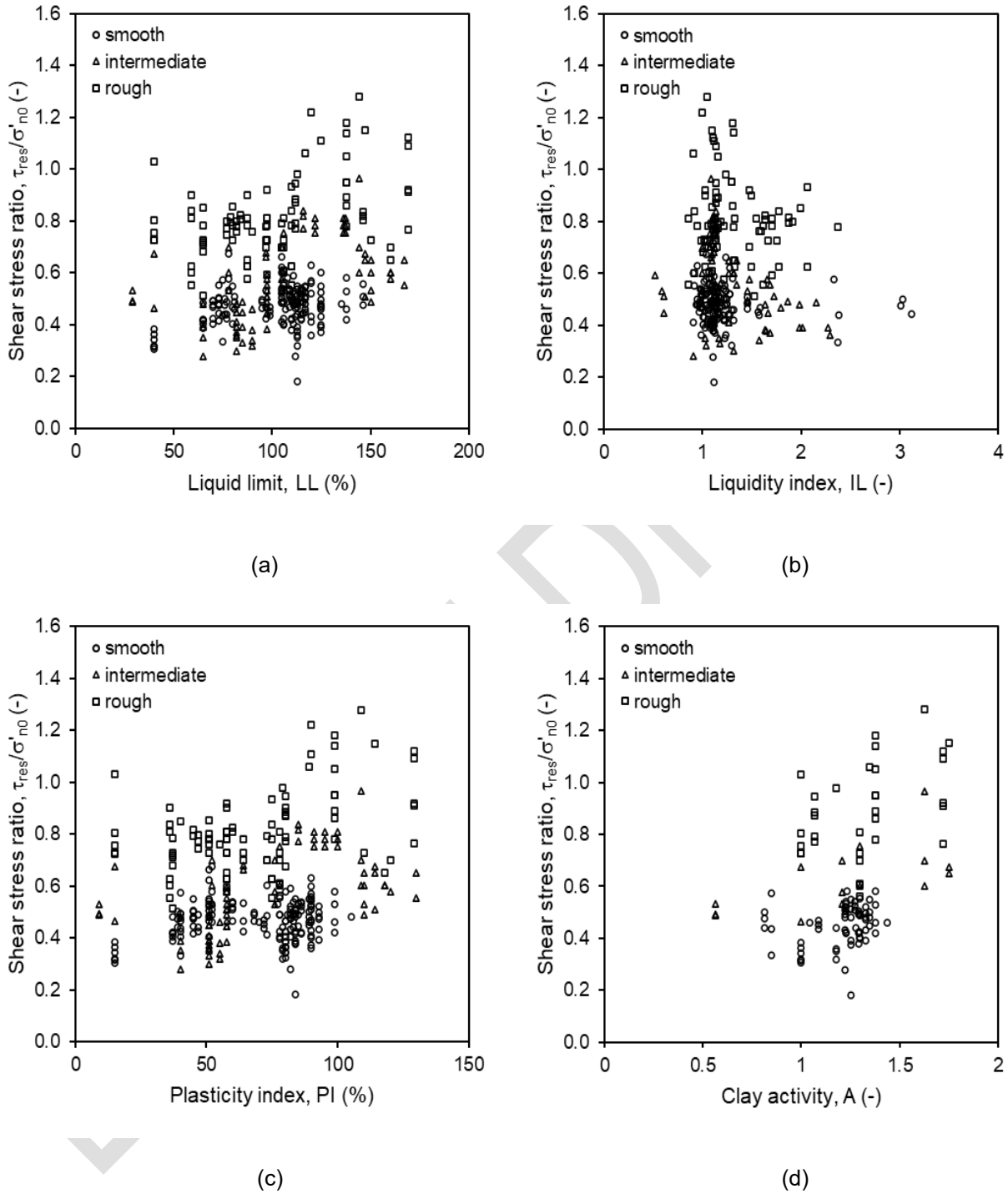

Figure 17 – Dataset A (all fine-grained, non-carbonate/calcareous): effect of index properties on residual shear strength trends for drained soils (all surfaces and normal stress values): (a) liquid limit, (b) liquidity index, (c) plasticity index, and (d) clay activity

4.3.2 Dataset B

Results for Dataset B are presented in the following figures as noted in Table 4-4. A summary of statistics for Dataset B is presented in Table 4-5.

Table 4-4 – List of figures for Dataset B results

Plot description	Figure No.
Shear stress ratio histograms for undrained, normally-consolidated conditions	Figure 18
Shear stress ratio histograms for drained conditions (all OCR values)	Figure 19
Normal stress trends for undrained, normally-consolidated conditions	Figure 20
Normal stress trends for drained conditions (all OCR values)	Figure 21
Surface roughness trends for undrained, normally-consolidated conditions and drained conditions (all OCR values)	Figure 22
OCR m parameter histogram for all surfaces	Figure 23
Soil property trends for undrained, normally-consolidated conditions	Figure 24
Soil property trends for drained conditions (all OCR values)	Figure 25

Table 4-5 – Statistically-derived parameters for Dataset B: all fine-grained, non-carbonate data

Parameter		Und, all data	Und, smooth data	Und, interm data	Und, rough data	Und, NC data	Und, NC smooth data	Und, NC interm data	Und, NC rough data	Dr, all data	Dr, smooth data	Dr, interm data	Dr, rough data
	n	113	54	35	24	272	80	131	61	493	169	182	133
Shear stress ratio, τ_{res}/σ'_{n0}	μ	-	-	-	-	0.36	0.30	0.36	0.44	0.57	0.46	0.53	0.76
	σ	-	-	-	-	0.12	0.08	0.13	0.12	0.18	0.08	0.16	0.14
	cv	-	-	-	-	0.34	0.26	0.36	0.26	0.32	0.17	0.30	0.19
	P_5	-	-	-	-	0.20	0.21	0.16	0.30	0.33	0.33	0.30	0.54
	P_{50}	-	-	-	-	0.34	0.28	0.34	0.43	0.52	0.47	0.50	0.76
	P_{95}	-	-	-	-	0.60	0.43	0.61	0.68	0.87	0.56	0.81	1.03
Normal stress 'a' parameter	μ	-	-	-	-	0.25	0.16	0.28	0.28	0.38	0.30	0.27	0.71
	σ	-	-	-	-	0.08	0.04	0.10	0.07	0.12	0.05	0.08	0.13
	cv	-	-	-	-	0.33	0.24	0.35	0.23	0.31	0.16	0.27	0.19
	P_5	-	-	-	-	0.13	0.11	0.13	0.19	0.24	0.23	0.15	0.51
	P_{50}	-	-	-	-	0.23	0.15	0.27	0.28	0.34	0.30	0.26	0.72
	P_{95}	-	-	-	-	0.38	0.23	0.45	0.38	0.58	0.36	0.40	0.96
Normal stress 'b' parameter	b	-	-	-	-	0.88	0.80	0.92	0.85	0.88	0.87	0.79	0.98
OCR 'm' parameter	μ	0.46	0.40	0.53	0.50	-	-	-	-	-	-	-	-
	σ	0.23	0.20	0.25	0.24	-	-	-	-	-	-	-	-
	cv	0.49	0.48	0.47	0.48	-	-	-	-	-	-	-	-
	P_5	0.11	0.13	0.11	0.10	-	-	-	-	-	-	-	-
	P_{50}	0.45	0.37	0.54	0.50	-	-	-	-	-	-	-	-
	P_{95}	0.87	0.76	0.98	0.86	-	-	-	-	-	-	-	-

Notes: n = number of data points; cv = coefficient of variation; Und = undrained (fast shearing rate); Dr = drained (slow shearing rate)

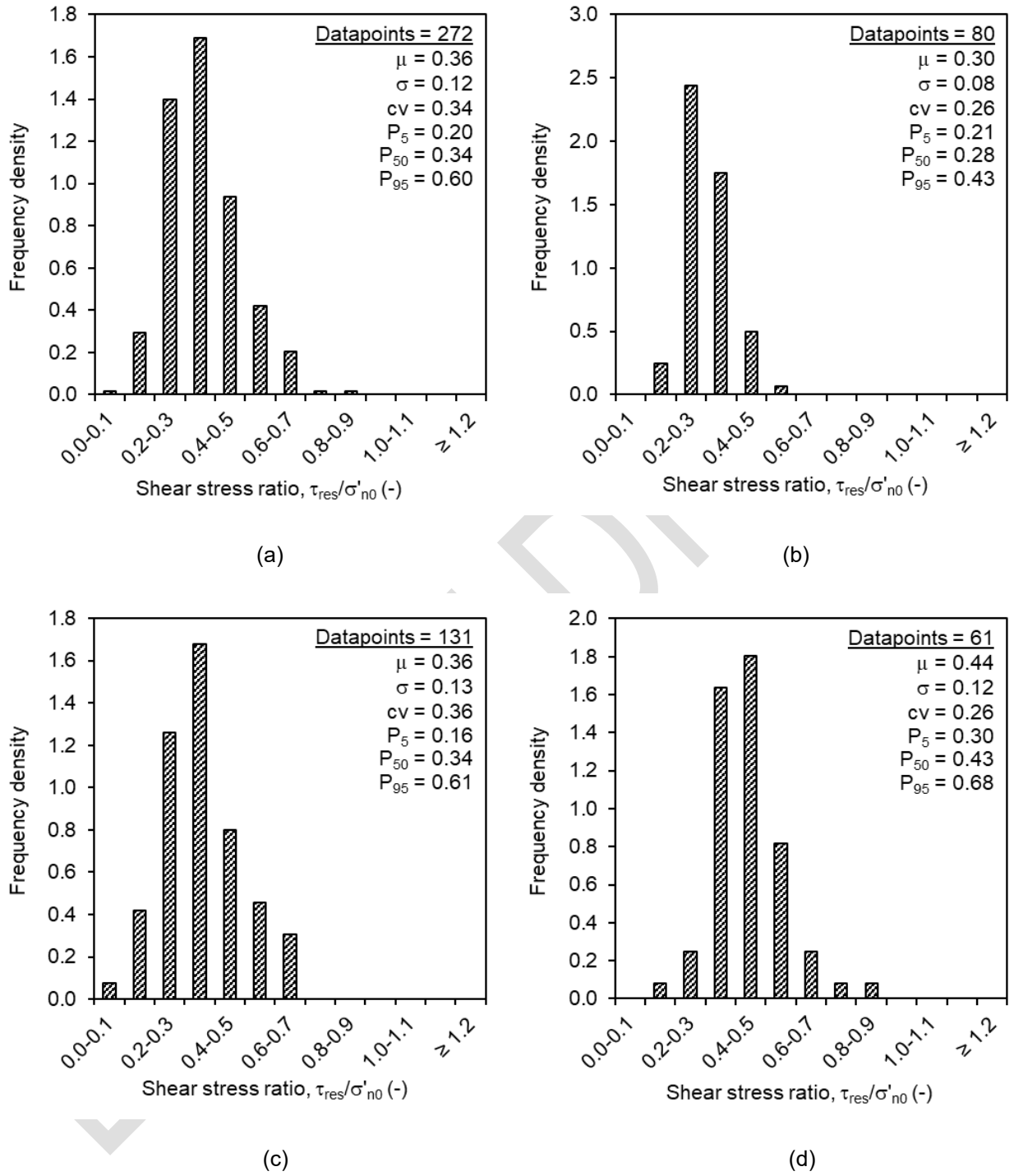

Figure 18 – Dataset B (all fine-grained, non-carbonate): distributions of residual strength ratio for undrained normally-consolidated soils: (a) all surfaces, (b) smooth surfaces, (c) intermediate surfaces, and (d) rough surfaces

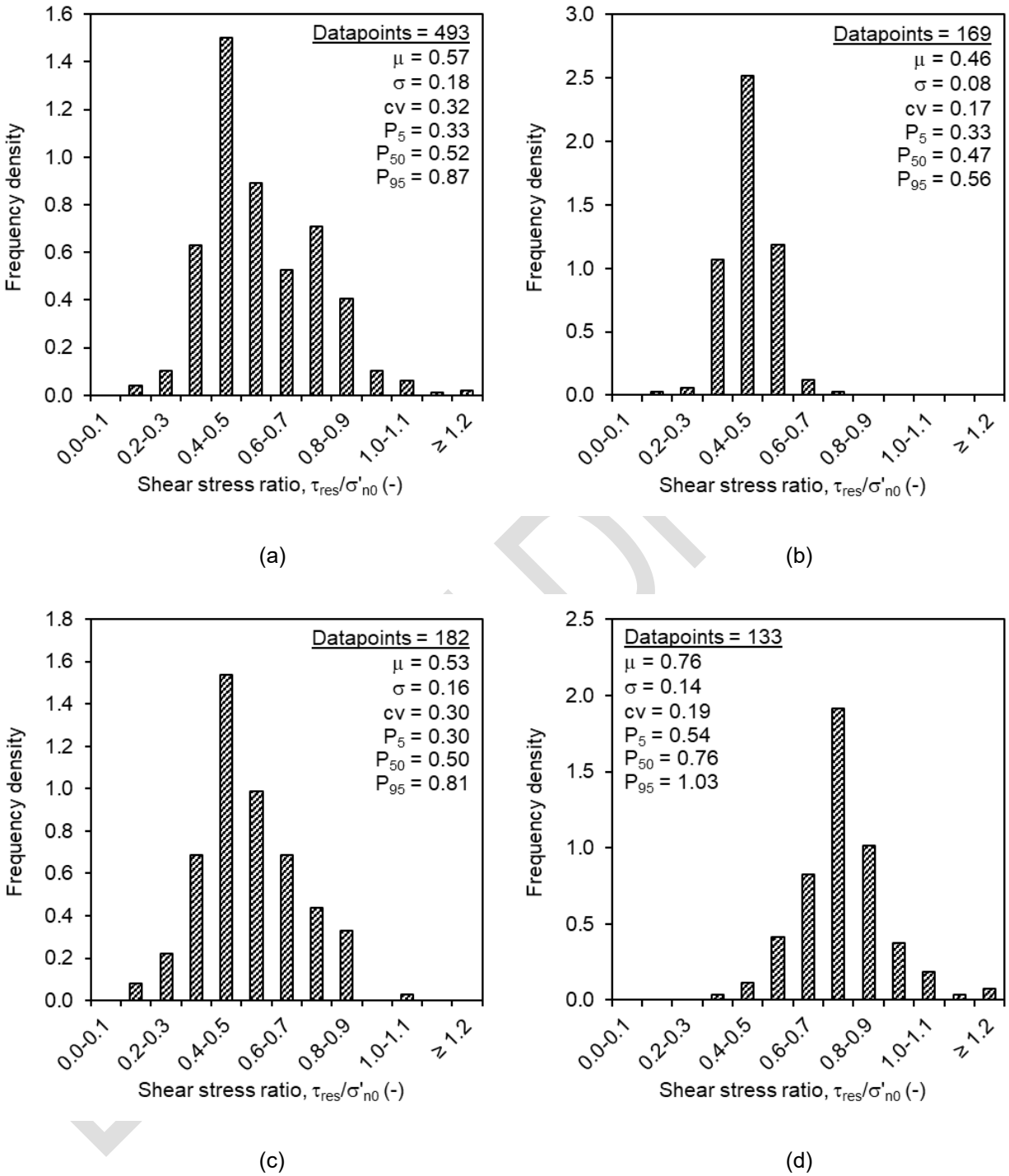

Figure 19 – Dataset B (all fine-grained, non-carbonate): distributions of residual strength ratio for drained soils: (a) all surfaces (including nine unknown roughness values), (b) smooth surfaces, (c) intermediate surfaces, and (d) rough surfaces

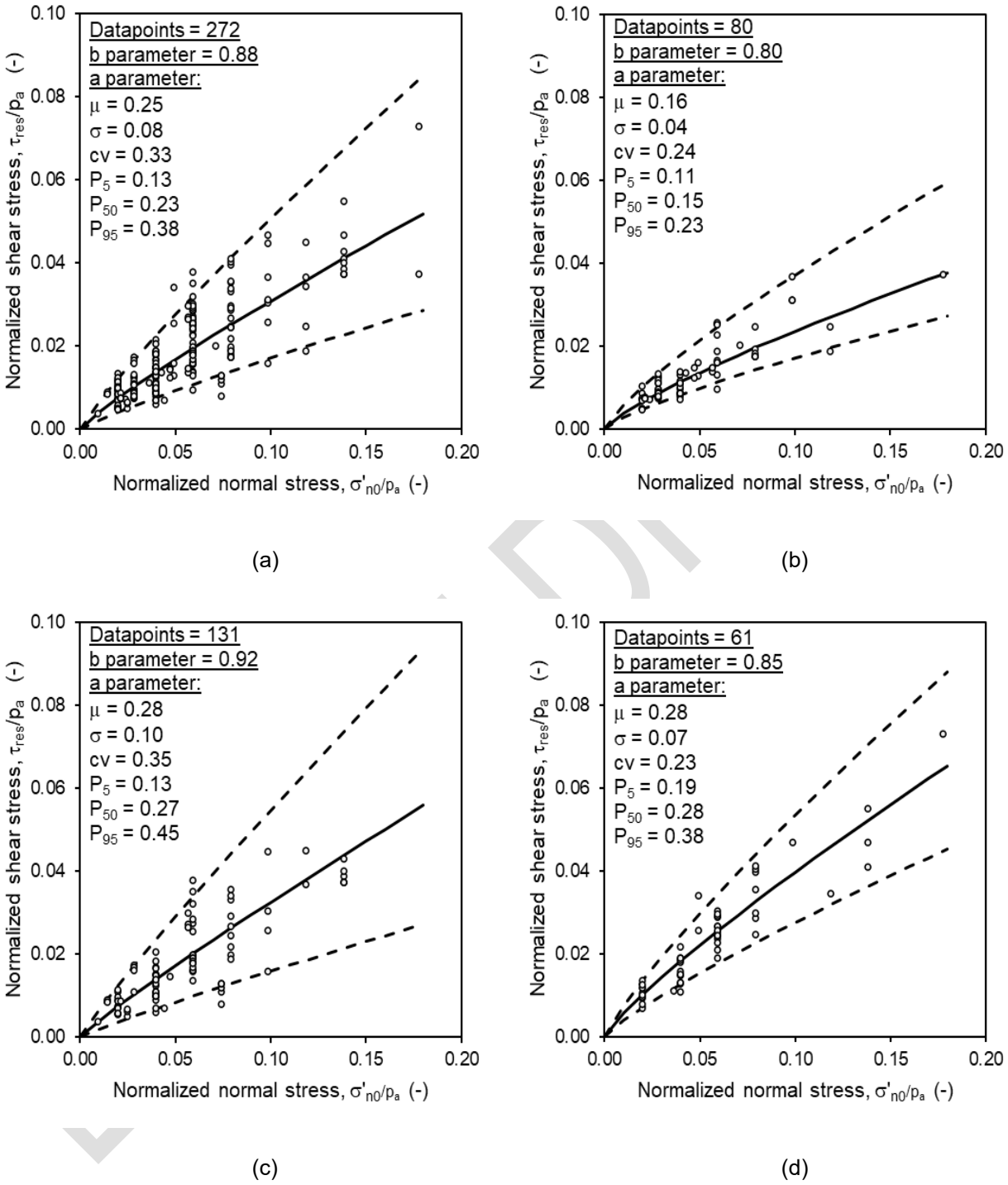

Figure 20 – Dataset B (all fine-grained, non-carbonate): normal stress trends of residual strength ratio for undrained normally-consolidated soils: (a) all surfaces, (b) smooth surfaces, (c) intermediate surfaces, and (d) rough surfaces

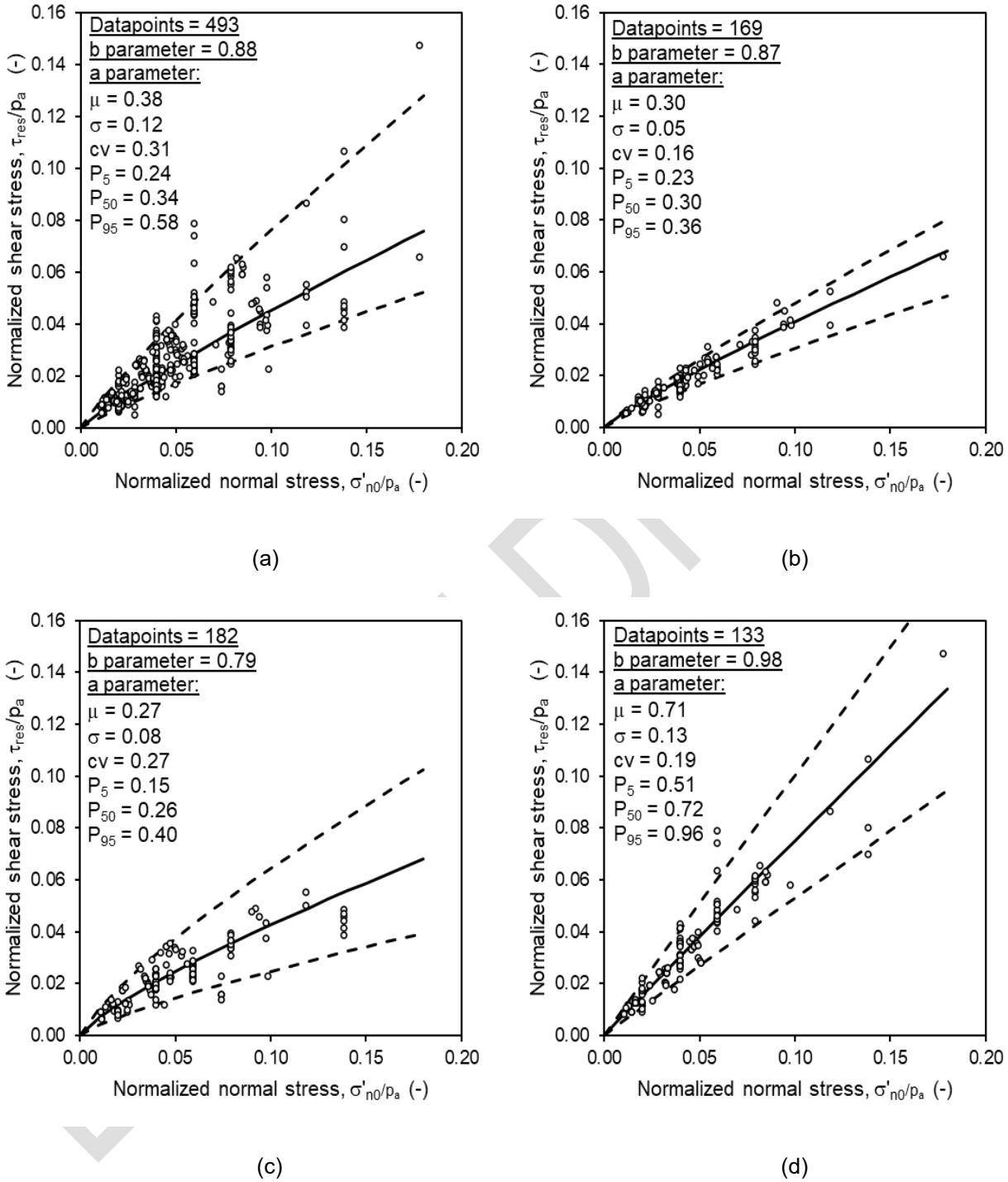

Figure 21 – Dataset B (all fine-grained, non-carbonate): normal stress trends of residual strength ratio for drained soils: (a) all surfaces (including nine unknown roughness values), (b) smooth surfaces, (c) intermediate surfaces, and (d) rough surfaces

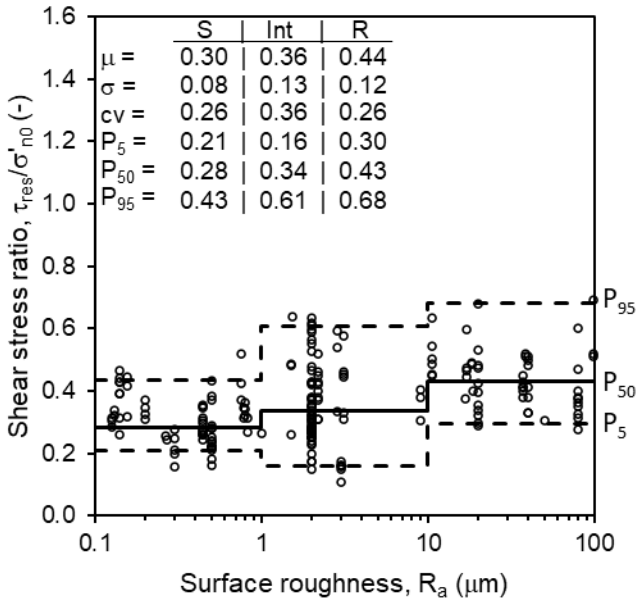

(a)

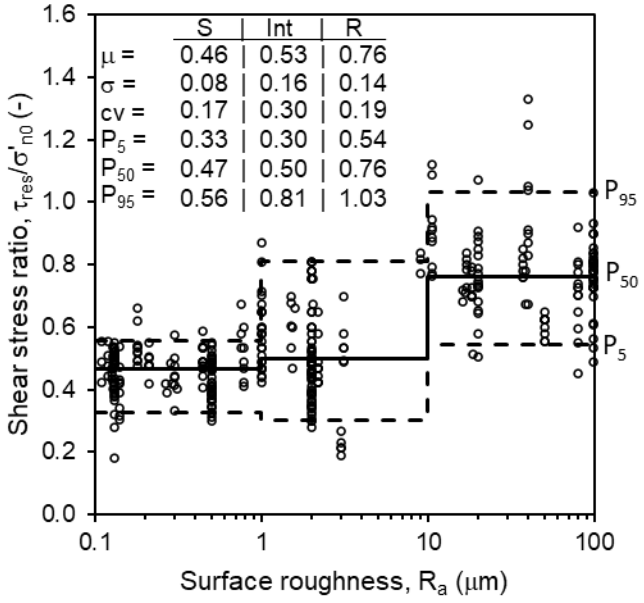

(b)

Figure 22 – Dataset B (all fine-grained, non-carbonate): surface roughness trends of residual strength ratio for (a) undrained, normally-consolidated soils and (b) drained soils: S = smooth surfaces, Int = intermediate surfaces, and R = rough surfaces

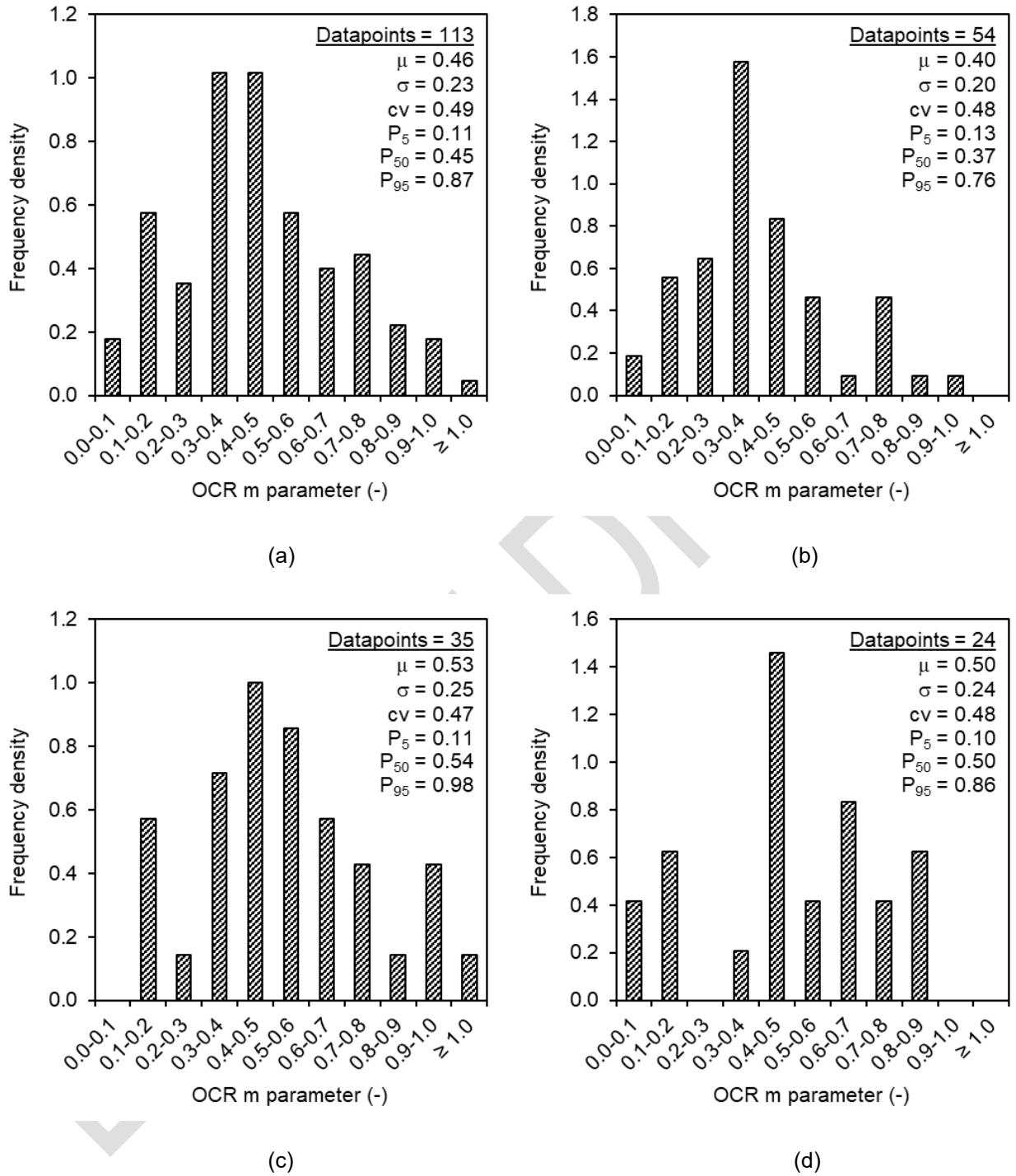

Figure 23 – Dataset B (all fine-grained, non-carbonate): distributions of overconsolidation 'm' parameter for undrained soils: (a) all surfaces, (b) smooth surfaces, (c) intermediate surfaces, and (d) rough surfaces

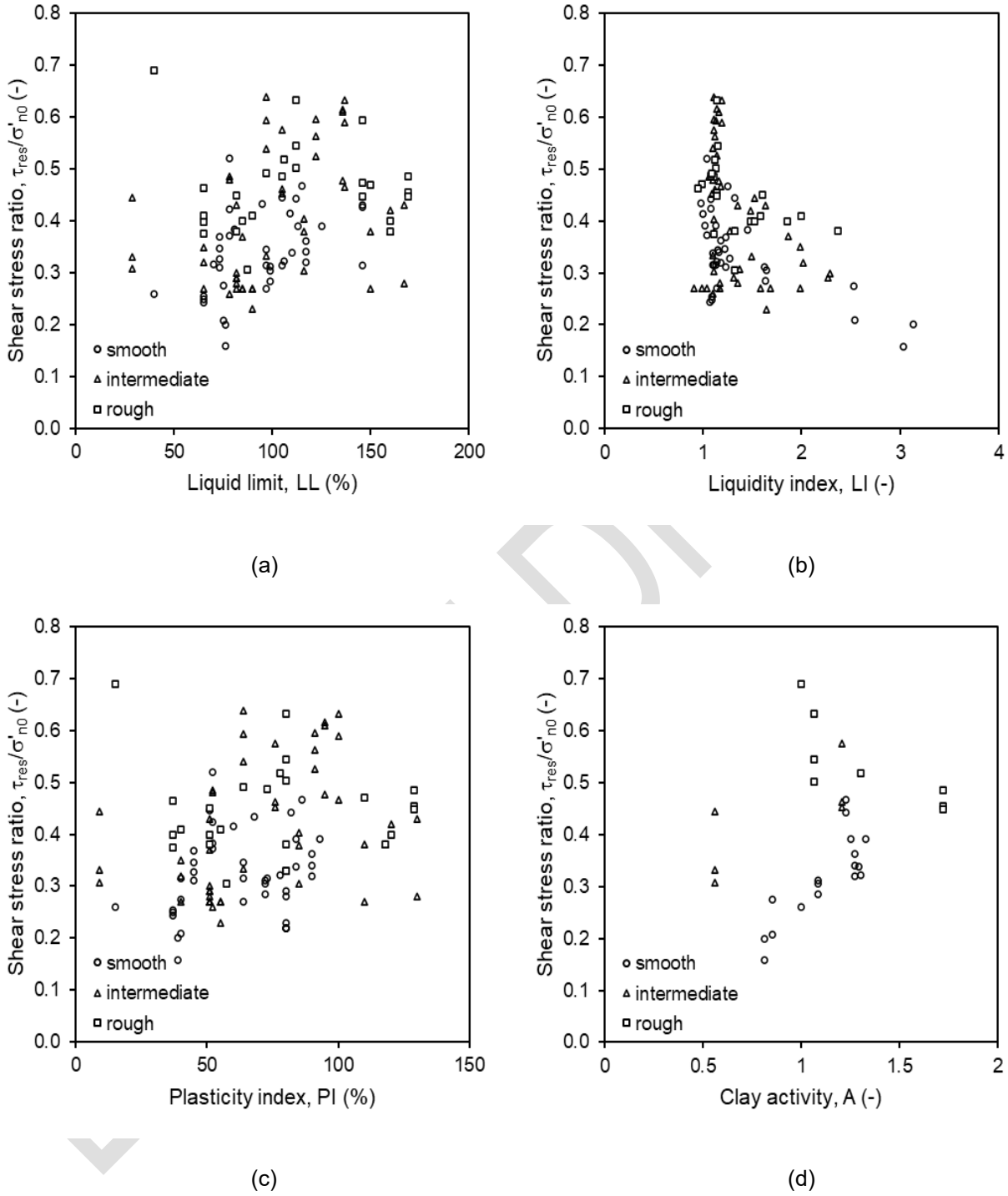

Figure 24 – Dataset B (all fine-grained, non-carbonate): effect of index properties on residual shear strength trends for undrained, normally-consolidated soils (all surfaces and normal stress values): (a) liquid limit, (b) liquidity index, (c) plasticity index, and (d) clay activity

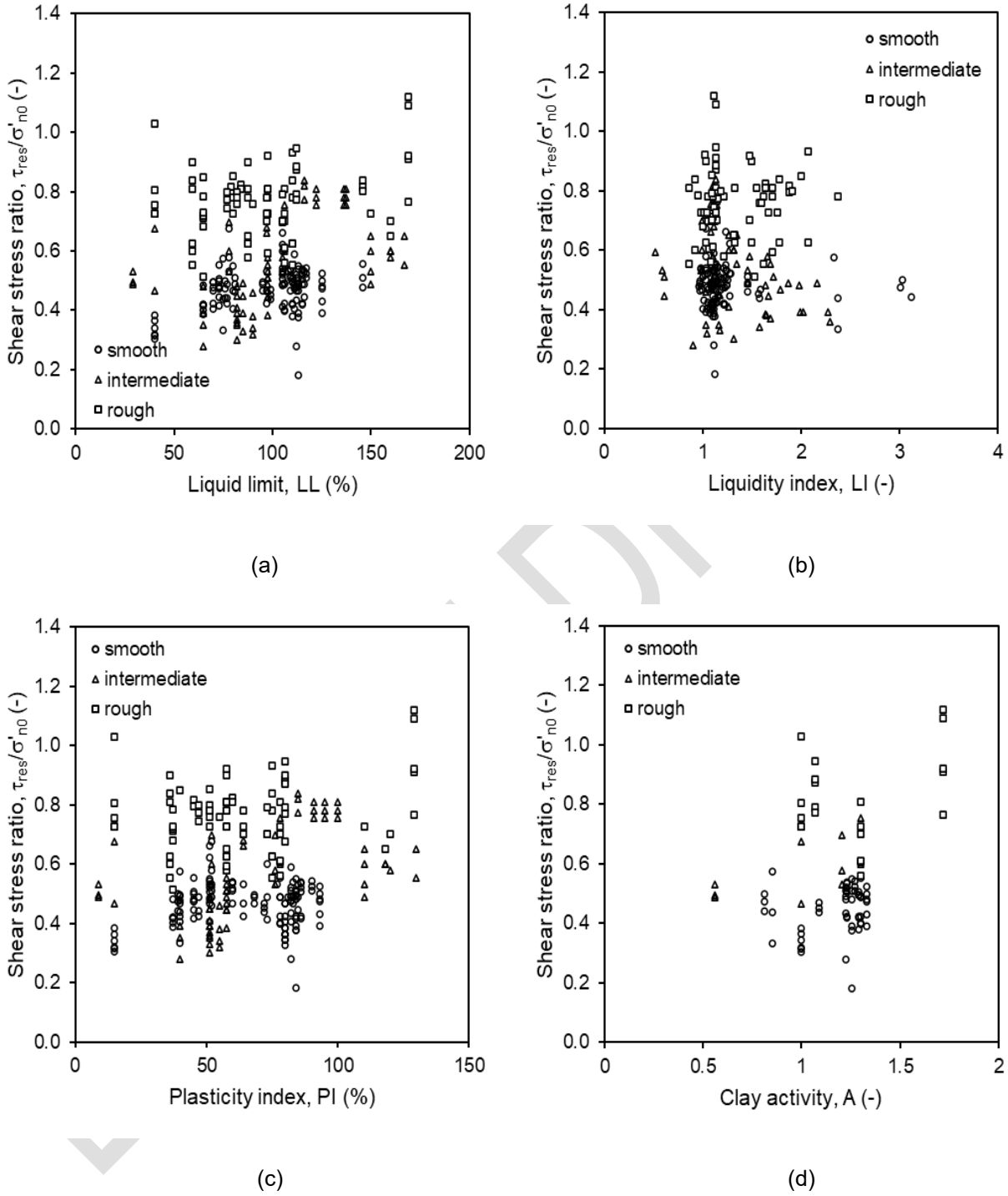

Figure 25 – Dataset B (all fine-grained, non-carbonate): effect of index properties on residual shear strength trends for drained soils (all surfaces and normal stress values): (a) liquid limit, (b) liquidity index, (c) plasticity index, and (d) clay activity

4.3.3 Dataset C

Results for Dataset C are presented in the following figures as noted in Table 4-6. A summary of statistics for Dataset C is presented in Table 4-7.

Table 4-6 – List of figures for Dataset C results

Plot description	Figure No.
Shear stress ratio histograms for undrained, normally-consolidated conditions	Figure 26
Shear stress ratio histograms for drained conditions (all OCR values)	Figure 27
Normal stress trends for undrained, normally-consolidated conditions	Figure 28
Normal stress trends for drained conditions (all OCR values)	Figure 29
Surface roughness trends for undrained, normally-consolidated conditions and drained conditions (all OCR values)	Figure 30
OCR m parameter histogram for all surfaces	Figure 31
Soil property trends for undrained, normally-consolidated conditions	Figure 32
Soil property trends for drained conditions (all OCR values)	Figure 33

Table 4-7 – Statistically-derived parameters for Dataset C: high-plasticity, fine-grained, non-carbonate data

Parameter		Und, all data	Und, smooth data	Und, interm data	Und, rough data	Und, NC data	Und, NC smooth data	Und, NC interm data	Und, NC rough data	Dr, all data	Dr, smooth data	Dr, interm data	Dr, rough data
	n	97	48	30	18	220	69	104	47	431	149	160	113
Shear stress ratio, τ_{res}/σ'_{n0}	μ	-	-	-	-	0.37	0.31	0.38	0.44	0.57	0.47	0.54	0.75
	σ	-	-	-	-	0.11	0.07	0.13	0.09	0.17	0.08	0.16	0.12
	cv	-	-	-	-	0.31	0.24	0.34	0.20	0.29	0.17	0.30	0.16
	P_5	-	-	-	-	0.21	0.21	0.16	0.32	0.34	0.34	0.30	0.55
	P_{50}	-	-	-	-	0.35	0.31	0.36	0.43	0.53	0.48	0.52	0.76
	P_{95}	-	-	-	-	0.60	0.44	0.61	0.60	0.85	0.57	0.82	0.92
Normal stress 'a' parameter	μ	-	-	-	-	0.26	0.16	0.25	0.30	0.36	0.30	0.25	0.64
	σ	-	-	-	-	0.08	0.04	0.08	0.05	0.10	0.05	0.07	0.10
	cv	-	-	-	-	0.30	0.22	0.34	0.18	0.29	0.15	0.27	0.15
	P_5	-	-	-	-	0.15	0.11	0.12	0.22	0.23	0.23	0.15	0.47
	P_{50}	-	-	-	-	0.25	0.16	0.23	0.30	0.32	0.31	0.24	0.64
	P_{95}	-	-	-	-	0.40	0.24	0.40	0.38	0.54	0.36	0.35	0.77
Normal stress 'b' parameter	b	-	-	-	-	0.89	0.80	0.86	0.88	0.86	0.87	0.75	0.95
OCR 'm' parameter	μ	0.48	0.40	0.55	0.54	-	-	-	-	-	-		-
	σ	0.23	0.19	0.27	0.23	-	-	-	-	-	-		-
	cv	0.48	0.47	0.48	0.42	-	-	-	-	-	-		-
	P_5	0.13	0.13	0.10	0.18	-	-	-	-	-	-		-
	P_{50}	0.45	0.37	0.55	0.51	-	-	-	-	-	-		-
	P_{95}	0.88	0.76	0.98	0.87	-	-	-	-	-	-		-

Notes: n = number of data points; cv = coefficient of variation; Und = undrained (fast shearing rate); Dr = drained (slow shearing rate)

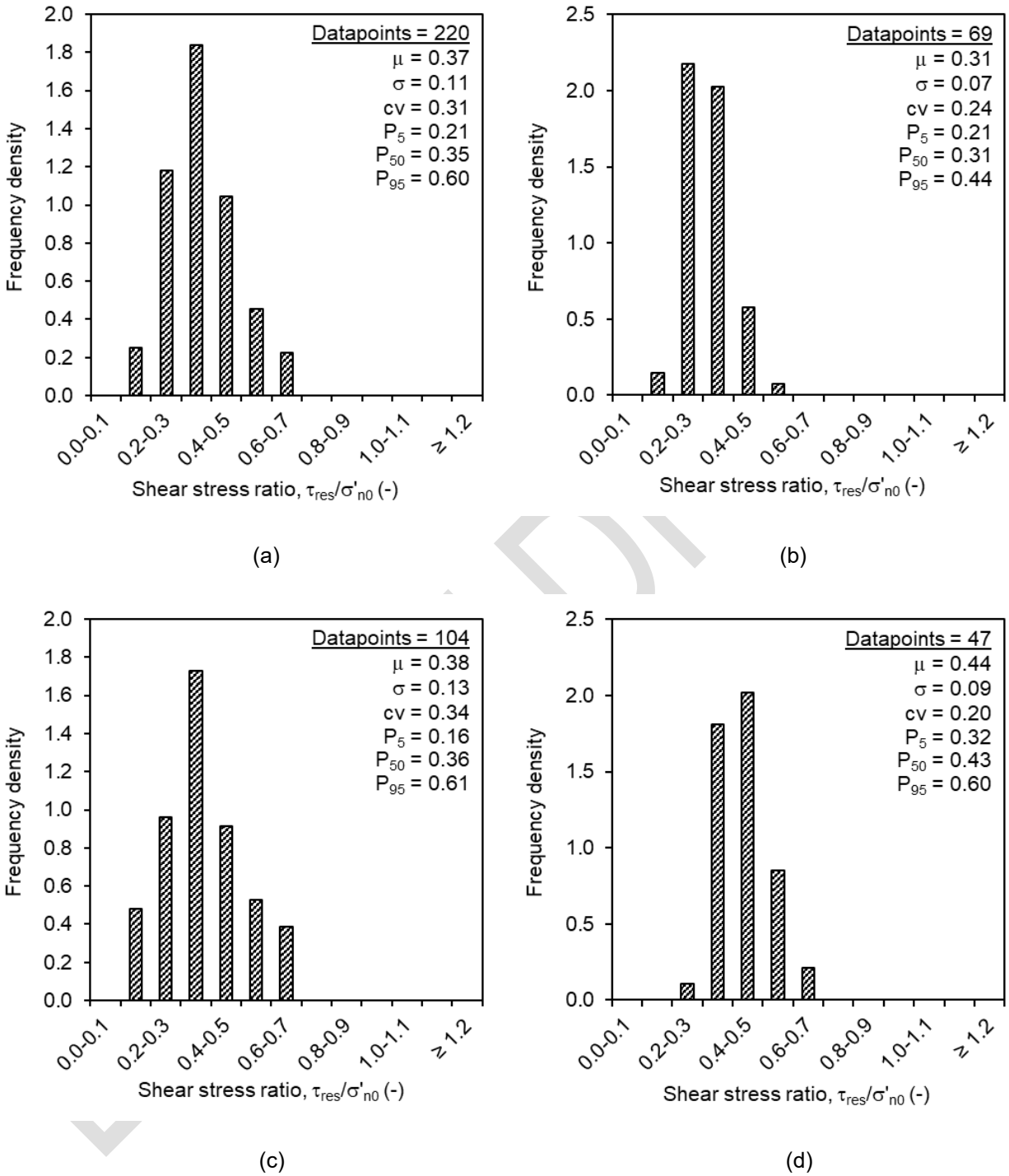

Figure 26 – Dataset C (high-plasticity, fine-grained, non-carbonate): distributions of residual strength ratio for undrained normally-consolidated soils: (a) all surfaces, (b) smooth surfaces, (c) intermediate surfaces, and (d) rough surfaces

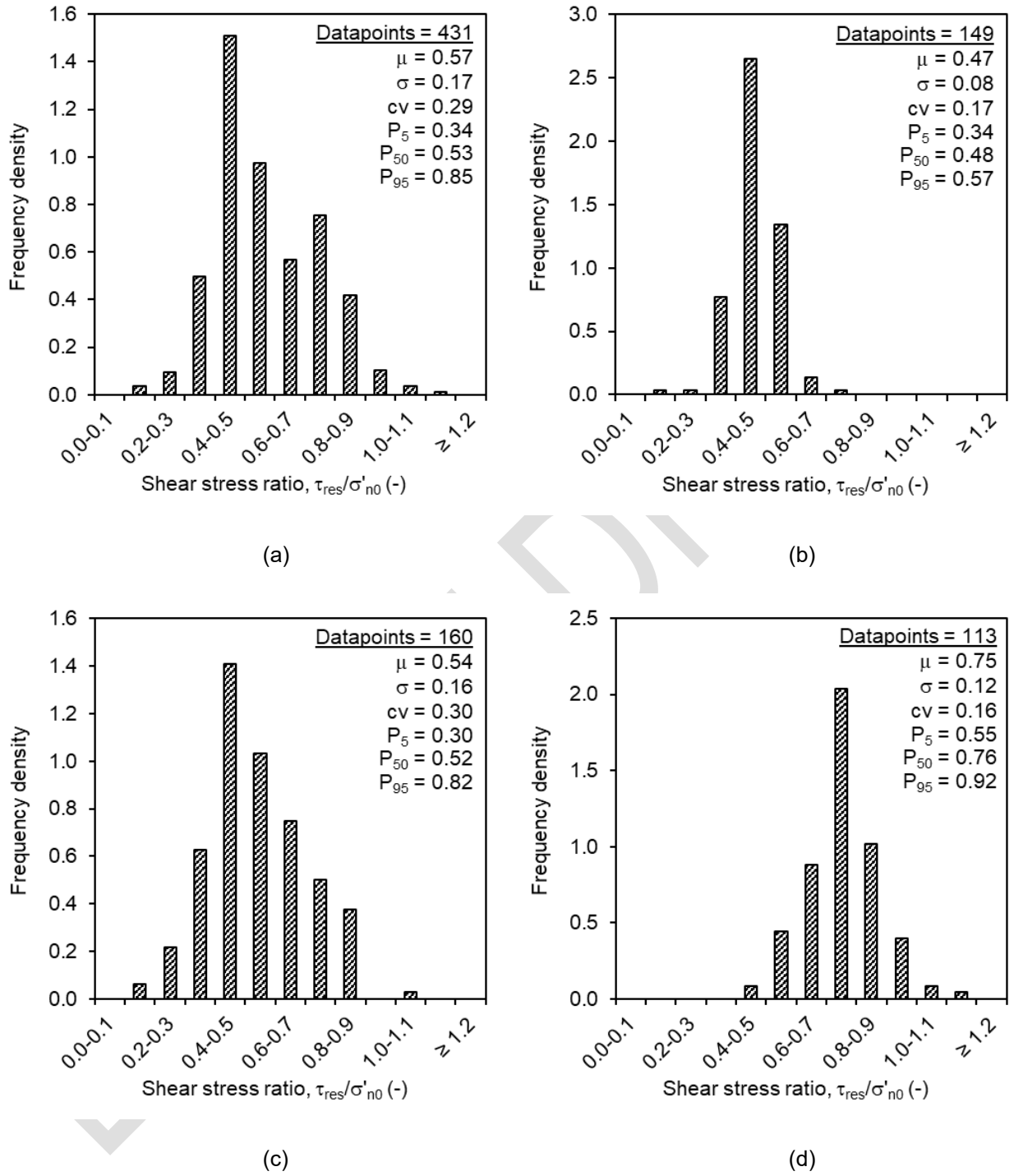

Figure 27 – Dataset C (high-plasticity, fine-grained, non-carbonate): distributions of residual strength ratio for drained soils: (a) all surfaces (including nine unknown roughness values), (b) smooth surfaces, (c) intermediate surfaces, and (d) rough surfaces

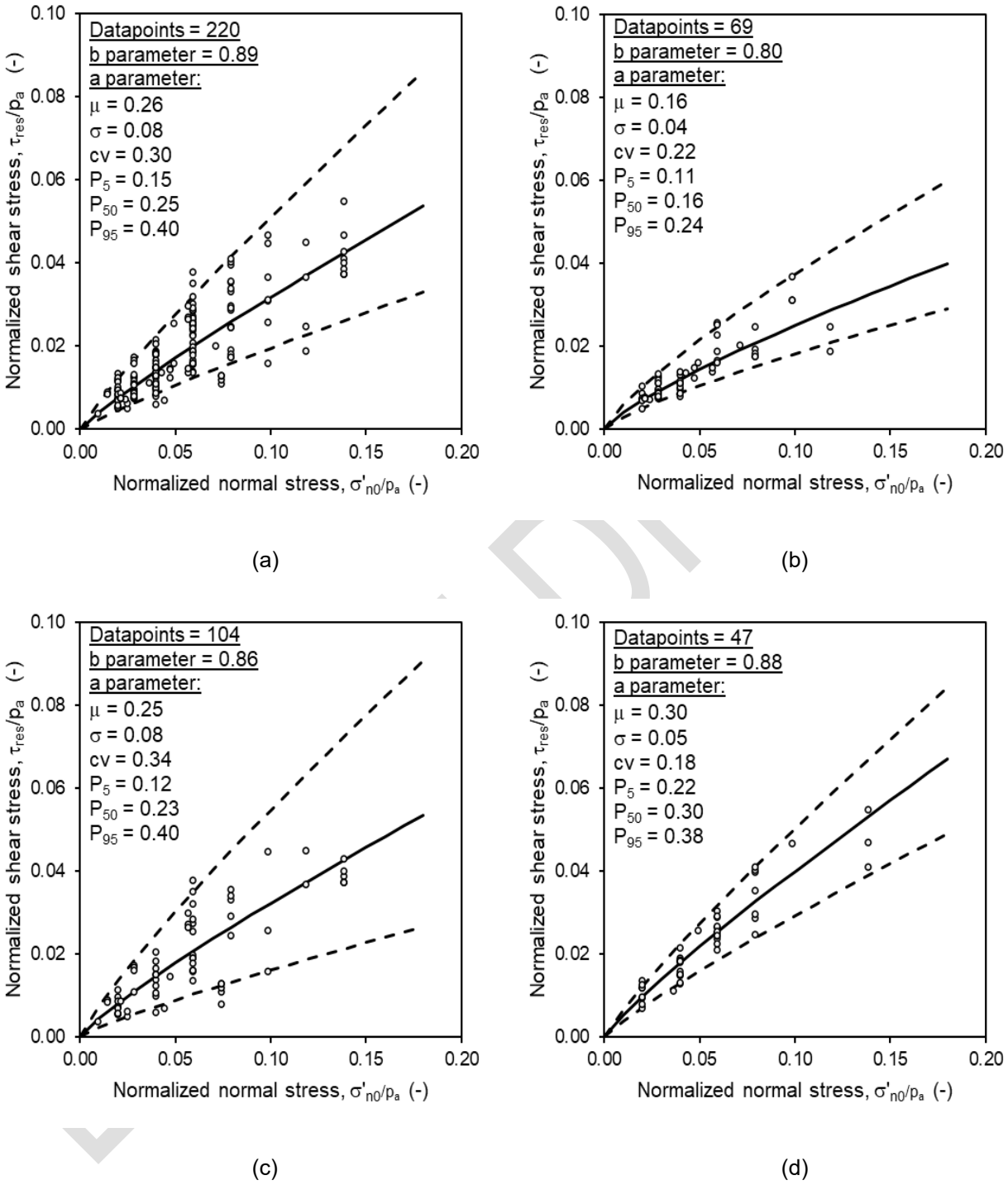

Figure 28 – Dataset C (high-plasticity, fine-grained, non-carbonate): normal stress trends of residual strength ratio for undrained normally-consolidated soils: (a) all surfaces, (b) smooth surfaces, (c) intermediate surfaces, and (d) rough surfaces

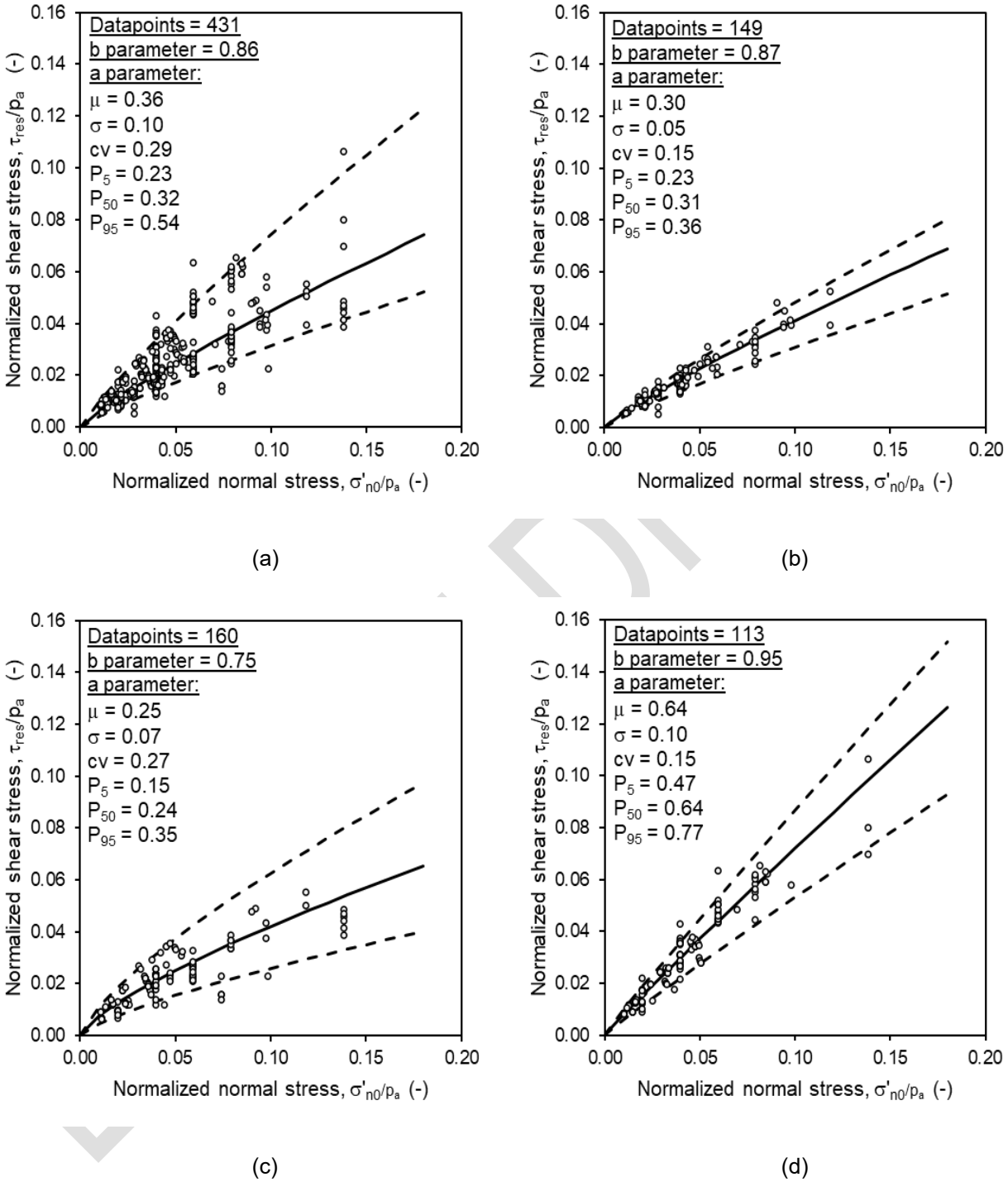

Figure 29 – Dataset C (high-plasticity, fine-grained, non-carbonate): normal stress trends of residual strength ratio for drained soils: (a) all surfaces (including nine unknown roughness values), (b) smooth surfaces, (c) intermediate surfaces, and (d) rough surfaces

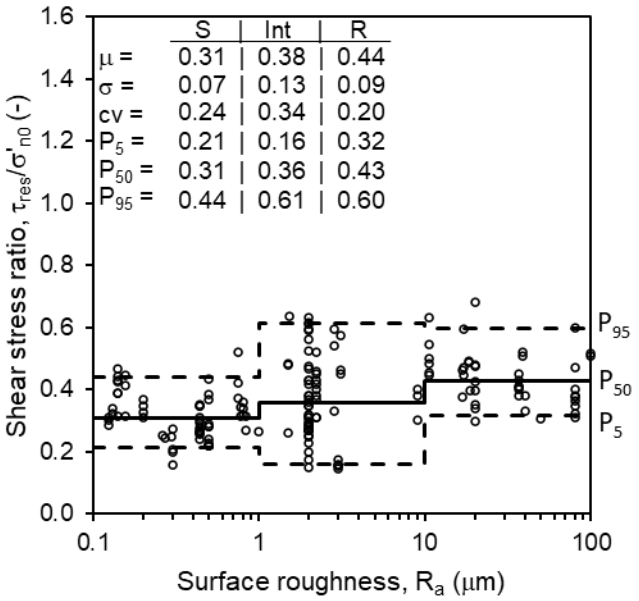

(a)

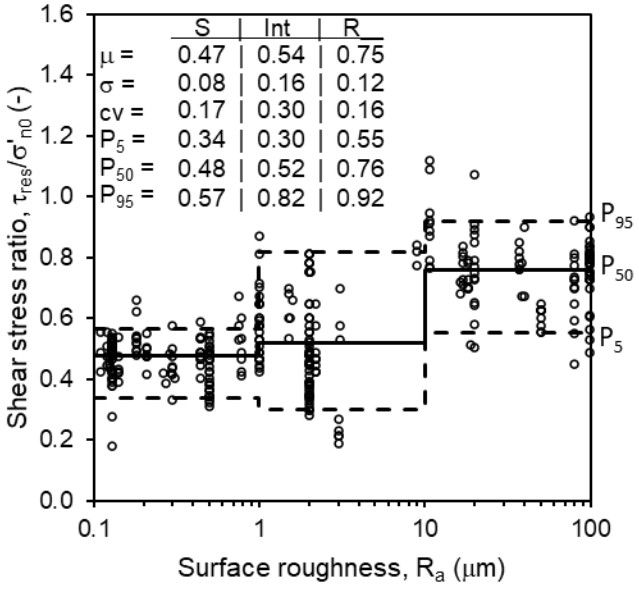

(b)

Figure 30 – Dataset C (high-plasticity, fine-grained, non-carbonate): surface roughness trends of residual strength ratio for (a) undrained, normally-consolidated soils and (b) drained soils: S = smooth surfaces, Int = intermediate surfaces, and R = rough surfaces

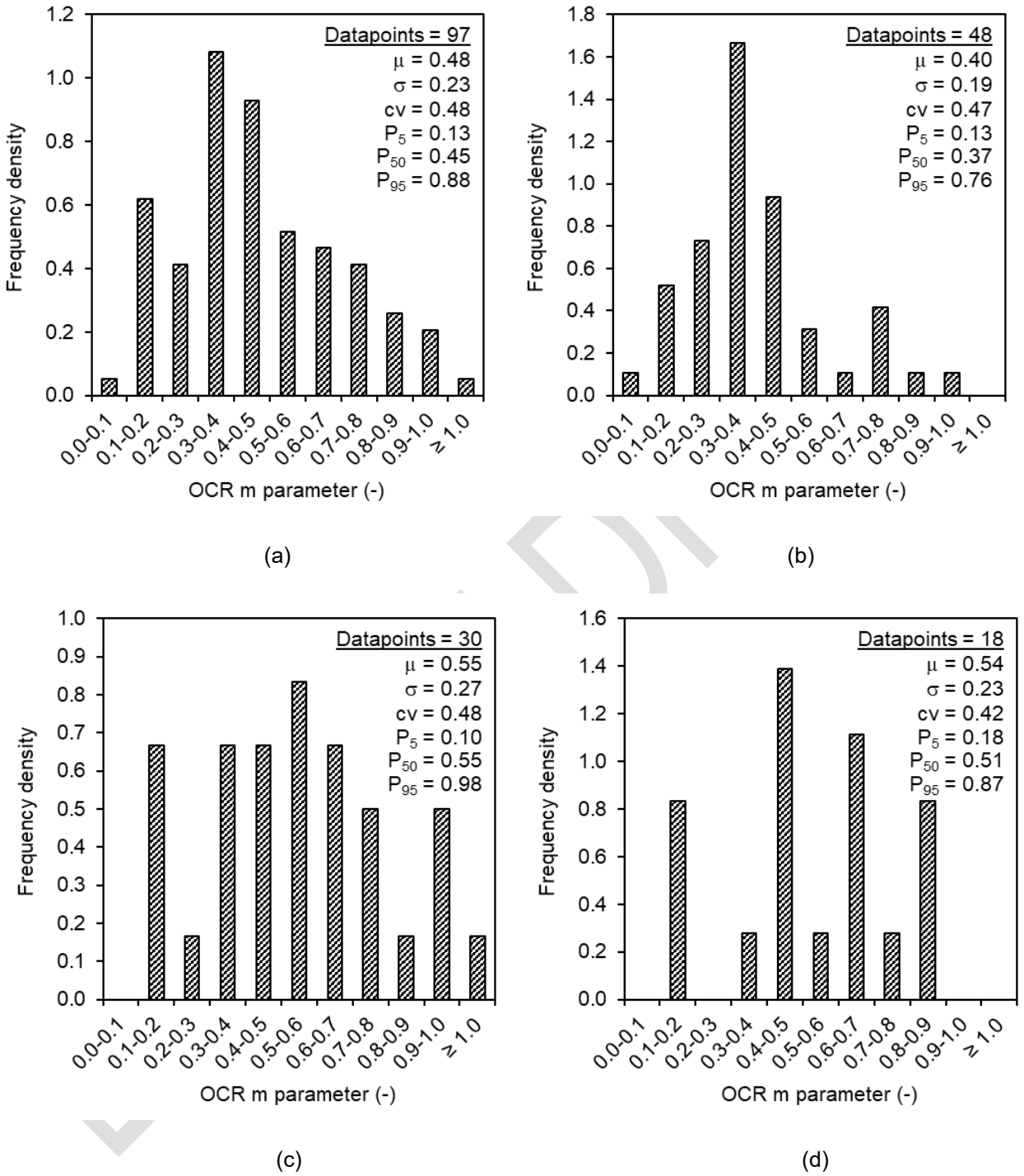

Figure 31 – Dataset C (high-plasticity, fine-grained, non-carbonate): distributions of overconsolidation 'm' parameter for undrained soils: (a) all surfaces, (b) smooth surfaces, (c) intermediate surfaces, and (d) rough surfaces

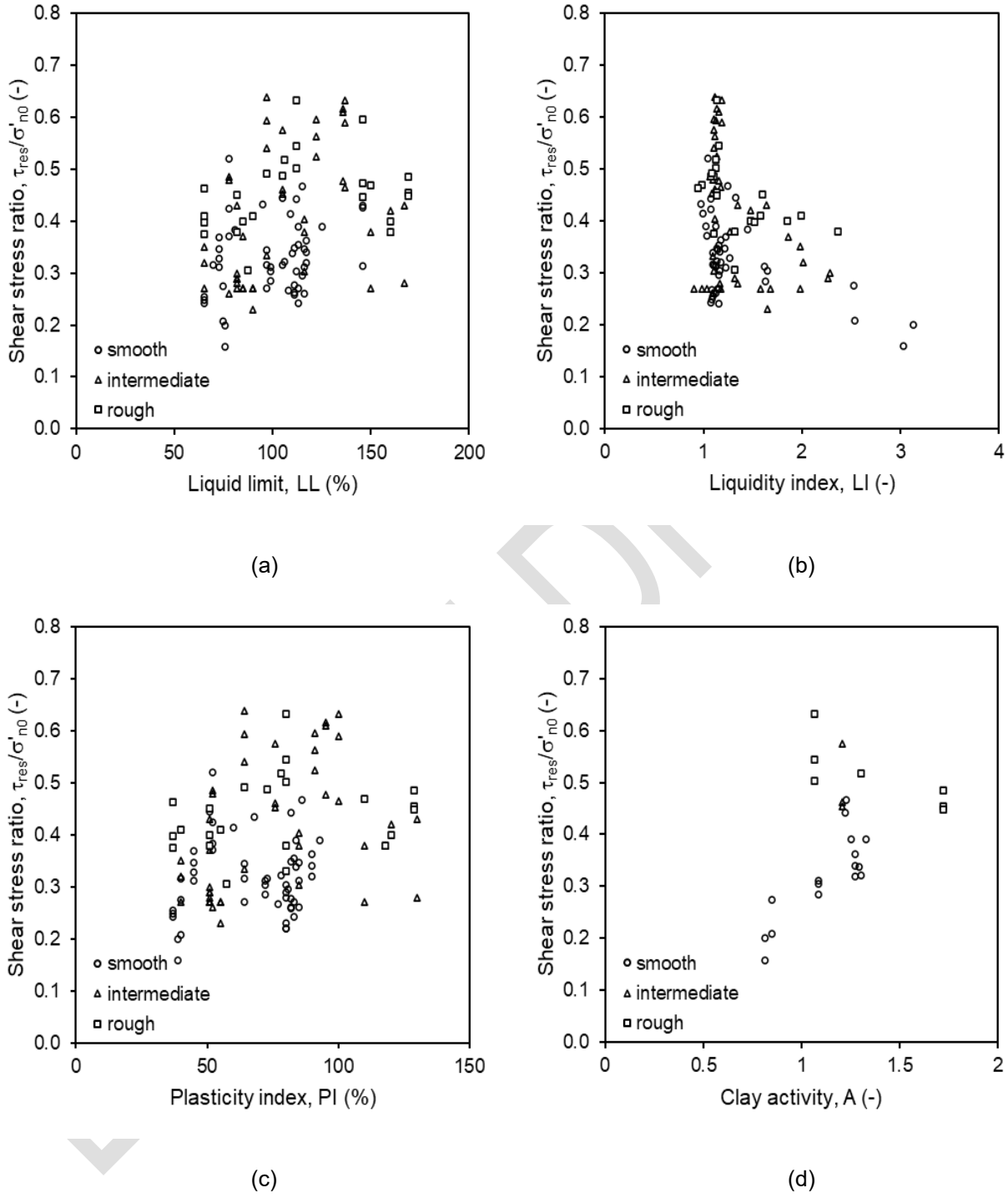

Figure 32 – Dataset C (high-plasticity, fine-grained, non-carbonate): effect of index properties on residual shear strength trends for undrained, normally-consolidated soils (all surfaces and normal stress values): (a) liquid limit, (b) liquidity index, (c) plasticity index, and (d) clay activity

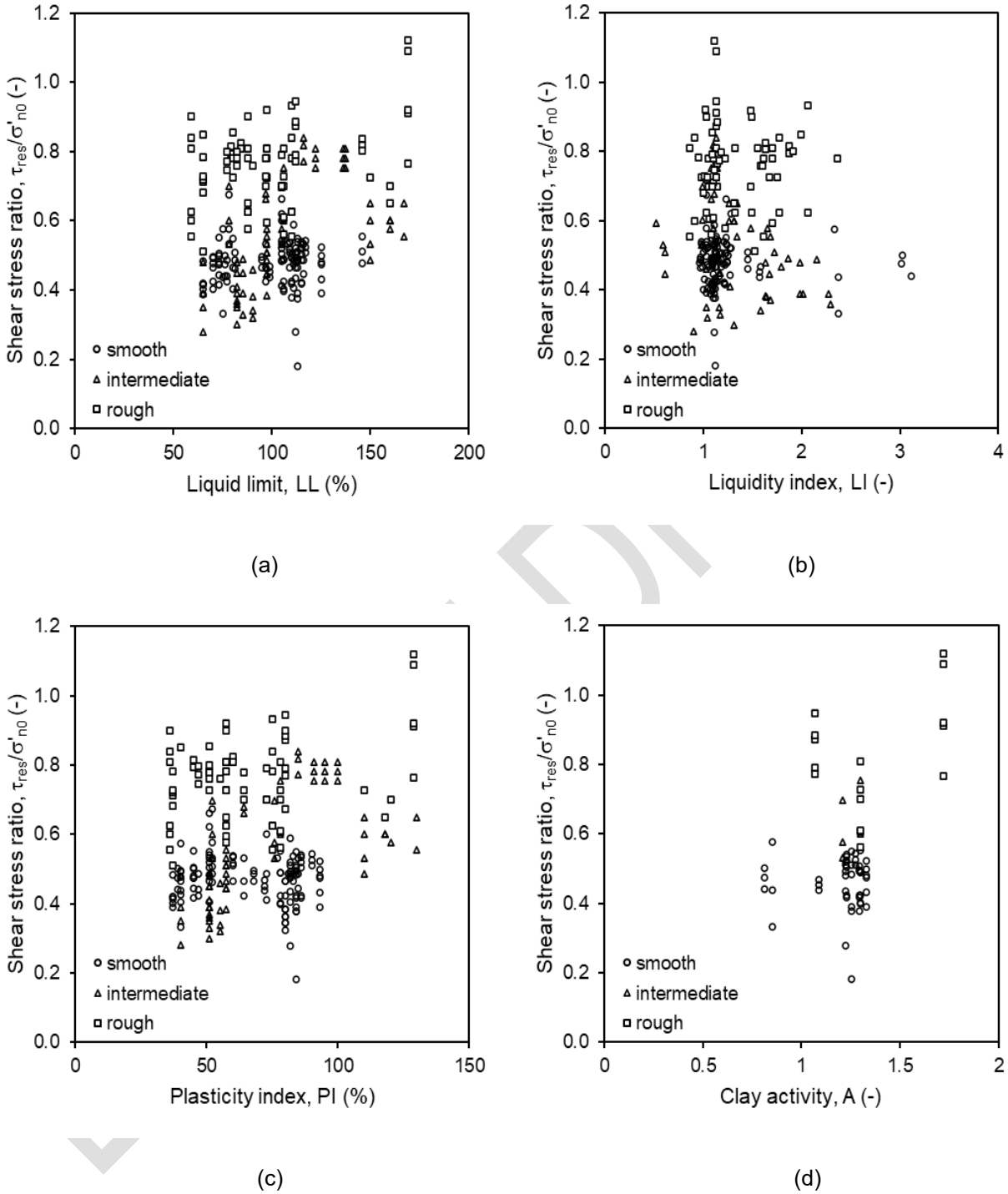

Figure 33 – Dataset C (high-plasticity, fine-grained, non-carbonate): effect of index properties on residual shear strength trends for drained soils (all surfaces and normal stress values): (a) liquid limit, (b) liquidity index, (c) plasticity index, and (d) clay activity

4.3.4 Dataset D

Results for Dataset D are presented in the following figures as noted in Table 4-8. A summary of statistics for Dataset D is presented in Table 4-9.

Table 4-8 – List of figures for Dataset D results

Plot description	Figure No.
Shear stress ratio histograms for undrained, normally-consolidated conditions	Figure 34
Shear stress ratio histograms for drained conditions (all OCR values)	Figure 35
Normal stress trends for undrained, normally-consolidated conditions	Figure 36
Normal stress trends for drained conditions (all OCR values)	Figure 37
Surface roughness trends for undrained, normally-consolidated conditions and drained conditions (all OCR values)	Figure 38
OCR m parameter histogram for all surfaces	Figure 39
Soil property trends for undrained, normally-consolidated conditions	Figure 40
Soil property trends for drained conditions (all OCR values)	Figure 41

Table 4-9 – Statistically-derived parameters for Dataset D: high-plasticity, fine-grained, non-carbonate data for plastic, sandpaper and concrete surfaces with $R_a \geq 0.2$ μm

Parameter		Und, all data	Und, smooth data	Und, interm data	Und, rough data	Und, NC data	Und, NC smooth data	Und, NC interm data	Und, NC rough data	Dr, all data	Dr, smooth data	Dr, interm data	Dr, rough data
	n	64	26	20	18	170	52	71	47	316	83	111	113
Shear stress ratio, τ_{res}/σ'_{n0}	μ	-	-	-	-	0.35	0.29	0.33	0.44	0.58	0.46	0.49	0.75
	σ	-	-	-	-	0.10	0.07	0.10	0.09	0.17	0.08	0.13	0.12
	cv	-	-	-	-	0.30	0.24	0.31	0.20	0.30	0.18	0.27	0.16
	P_5	-	-	-	-	0.20	0.21	0.16	0.32	0.34	0.33	0.29	0.55
	P_{50}	-	-	-	-	0.34	0.28	0.32	0.43	0.53	0.47	0.48	0.76
	P_{95}	-	-	-	-	0.52	0.40	0.48	0.60	0.87	0.58	0.71	0.92
Normal stress 'a' parameter	μ	-	-	-	-	0.25	0.17	0.23	0.30	0.32	0.29	0.20	0.64
	σ	-	-	-	-	0.07	0.04	0.07	0.05	0.09	0.05	0.04	0.10
	cv	-	-	-	-	0.29	0.22	0.30	0.18	0.29	0.16	0.22	0.15
	P_5	-	-	-	-	0.14	0.12	0.11	0.22	0.20	0.22	0.12	0.47
	P_{50}	-	-	-	-	0.24	0.16	0.23	0.30	0.29	0.29	0.21	0.64
	P_{95}	-	-	-	-	0.38	0.26	0.34	0.38	0.49	0.36	0.27	0.77
Normal stress 'b' parameter	b	-	-	-	-	0.89	0.83	0.88	0.88	0.82	0.86	0.72	0.95
OCR 'm' parameter	μ	0.48	0.45	0.47	0.54	-	-	-	-	-	-	-	-
	σ	0.22	0.21	0.23	0.23	-	-	-	-	-	-	-	-
	cv	0.46	0.47	0.50	0.42	-	-	-	-	-	-	-	-
	P_5	0.13	0.14	0.11	0.18	-	-	-	-	-	-	-	-
	P_{50}	0.48	0.40	0.47	0.51	-	-	-	-	-	-	-	-
	P_{95}	0.86	0.82	0.81	0.87	-	-	-	-	-	-	-	-

Notes: n = number of data points; cv = coefficient of variation; Und = undrained (fast shearing rate); Dr = drained (slow shearing rate)

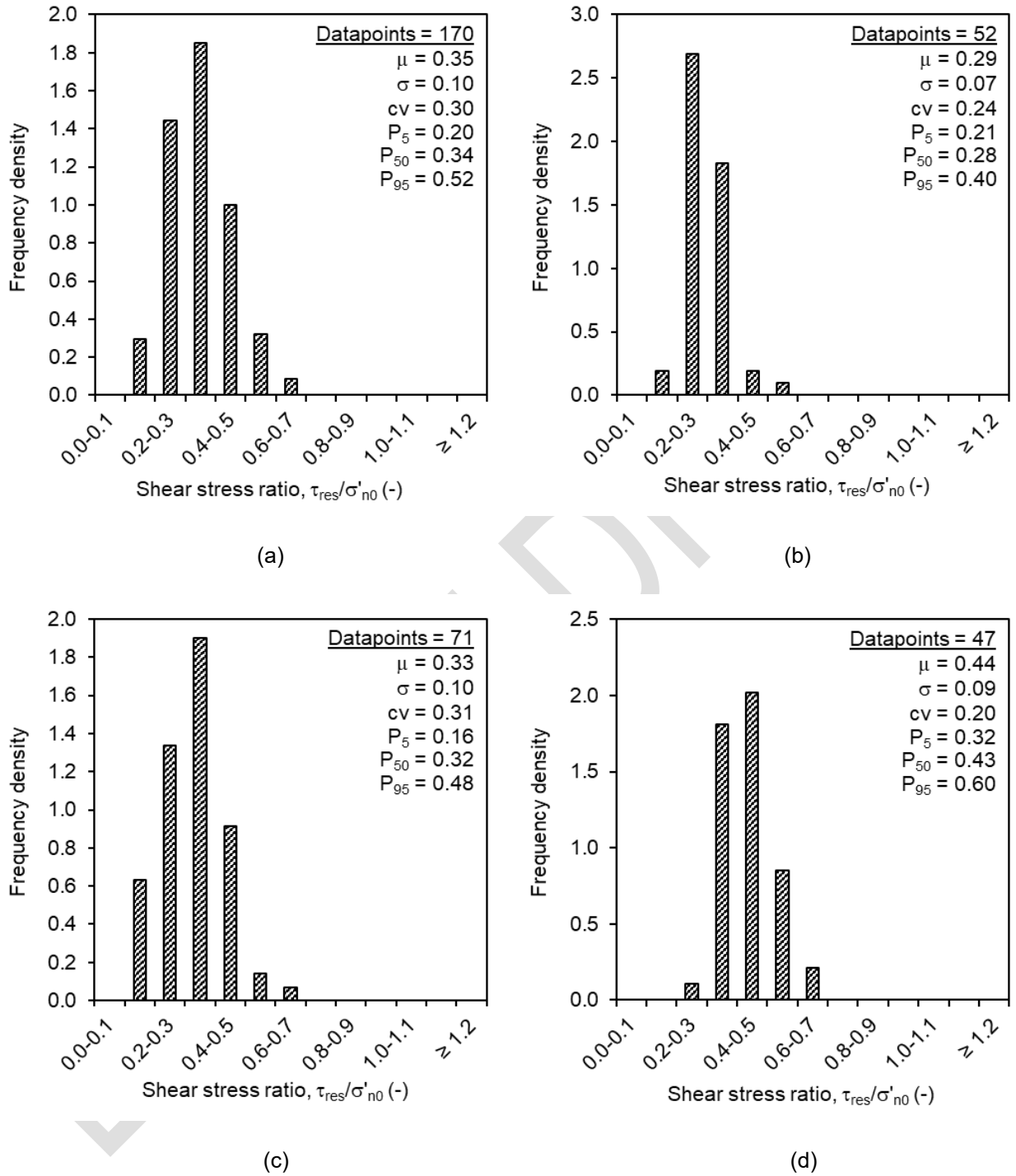

Figure 34 – Dataset D (high-plasticity, fine-grained, non-carbonate, excluding bare steel and surfaces with R_a < 0.2 μm): distributions of residual strength ratio for undrained normally-consolidated soils: (a) all surfaces, (b) smooth surfaces, (c) intermediate surfaces, and (d) rough surfaces

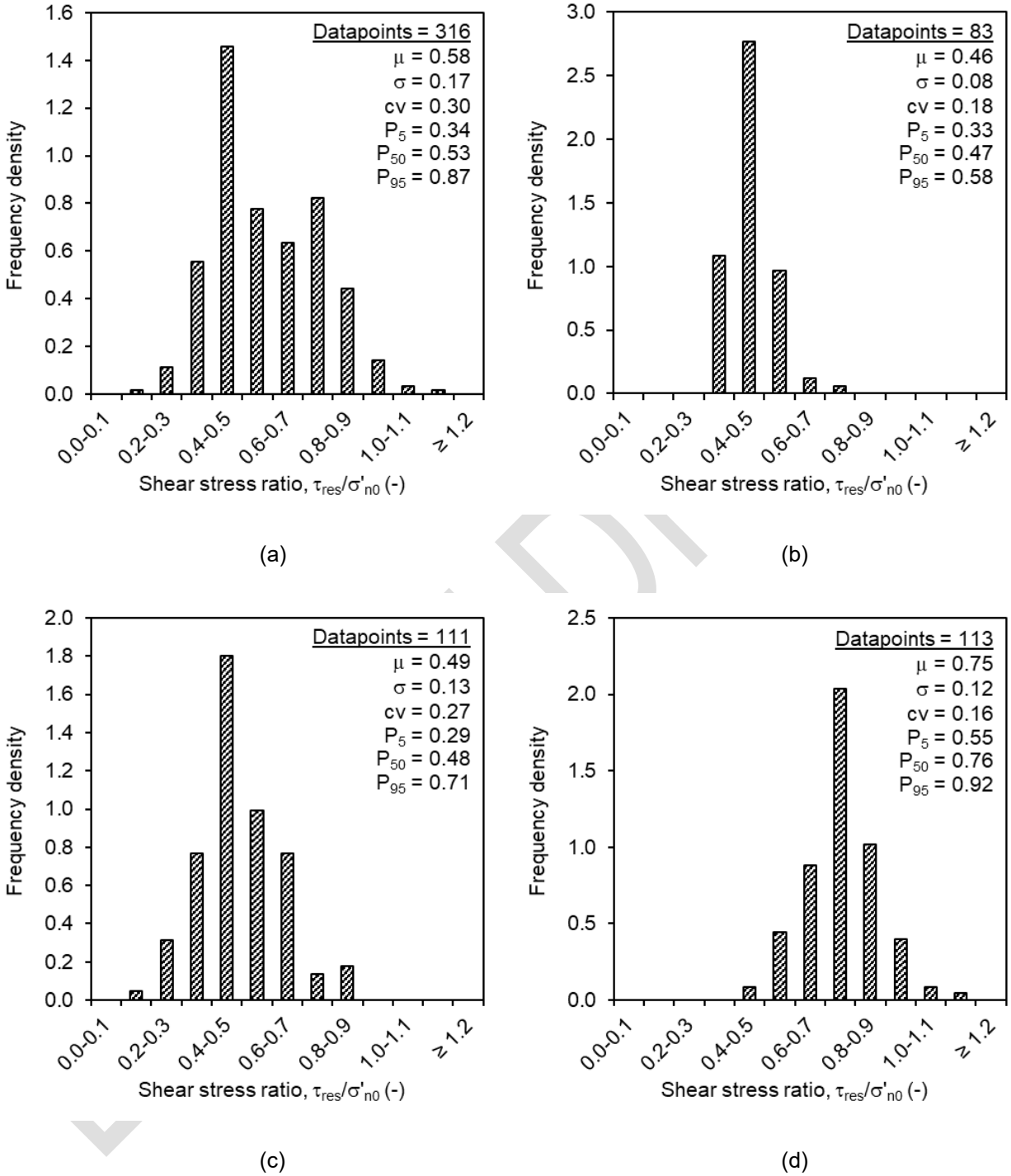

Figure 35 – Dataset D (high-plasticity, fine-grained, non-carbonate, excluding bare steel and surfaces with R_a < 0.2 μm): distributions of residual strength ratio for drained soils: (a) all surfaces (including nine unknown roughness values), (b) smooth surfaces, (c) intermediate surfaces, and (d) rough surfaces

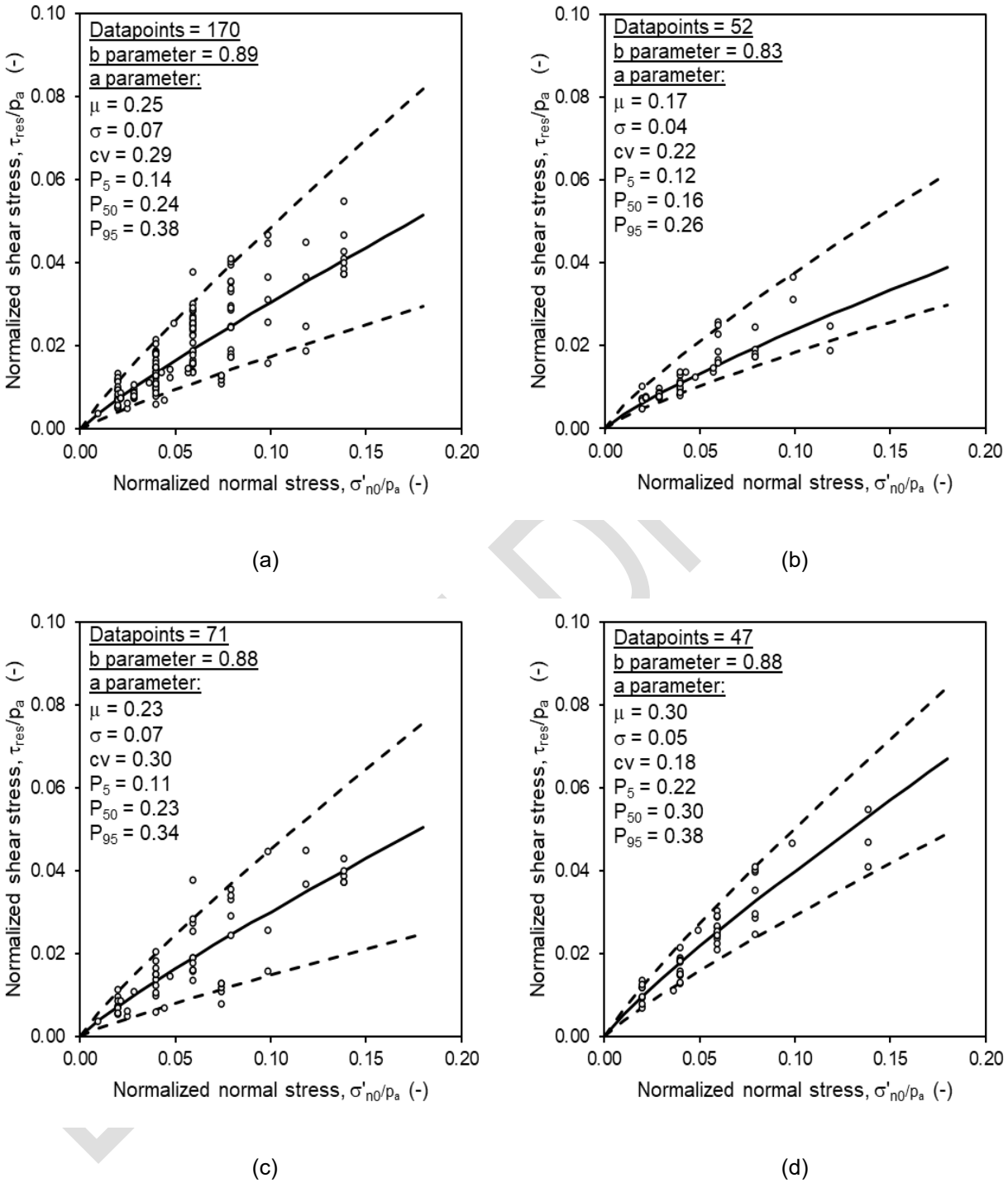

Figure 36 – Dataset D (high-plasticity, fine-grained, non-carbonate, excluding bare steel and surfaces with R_a < 0.2 μm): normal stress trends of residual strength ratio for undrained normally-consolidated soils: (a) all surfaces, (b) smooth surfaces, (c) intermediate surfaces, and (d) rough surfaces

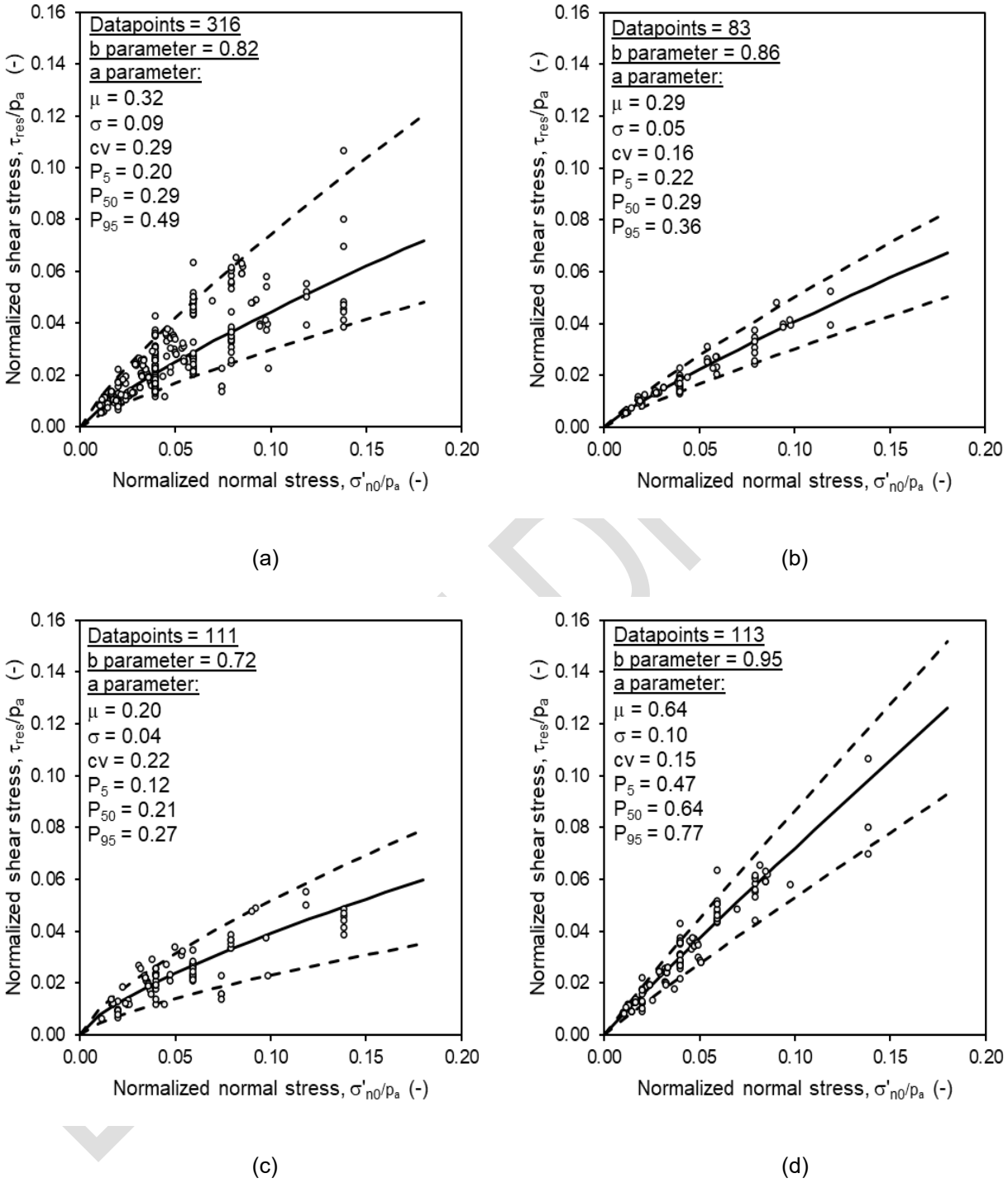

Figure 37 – Dataset D (high-plasticity, fine-grained, non-carbonate, excluding bare steel and surfaces with R_a < 0.2 μm): normal stress trends of residual strength ratio for drained soils: (a) all surfaces (including nine unknown roughness values), (b) smooth surfaces, (c) intermediate surfaces, and (d) rough surfaces

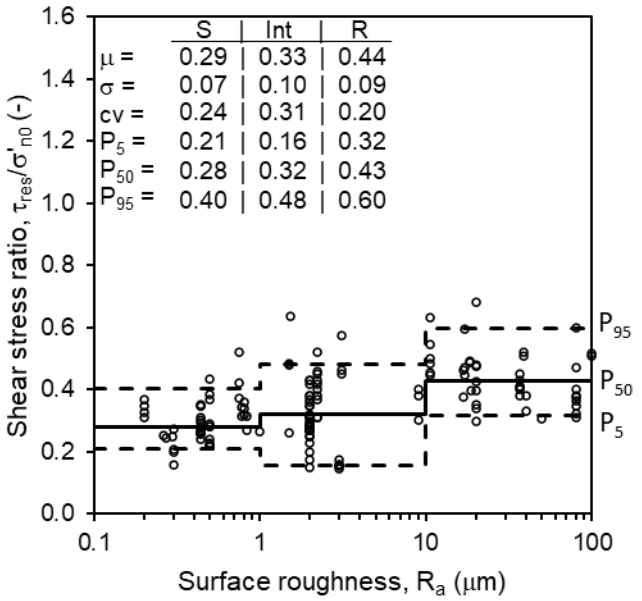

(a)

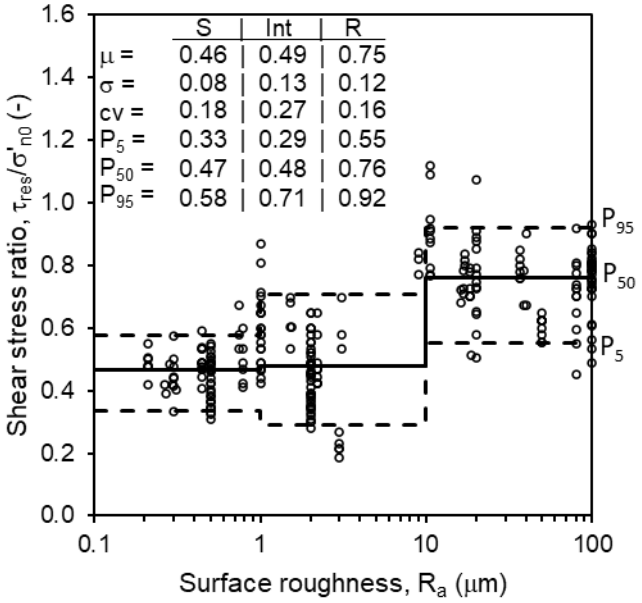

(b)

Figure 38 – Dataset D (high-plasticity, fine-grained, non-carbonate, excluding bare steel and surfaces with R_a < 0.2 μm): surface roughness trends of residual strength ratio for (a) undrained, normally-consolidated soils and (b) drained soils: S = smooth surfaces, Int = intermediate surfaces, and R = rough surfaces

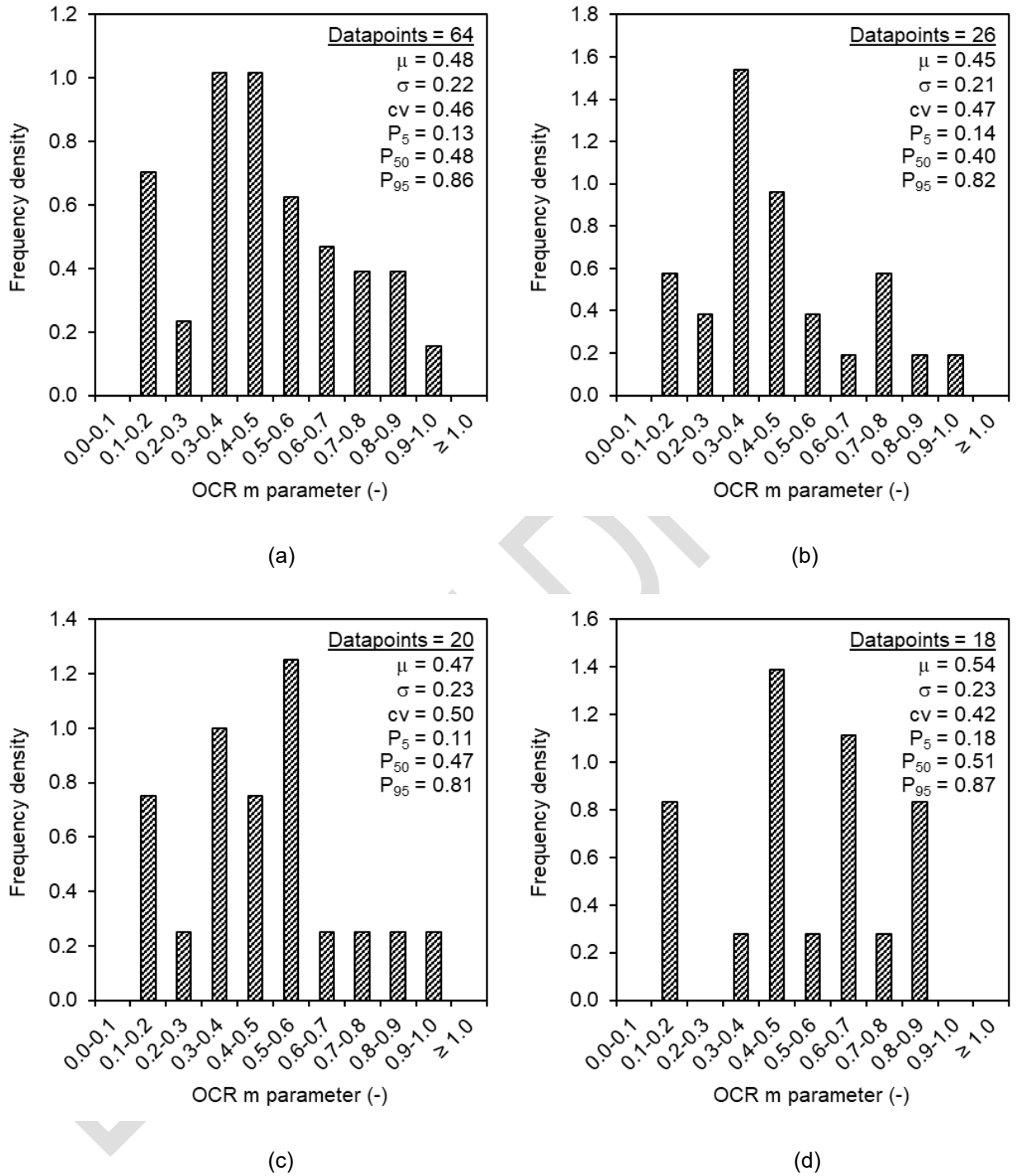

Figure 39 – Dataset D (high-plasticity, fine-grained, non-carbonate, excluding bare steel and surfaces with R_a < 0.2 μm): distributions of overconsolidation 'm' parameter for undrained soils: (a) all surfaces, (b) smooth surfaces, (c) intermediate surfaces, and (d) rough surfaces

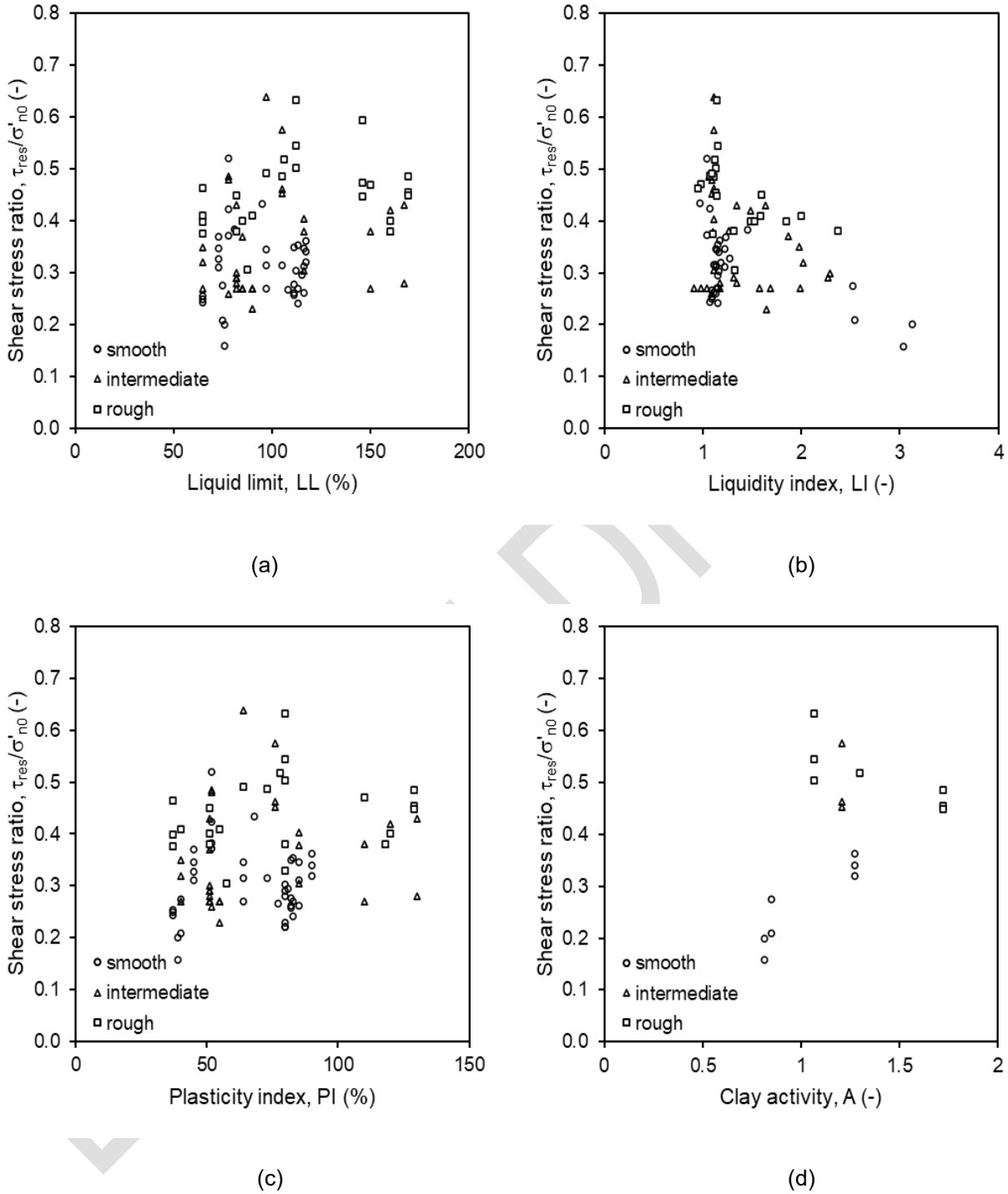

Figure 40 – Dataset D (high-plasticity, fine-grained, non-carbonate, excluding bare steel and surfaces with R_a < 0.2 μm): effect of index properties on residual shear strength trends for undrained, normally-consolidated soils (all surfaces and normal stress values): (a) liquid limit, (b) liquidity index, (c) plasticity index, and (d) clay activity

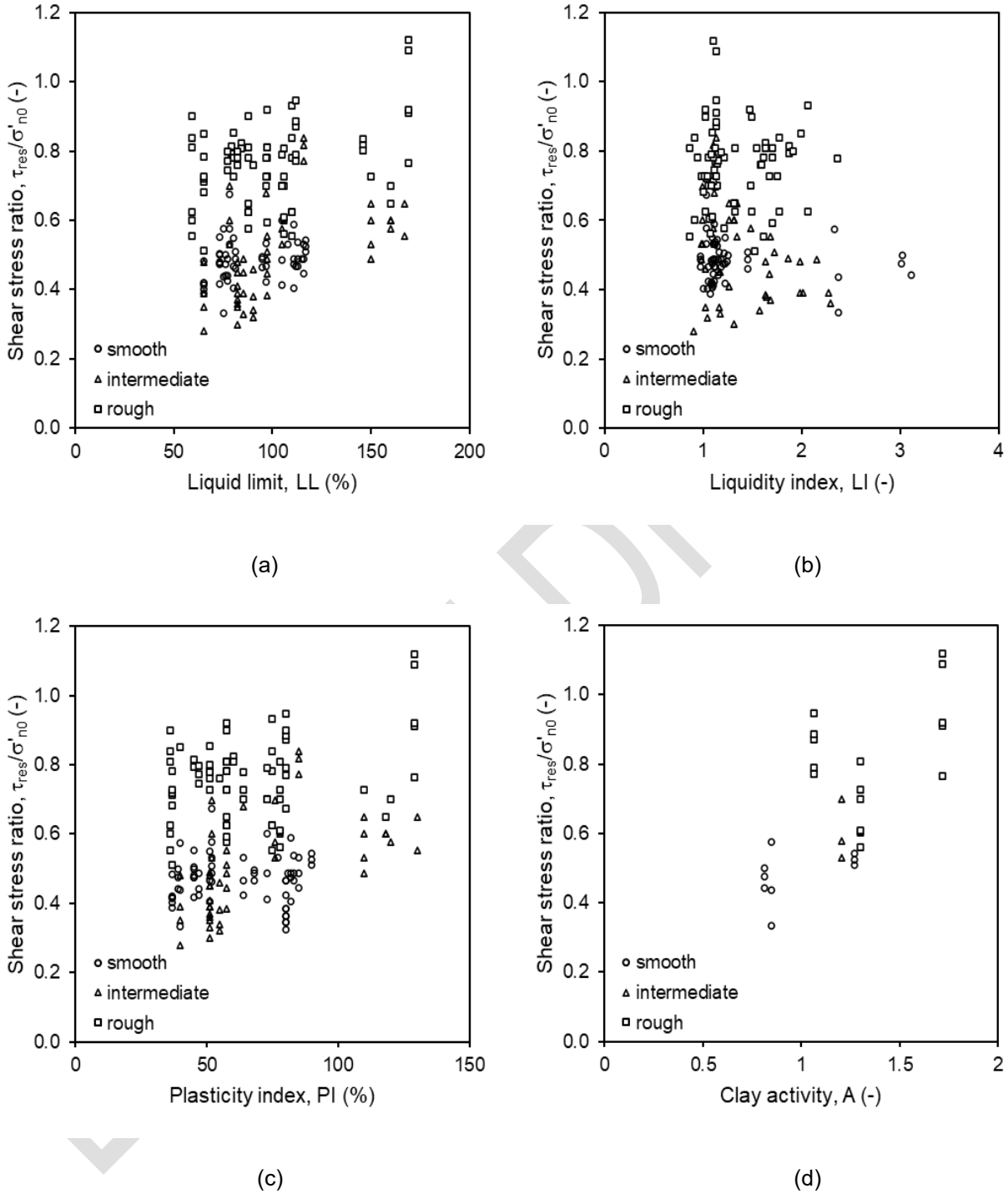

Figure 41 – Dataset D (high-plasticity, fine-grained, non-carbonate, excluding bare steel and surfaces with R_a < 0.2 μm): effect of index properties on residual shear strength trends for drained soils (all surfaces and normal stress values): (a) liquid limit, (b) liquidity index, (c) plasticity index, and (d) clay activity

4.4 Supplementary figures

This section presents effects of testing device, testing facility, and testing procedures to support explanation of underlying trends in the data and development of guidance for test planning, execution, and interpretation. Dataset D was used for these comparisons.

4.4.1 Effect of testing device

While several types of modified direct shear box and interface shear devices were utilized in the database, it is useful to compare the overall results from the range of the ISB devices against tilt table test results. Tilt table testing is generally considered to mobilize fully drained conditions, so it useful as drainage check against ISB tests performed at slow shearing rates. This is illustrated using the shear stress ratio histogram presented in Figure 42a, and the shear stress ratio versus surface roughness presented in Figure 42b. The tilt table tests (black columns) produce a 17% higher drained mean shear stress ratio compared to slow ISB tests (patterned columns), as well as a lower coefficient of variation despite the lower number of tests. This can also be observed when examining shear stress ratio versus surface roughness, though not as explicitly due to the large number of datapoints somewhat masking the differences. The lower ISB stress ratios are likely caused by less than complete excess pore pressure dissipation.

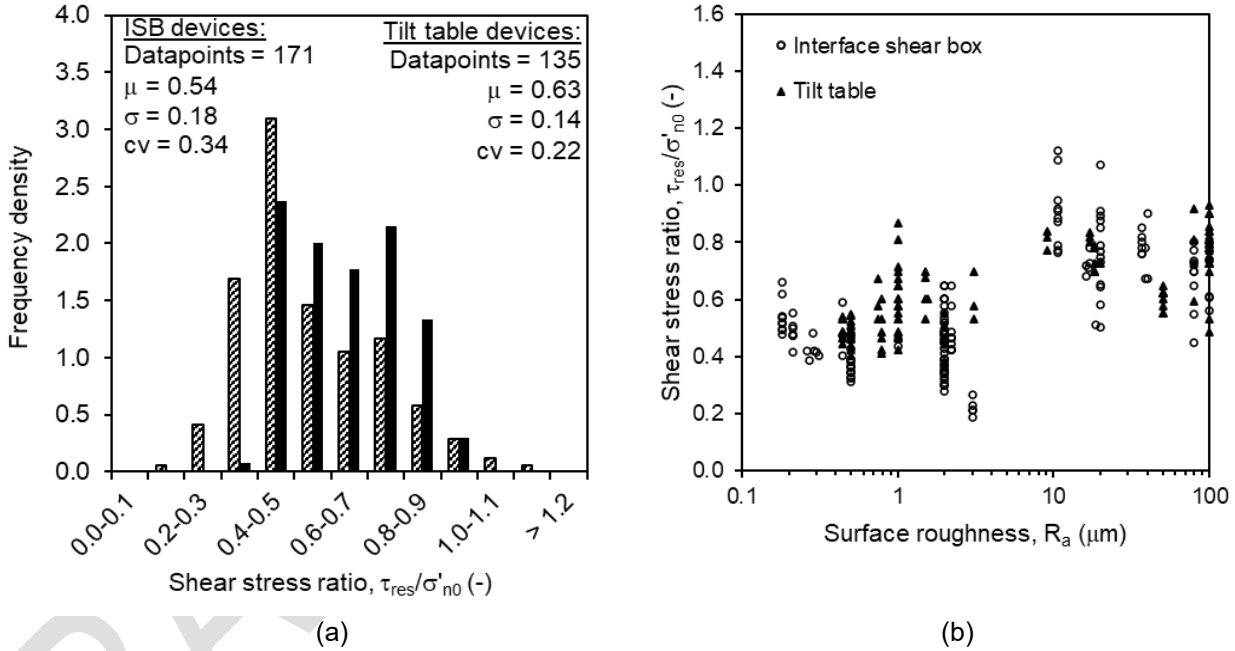

(a) (b)

Figure 42 – Dataset D (high plasticity, fine-grained, non-carbonate, excluding steel surfaces and surfaces with $R_a < 0.2$ μm): effect of device type on drained strength ratio showing (a) distribution for all surfaces and normal stress values and (b) surface roughness effect for all normal stress values

4.4.2 Effect of laboratory contractor

The bulk of testing was performed by two contractors. A comparison of results between the two contractors is presented in Figure 43, showing histograms of OCR *m* parameter values for all surfaces tested (Figure 43a)

and trends of OCR *m* versus surface roughness (Figure 43b). The OCR *m* parameter was selected for comparison as the method of interpretation of *m* requires selecting the residual shear resistance from either cycle 1 or 2 from a cyclic test where OCR > 1, or from a monotonic test. Therefore, the *m* parameter comparison captures multiple epistemic uncertainties between the two contractors, including the contractors' own intra-laboratory differences, technician influence, equipment influence, and data interpretation differences. As shown, Contractor B (black columns) produces a 22% higher mean stress ratio compared to Contractor A (patterned columns) despite similar cv values. Given the limited number of datapoints it is difficult to draw any conclusions from this.

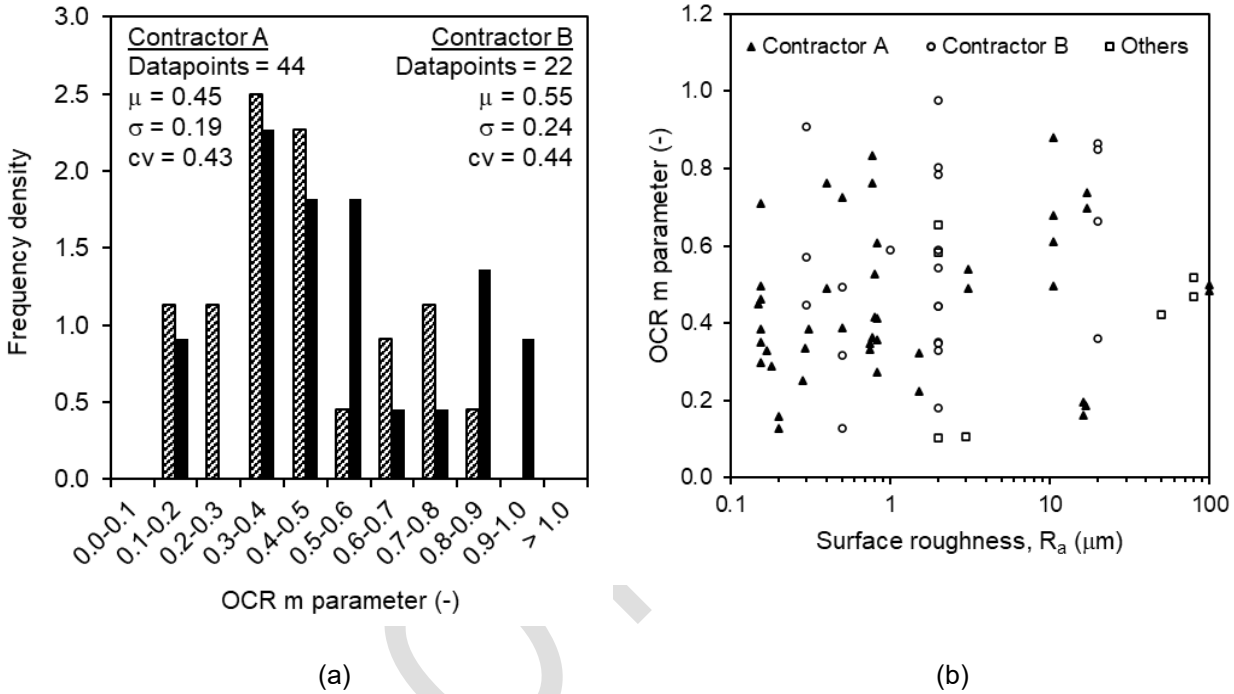

(a) (b)

Figure 43 – Dataset D (high plasticity, fine-grained, non-carbonate, excluding steel surfaces and surfaces with R_a < 0.2 μm): contractor influence on overconsolidation 'm' parameter showing (a) distribution for all surfaces and normal stress values and (b) versus surface roughness for all normal stress values

4.4.3 Effect of testing procedure

As discussed in Section 4.1, the test procedure of ISB tests can have an influence on the selected residual shear strength, specifically whether monotonic tests are performed that limit the amount of shearing displacement or cyclic tests are performed, which allow continued strain accumulation resulting in a lower undrained residual strength (even in the presence of episodic consolidation periods during testing). This is evident in the overall database trends, illustrated in the normally-consolidated undrained shear stress ratio histogram of Figure 44a and the normally-consolidated undrained shear stress ratio versus surface roughness of Figure 44b. Monotonic tests (patterned columns) produce a ~25% higher mean stress ratio than cyclic tests (black columns), with a relatively low coefficient of variation despite 27 tests performed monotonically. In this comparison, both Type A (18 cycles of fast shear) and Type B (2 cycles of fast shear) are included; however, comparing the statistical data shown on Figure 44a it is clear that there is no significant difference between Type A and Type B in terms of the mean undrained shear stress ratio.

For drained conditions, the trends are opposite (Figure 45a), with monotonic tests showing a lower mean strength ratio than cyclic tests. However, the number of monotonic tests is quite limited and concentrated around very low to low surface roughness values (Figure 45b), which may explain the lower mean value. There is a significant difference between the Type A and Type B cyclic tests, with Type A showing 25% higher mean stress ratio than Type B. This could be due to soil becoming trapped between the shear ring and the surface, but could also be due to greater dissipation of excess pore pressure during fast cycles, creating a stronger shear zone at the interface.

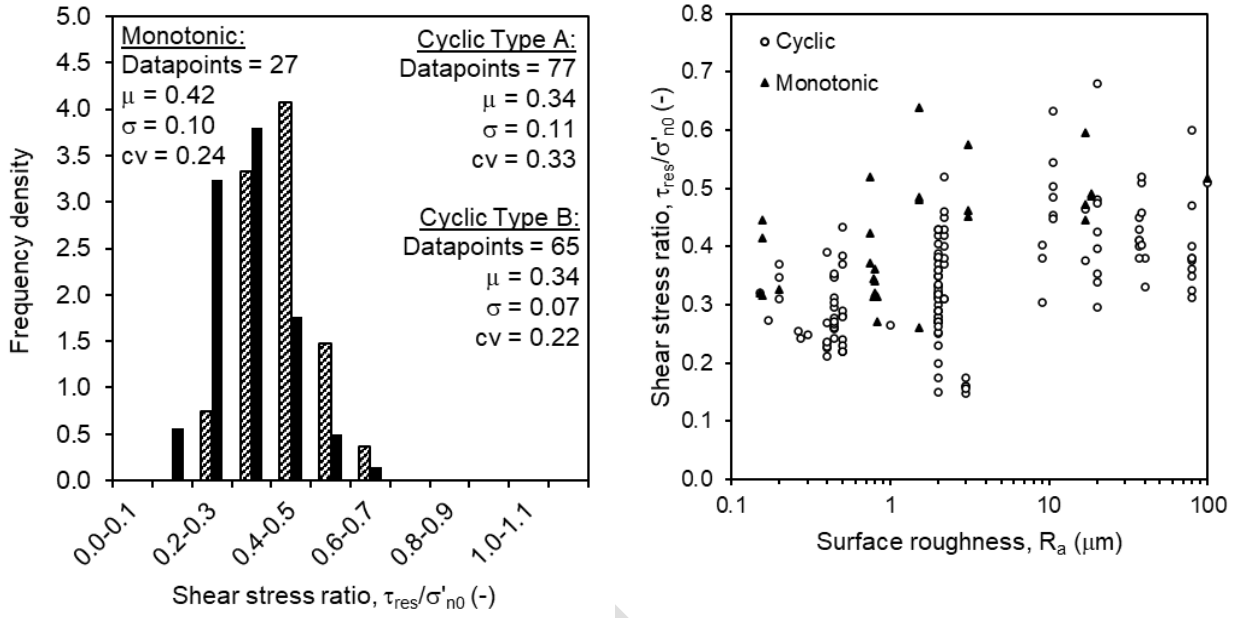

(a) (b)

Figure 44 – Dataset D (high plasticity, fine-grained, non-carbonate, excluding steel surfaces and surfaces with R_a < 0.2 μm): effect of shearing procedure on undrained, normally-consolidated strength ratio showing (a) distribution for all surfaces and normal stress values and (b) versus surface roughness for all normal stress values

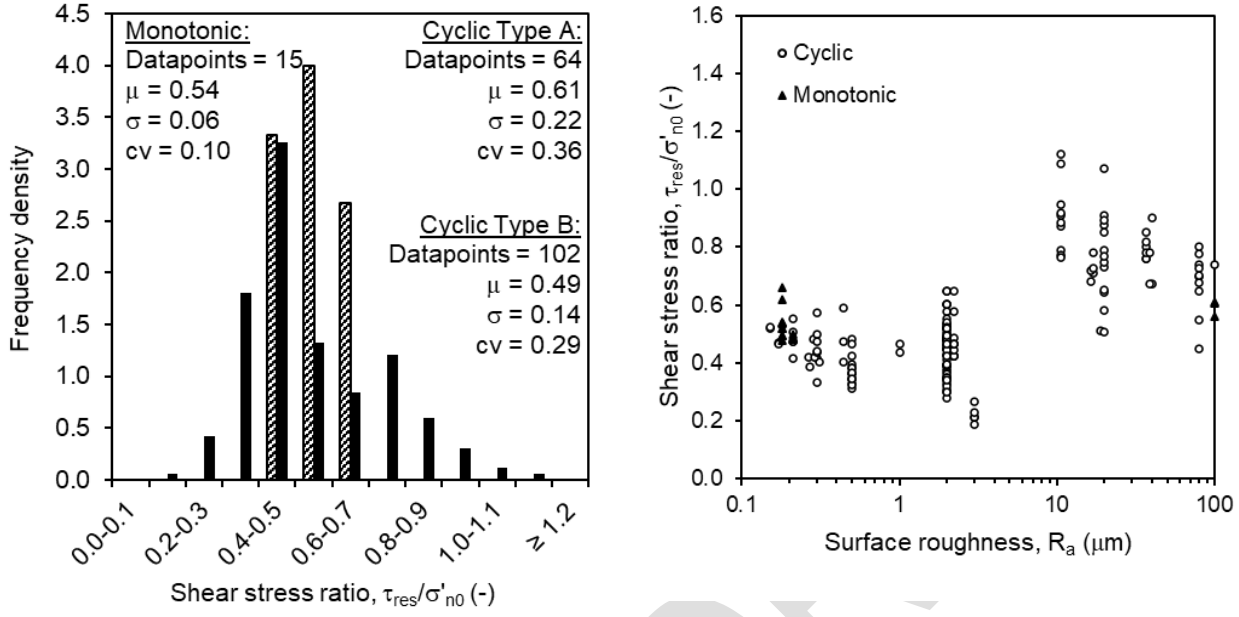

(a) (b)

Figure 45 – Dataset D (high plasticity, fine-grained, non-carbonate, excluding steel surfaces and surfaces with R_a < 0.2 μm): effect of shearing procedure on drained strength ratio showing (a) distribution for all surfaces and normal stress values and (b) versus surface roughness for all normal stress values

4.5 Limitations

No reinterpretation of project-specific datasets has been performed during this study due to a lack of access to detailed records of all tests. A reinterpretation of all test data using the cumulative knowledge gained over the past two decades may allow for further refinements in model parameter ranges.

As noted by several researchers, there are several limitations to shear testing using modified direct shear or interface shear devices, including lack of direct measurement of principal stresses, uncertain impact of boundary effects, and uncontrolled volume changes due to soil loss through the gap between the shear rings or shear ring and interface plate (e.g. Potts 1987).

Additional challenges with low normal stress interface testing have been encountered which may contribute to scatter within the database results, as described below:

- **Overconsolidated residual undrained strength mobilization**: The selection of residual undrained shear strength for an overconsolidated specimen requires judgement and consideration of the design application. Following mobilization of the peak resistance, the specimen will begin to swell due to development of negative excess pore pressures during shearing and availability of free water. This can result in rapid reductions in shear resistance, and inconsistencies as to where to select a representative residual value. For cyclic tests with short displacement limits (e.g. 5 mm), the cumulative shear displacement at (still) overconsolidated conditions during cycle 2 may be similar to a monotonic test with a relatively long travel limit, e.g. 25 mm. For cyclic tests with long displacement limits, the

cumulative shear displacement may be significantly larger than short displacement cyclic tests or monotonic tests. Care is recommended when selecting the overconsolidated residual resistance to ensure it is consistent with the intended design application and noted in the project reporting. For example, when performing axial anchor load checks, a high estimate axial resistance will increase the anchor load. When performing lateral buckling and pipeline expansion checks, a low estimate axial resistance will increase the pipeline expansion and buckle feed-in.

- **Normally-consolidated residual undrained strength mobilization**: The displacement required to mobilize true residual strength can require multiple cycles allowing for accumulation of shear displacement similar to ring shear testing, i.e. several hundred millimeters. For monotonic tests and cyclic Type B tests (i.e. N = 2 fast cycles) within the database, the minimum (true) residual resistance may be lower than reported values. While comparisons within Dataset D showed lower undrained residual strength for cyclic tests (see Section 4.4.3), comparisons using the same soil and test input conditions have not been performed for any of the projects within the database. Note that the majority of cyclic tests included 30-minute consolidation periods between pairs of fast shearing cycles, thus allowing the soil strength to recover through consolidation and thereby potentially prohibiting measurement of true residual strength, since some recovery occurs during each consolidation period.

- **Machine friction corrections**: Machine friction has long been a key challenge with direct and interface shear tests, and it becomes critical when performing tests at low normal stress when the machine friction itself can comprise a significant portion of the total measured resistance (e.g. up to values around 20 to 30% for tests performed at 2 kPa). Several of the devices used in the database have been modified to minimize machine friction. In each test (or each test program for a given interface surface), machine friction was measured using an empty shear box/ring and was then subtracted from the interpreted residual shear strength. However, additional machine friction can develop from down drag effects due to friction between the soil and sidewalls of the shear box/ring, as well as from the additional shear resistance from soil escaping the box/ring and the interface surface. Use of Telfon or silicon grease-coated side walls, thin walls, and avoidance of initial gapping between the box/ring and interface surface have been employed to minimize these effects, yet they are challenging to measure and difficult to account for in the corrections. Some of the reported resistance values may be higher than the true soil-interface (or soil-soil) shear strength due to added friction that could not be measured using standard test procedures.

- **Surface roughness measurements**: Due to limitations with profilometers used to measure surface roughness, many of the roughest surfaces tested are reported with a nominal R_a = 80 μm, which represents the maximum value measured by the profilometer used. Some of these surfaces may have higher R_a values; however, given the database is limited to fine-grained soils this has limited effect on the interpreted statistical values and model fits, since 80 μm is well within the 'fully rough' range of surface roughness. Similarly, soil-soil tests are assigned a roughness of R_a = 99 μm for plotting purposes, even though the actual 'roughness' is undefined and linked to the particle size distribution within the shear zone. Some of the reported roughness values have been assumed based on visual estimates (< 1% of the overall database). Furthermore, some roughness values may have evolved during testing due to abrasion from soil particles.

- **Combining effects of normal stress, roughness, and stress history for design:** Division of the datasets have been selected to aid the designer for categorical conditions, i.e. undrained versus drained and smooth versus intermediate versus rough surfaces. It is left to the designer to select which datasets are most applicable to their project and pipeline conditions, and which input values hold greater confidence. For example, if the roughness of the pipeline coating is unknown, then application of the normal stress statistical dataset, or the normal stress model (including stress history effects for undrained resistance) would be more appropriate. Conversely, the roughness statistical datasets would

be more appropriate for cases where the pipeline coating surface roughness is relatively certain (or at least planned to be smooth, intermediate, or rough) and the pipeline embedment (and therefore the normal stress) is unknown. In cases where both the normal stress and roughness is relatively certain, the normal stress model subsets may be used to narrow the design range of shear strength.

5 Guidance for test planning, execution, and interpretation

This section provides guidance for test planning, execution, and interpretation. Suggestions are also included on capturing uncertainty for derivation of design ranges in shear resistance for use in axial PSI analysis.

5.1 Site investigation

5.1.1 Seabed sampling method

Box coring provides a rapid method for obtaining surficial soils that does not require a drilling system or actuated seabed frame. Thus, box cores can be deployed from a geophysical survey vessel or from a vessel of opportunity. Box cores also allow for accurate visual inspection and logging of surficial soils and can be sub-sampled to gather intact material for subsequent laboratory testing. Piston cores can also be appropriate but do not generate large volumes of soil if required for model testing.

5.1.2 Supplementary laboratory testing

Supplementary laboratory testing to support interface shear test interpretation is recommended to include water content, unit weight, particle size distribution, and Atterberg limits tests. Specific gravity can also be helpful when testing in frontier regions or in unique soils such as fecal pellets (low specific gravity) or glauconitic particles (high specific gravity), as well as mineralogical tests. Particle size distribution tests include hydrometers extending through the standard (ASTM D7928) 24-hour reading to obtain the clay fraction (2 μm). For soils with significant colloidal content, other methods may be needed to obtain D_{50} for use in calculating clay activity.

5.2 Specimen preparation

5.2.1 Sample selection

For sites with similar surface soil conditions along a pipeline route, it may be appropriate to assign several soil cores to a single soil zone and combine these cores to create a single batch sample. The batch sample approach, versus performing sets of tests on sub-samples from individual cores, reduces the number of tests to be performed. It also aids the parameter fitting process since minor differences between individual core properties do not add to scatter within the data (see further discussion in Section 5.5.3). This averaging of soil conditions is generally acceptable since small local variations in axial shear resistance along the pipeline are averaged out during the build-up of effective force during heating and pressurization.

For sites where a surficial layer of slurry, biogenic material, sand or shells is present at the mudline, separate test sets on each soil layer may be warranted, particularly if the expected pipe embedment range extends into both layers. Different mixtures of each layer can be used to assess the influence of the mixture proportions that may result from the pipelaying process. This can be important for axial resistance since the coarse fraction can dominate the frictional response of the clay mixture, increasing shear strength. Conversely, a low permeability slurry or biogenic layer can govern the drainage characteristics of the clay mixture, delaying consolidation.

5.2.2 Specimen preparation

Due to the pipelaying process, surface soils are remolded from the cyclic motion of the pipeline, driven by the sea state (Westgate et al. 2010). Water entrainment is also possible, further reducing the soil strength (e.g. Sahdi et al. 2020). Because of this, performing interface shear tests on intact soil is generally not necessary. Instead, individual (or batch) samples are initially remolded to a (salt) water content value at or slightly (e.g. 10%) higher than the liquid limit. Care is needed here since the liquid limit depends on the pore water salt

concentration and the ASTM liquid limit is measured using distilled water. The objective is to simulate the effects of the pipelaying process (i.e. remolding the soil through mechanical means and water entrainment) and to prepare a homogeneous, reconstituted specimen within the shear box/ring for testing. Another advantage of reconstituting the soil samples for testing is that the (induced) OCR is known, since the normal stress during consolidation and shearing are specified test inputs.

5.3 Development of laboratory test program

5.3.1 Normal stress selection

The test program is recommended to include normal stresses that cover the full range of empty through flooded pipeline submerged bearing pressures (W′/D), including wedging effects where appropriate. As observed for the test database, the tests have been performed using a normal stress range of 1 to 18 kPa, which is sufficient for nearly all types of subsea pipelines. A wide range of normal stress helps to capture the stress effect curvature associated with the power law fitting parameters *a* and *b*. A minimum of three normal stress values is needed to capture the curvature of the stress effect.

5.3.2 Consolidation stress selection

Due to the very soft nature of saturated, remolded clay, it may be necessary to first consolidate the sample in a consolidometer (outside of the shear box/ring) under an initially low stress level to create a workable sample, e.g. half of the target normal stress level for the test. After the sample is transferred into the shear box/ring, it is useful to monitor the sample settlement during consolidation phase, which may be performed in multiple increments of stress. The settlement response can provide an estimate of the coefficient of consolidation of the soil, which is useful in various aspects of PSI analysis.

It is important for accurate shear strength assessment to capture the preloading effect from changes in pipe weight through the pre-commissioning phase. For some projects, particularly in regions where oil (rather than gas) is produced, the difference between the flooded and operating pipeline weights is minimal, e.g. induced OCR values less than 1.1. For such low values of mobilized OCR, the uncertainty in the *m* parameter may have no practical effect on the undrained shear resistance, and OCR does not affect drained residual shear strength.

For light oil, gas, or thin-walled lines, the OCR effect can be important, and for gas lines the OCR caused by flooding may exceed 10. Generally, tests at higher values of OCR give a more precise assessment of the *m* parameter. Note that the degree of excess pore pressure dissipation through the pre-commissioning phase can affect the mobilized OCR at the pipe-soil interface, which can increase the OCR to values greater than simply the ratio of flooded to empty (or flooded to operating) pipe weight (see e.g. Low et al. 2017). A minimum of three OCR values is recommended (e.g. 1, 2, and 4, up to 10 if relevant), using the best estimate (BE) normal stress during shear for all three tests.

As discussed in Section 4.5, ignoring the OCR effect can be conservative for specific design checks where low axial resistance is critical, such as initial pipeline expansion, pipeline walking, and pipeline feed-in during rogue buckle formation. In cases where high axial resistance is critical, e.g. anchor loads to resist pipeline expansion and walking, a higher OCR value will lead to higher loads. When there is uncertainty in the time periods during flooded (i.e. wet-parked) pipeline conditions, it is recommended to consider a range of induced OCR values wider than calculated from the changes in pipe weight.

5.3.3 Interface surface selection

Testing is ideally performed on representative pipeline coatings, i.e. on samples provided by the coating supplier. Coated pipeline sections (e.g. 1 foot lengths) can be used to extract a sample coating surface and flatten it for use in shear testing. This has the advantage of avoiding uncertainties in the effects of surface

material roughness or hardness (more critical for coarse-grained soil), or the directionality of any roughness patterns such as spiral scoring or clamping during the coating process along the pipeline assembly (i.e. firing) line. When using sandpaper as a proxy for a roughened surface, a waterproof (i.e. waxed) paper base is recommended to ensure surface integrity throughout the test program. It is advisable to avoid bare steel coatings due to potential physicochemical interactions between the soil and the steel, including corrosion due the presence of salt. An example of a bare steel coating used for testing is shown in Figure 46, illustrating rust development during the testing program and changes in bonding between the soil and surface during an individual shear test.

(a) (b)

Figure 46 – Pre-test and post-test images of bare steel surface test showing (a) rust developing between tests and (b) changes in bonding between the soil and the surface during shear (Das et al. 2024)

It may be necessary to resurface interface plates throughout the testing program to avoid variations in roughness from test to test. This is important for both smooth coatings which can scour and abrade (particularly for soft plastics tested against soil with significant coarse fractions) and rough coatings that can become worn through removal of surface asperities such as fusion-bonded epoxy. Surface roughness measurements are recommended to be taken parallel to the direction of shearing before and after each test, or at a sufficient frequency to ensure consistency across the test program. The diameter of the stylus tip, if using a profilometer type device, may affect the ability to measure rough surfaces accurately. Laser scans can be more accurate and provide more information than one-dimensional stylus profilometers. The average roughness R_a is generally the more common parameter used in quantifying surface roughness characteristics.

As shown in this study and others (e.g. Das et al. 2025), very smooth surfaces (R_a < 0.2 μm) can exhibit higher shear resistance than other smooth surfaces near the smooth-intermediate roughness transition. Extremely smooth surfaces may lead to unrepresentatively high values of undrained shear resistance, particularly for high plasticity soils. In projects where a roughened pipeline coating is planned, but the type of material or roughening method is unknown, soil-soil (i.e. direct shear) tests could be performed to provide the upper bound to the interface shear resistance. These can be performed using the same device used for the interface tests, replacing the interface with the bottom half of a shear box, or equivalent approach. As shown in this study, a fully rough coating response (representing soil-soil shearing) may be mobilized at relatively low values of

surface roughness ($R_a \geq 10$ μm). Most roughened plastic coatings, and nearly all concrete coatings, exhibit surface roughness values greater than 10 μm.

5.3.4 Test procedures

Test procedures may be constrained by the testing facility capabilities and available shear devices. Monotonic testing and cyclic testing with short displacement limits can overestimate the residual value. It is recommended to maximize shearing displacement as much as practical within the constraints of the equipment and consideration of potential soil loss during shear. Starting a cyclic test at one end of the displacement limit (e.g. as shown in Figure 7a) allows for a full sweep to achieve residual conditions without the influence of displacement reversal.

For cyclic testing, a decision will need to be made on whether to include episodic consolidation periods between cycles or pairs of cycles. While continuous shearing without episodic consolidation enables a more accurate (i.e. lower) measurement of undrained residual strength, including episodic consolidation allows for calibration of drainage models that capture the effects of pipeline startup and shutdown events. A hybrid approach of continuous cycling during, e.g., the first 10 cycles following by episodic consolidation (e.g. 30-minute pause periods) between pairs of the final 8 cycles could capture both types of data.

Larger numbers of cycles also may be warranted, subject to sufficient sample height remaining within the shear box/ring throughout the duration of shearing. The number of cycles and duration of any episodic consolidation periods may consider the permeability of the soil and practicalities of test program duration. Settlement of the top load platen can be monitored to assess the degree of dissipation occurring through the consolidation stages.

Cycling can lead to more soil loss during shearing, and therefore it must be decided whether to impose an initial gap between the box/ring and the interface surface. For smooth surfaces, use of a no-gap condition may be most appropriate and machine friction is generally consistent. For rough surfaces, an initial gap can reduce the potential for larger particles to add artificial friction when interacting with the edges of the box/ring but generally leads to greater specimen loss. This can create berms of soil that increase the initial shear resistance during cyclic reversal (if the berm mobilizes tension on the back of the retracting box/ring) or increase the shear resistance near the cyclic limits (if the berm imposes passive resistance onto the advancing box/ring). Post-test pictures of the interface and soil specimen can help to validate assumptions in the machine friction corrections and explain unexpected behavior in the data resulting from soil berms.

Tilt table testing has been shown in this study to provide a benchmark drained value of residual shear resistance. Tilt table testing entails multiple shearing episodes to ensure the residual shear strength is attained, i.e. resetting the interface plate onto the soil and repeating the tilting procedure. The rate of tilt can be increased to ensure rate effects do not change the result; i.e. once critical state conditions are attained. Cyclic tilt table tests can also be employed by alternating the tilt direction to avoid resetting the interface plate. Key advantages of tilt table testing are (i) the absence of machine friction and (ii) normal stress trends emerging from tilt table data are often highly repeatable.

Regardless of test procedure (ISB, tilt table, monotonic, cyclic), repeat tests performed for a given set of project conditions assess how consistent (or inconsistent) the results are. This helps to quantify epistemic uncertainty related to equipment and test procedures, allowing for greater confidence in the application of statistical data (see Section 5.5.3).

5.4 Interpretation of shear strength

5.4.1 Peak resistance

A peak in shear resistance can occur during the initial undrained movement, and a smaller peak is sometimes observed during subsequent undrained movements following each rest period or each cyclic reversal. Peak shear resistance may be estimated from shear box tests but is generally not relied on in pipeline design due to the low likelihood that the peak resistance will be mobilized simultaneously everywhere along an axially expanding pipeline. However, a peak resistance may be appropriate for short pipelines when performing buckle initiation reliability checks. This is similar in principle to selection of a higher residual shear resistance for an overconsolidated specimen, e.g. immediately post-peak during cycle 1 rather than further along the strain-softening/swelling response in cycle 2 or higher.

5.4.2 Residual resistance

The residual resistance is selected from portions of the tests where a stable value is observed, averaging over enough data points to eliminate noise. This is particularly important at very low stress levels when load cell noise could be significant and for rough surfaces that exhibit greater scatter. For example, using the test data presented in Figure 7, the shear resistance was averaged over horizontal displacement ranges from approximately 20 to 25 mm in the forward direction and from 0 to 5 mm in the backward direction. The absolute values of shear resistance in each direction are then averaged to remove any asymmetry in the data. Machine friction corrections in both forward and backward directions may be appropriate depending on the nature of the surface tested.

5.4.3 Mobilization displacement

In pipeline structural modelling, the axial response is usually modelled using a bilinear elastic – perfectly plastic model, which requires specification of the mobilization displacement, x_{res}. For assessments of pipe walking, a low (tangent) value of x_{res} creates a higher rate of walking (Hill et al. 2012) since it reduces the elastic recoverable part of the axial force-displacement model. For initial pipeline expansion, a higher (secant) value of x_{res} is conservative (Figure 1). However, since the mobilization displacement is known to be at least partly linked to the pipeline diameter, element testing is of limited use for selection of mobilization displacement.

5.4.4 Consolidation hardening parameters

The rate of increase in shear resistance with cycles from the initial undrained to final drained conditions is measured directly in ISB tests. It can also be predicted from critical state parameters, or these parameters can be calibrated to ISB test results (Boukpeti and White 2017). Also, scaling approaches exist to estimate the different levels of consolidation between cycles of movement around a pipeline compared to an ISB test, allowing for the different scales and for different levels of pore pressure dissipation between cycles (Low et al. 2017). This approach can be used to quantify the modest amount of pipeline walking that would accumulate before hardening occurred, bringing walking to a halt (White et al. 2015).

5.5 Development of design parameters

5.5.1 Epistemic uncertainty

As reported in this study, there is significant variability in the database results due to several epistemic factors, including the following:

- **Testing procedure**: most of the database tests performed were developed following test program design as described in Westgate et al. (2018); some of the early tests included additional variations include effect of shearing rate, effect of specimen preparation (intact, reconstituted, or remolded); in some cases, test program design was directed by the field operator which departed from the standard test program.

- **Laboratory influence**: 5 commercial laboratories and 2 university laboratories are included in the database, which leads to inherent uncertainty due to laboratory differences in specimen preparation and interpretation of design strength parameters.

- **Equipment influence**: 7 different devices were used in the database, including air-controlled, hydraulic, dead weight, and servo-controlled normal stress control, and various modifications for machine friction. Equipment functionality and data acquisition system quality, calibration, and maintenance may contribute to some scatter in the data.

- **Model uncertainty**: The undrained and drained shear resistance models for normal stress and overconsolidation are empirical and not mechanistic (developed from first principles or Newtonian mechanics) which lends to inherent uncertainty in model predictions. Statistical analysis was used to develop LE, BE and HE model parameters (e.g. normal stress *a* and *b* parameters, OCR *m* parameter).

5.5.2 Aleatoric variability

The limited number of tests typically completed as part of an interface shear testing program leads to a (potentially large) component of aleatoric variability ignored in the design process, thereby underestimating the uncertainty in the model predictions. Use of batch samples over individual samples can exacerbate this, since no aleatoric variability is captured. However, this is partially compensated by length averaging effects where the shear resistance during pipeline expansion is mobilized over a long (typically > 500 m) length of pipe. Batch sampling of several individual samples spaced evenly along a pipeline route can therefore provide a more representative BE design value for use in PSI analysis, but use of batch samples alone ignores the aleatoric uncertainty in the soil properties along the route.

While an attempt has been made to link residual shear strength to index properties including liquid limit, liquidity index, plasticity index and clay activity, no trends are evident. Therefore, it may be appropriate to simply measure the undrained soil strength on remolded soil samples to determine aleatoric variability most relevant to axial shear resistance. For sites with significant aleatoric variability, multiple batch samples may be required for different soil zones along a route.

5.5.3 Combining epistemic and aleatoric uncertainty in design

Since epistemic (database) uncertainty and aleatoric (site-specific) variability are not directly additive as they represent fundamentally different sources of uncertainties, they can be combined as part of total uncertainty assessment. Phoon and Kulhawy (1999) proposed a model for total uncertainty as follows:

$$cv_{total} = \sqrt{\frac{\delta}{L}(cv_{aleortic})^2 + (cv_{measurement})^2 + (cv_{statistical})^2 + (cv_{model})^2} \quad \text{Eq. (3)}$$

where:

cv_{total} is the total design uncertainty;

$cv_{aleatoric}$ is the inherent soil variability;

$cv_{measurement}$ is the measurement uncertainty;

$cv_{statistical}$ is the statistical uncertainty, i.e. the error of fitting a statistical model to actual distribution of the dataset;

cv_{model} is the transformational model uncertainty; and

and δ/L approximates variance reduction due to spatial averaging.

There are various approaches to handle spatial averaging for pipeline design; one approach is to consider the variation in pipeline embedment as a proxy for soil properties (e.g. Westgate and White (2015), whereas others take the spatial correlation of soil properties directly, such as Kriging. A high scale of fluctuation, relative to the length of pipeline mobilizing shear resistance, will reduce the effective variation in soil resistance 'felt' by the moving pipeline, as it will average out these local variations. A low scale of fluctuation will lead to inherent soil variability having a greater influence on the local shear resistance mobilization, dominating behavior over a portion of the characteristic length of pipeline. Without sufficient data, the spatial averaging effect can of course be ignored (i.e., assuming δ/L = 1 in Equation 3).

While no attempt has been made here to quantify the different types of epistemic uncertainty explicitly, one can argue that due to the wide range of conditions captured within the database, epistemic uncertainty and aleatoric variability are inherently included in the statistical values of the model parameters presented. Therefore, the coefficient of variation for a given dataset from those reported in this study ($cv_{database}$) could be used as a representative value to derive a design standard deviation (σ_{design}) of (e.g.) undrained strength ratio, using the local mean (μ_{local}) from site-specific testing on a batch sample:

$$\sigma_{design} = cv_{database}\ \mu_{local} \qquad \text{Eq. (4)}$$

The design standard deviation could then be used to derive low estimate (LE) and high estimate (HE) undrained strength ratios, e.g. using two standard deviations from the site-specific mean (i.e. based on 5th and 95th percentiles, respectively). The design LE, BE, and HE undrained strength ratios would then be used for calculation of axial shear resistance, accounting for other effects such as embedment (i.e. the wedging factor ζ) and overconsolidation, as appropriate to the design case being considered.

Alternative uncertainty quantification frameworks such Bayesian methods can also be used, which offer narrower design ranges than the simple summing of squares approach as illustrated in Das and Westgate (2023). However, this method is computationally intensive and is highly dependent on the selection of prior distributions of the model parameters.

6 Recommendations for further investigation

The following are suggestions for future investigation based on the outcomes of this study:

- Perform comparisons of cyclic testing with and without episodic consolidation periods to determine their influence on identification of minimum undrained residual shear resistance; investigate the number of cycles required to attain said condition for a range of fine-grained soils and surface roughness.

- Investigate potential modifications/development of low normal stress ring shear devices to achieve true undrained residual shear resistance and avoid cyclic effects of machine friction and berm development.

- Perform detailed investigations using a single soil sample and surface type to refine calibrations for and reduce epistemic uncertainty associated with normal stress, roughness, OCR and drainage models.

Bibliography

[1] API (2011). RP 2GEO: Recommended Practice for Geotechnical Engineering.

[2] ASTM (2021). ASTM D7928-21: Standard Test Method for Particle-Size Distribution (Gradation) of Fine-Grained Soils Using the Sedimentation (Hydrometer) Analysis, ASTM International, West Conshohocken, PA.

[3] Atkins. (2015). SAFEBUCK JIP - Safe Design of Pipelines with Lateral Buckling: Design Guideline, Report No. 5087471 / 01 / C, dated 15 January 2015.

[4] Bolton M.D., Ganesan S.A., and White D.J. (2007). SAFEBUCK Phase II: Axial pipe-soil interaction testing using the Cam-shear device, Report to Boreas Consultants, (SAFEBUCK JIP), ref. SC-CUTS-0609-R01. 56pp. (Confidential to JIP Participants).

[5] Boukpeti, N. and White, D.J. (2017). Interface shear box tests for assessing axial pipe-soil resistance, Géotechnique, Vol. 67, No. 1, pp. 18-30.

[6] Bransby, F., White, D., Low, H.E., and Westgate, Z. (2015). Accurate descriptions of pipe-soil interaction to facilitate the design of high temperature pipelines, Proc. Offshore Pipelines Technical Conf., Asia, October 21-22.

[7] Bruton, D., Sinclair, F., and Carr, M. (2010). Lessons learned from observed walking of pipelines with lateral buckles, including new driving mechanisms and updated analysis models, Proc. Offshore Technology Conference, Houston, USA, OTC 20750.

[8] Carr, M., Sinclair, F., and Bruton, D. (2006). Pipeline walking – understanding the field layout challenges, and analytical solutions developed for the SAFEBUCK JIP, Proc. Offshore Technology Conference, Houston, USA, OTC-17945.

[9] Clark, A.R. and Walker, B.F. (1977). A proposed scheme for the classification and nomenclature for use in engineering description of Middle Eastern sedimentary rocks, Géotechnique, Vol. 27, No. 1, pp. 93-99.

[10] Das, R. and Westgate, Z. (2023). Interpreting interface shear strength parameters for pipe-soil interaction analysis using Bayesian inference, SUT Offshore Site Investigation and Geotechnics Conference, London, U.K.

[11] Das, R., Westgate, Z., Seiphoori, A., and Garmon, S. (2024). Effect of clay activity and interface surface material on residual undrained interface strength: implications on pipeline-seabed interaction analysis, Proc. 7th Int. Conf. Geotechnical and Geophysical Site Characterization, Barcelona.

[12] Das, R., Garmon, S., and Westgate, Z. (2025). Effect of soil composition, interface roughness, and drainage response on shear strength during low normal stress interface shear box testing, Proc. Int. Symp. Frontiers in Offshore Geotechnics, Nantes.

[13] DNV (2021). Recommended Practice DNVGL-RP-F114: Pipe-soil interaction for submarine pipelines, Edition May 2021.

[14] Eid, H.T., Amarasinghe, R.S., Rabie, K.H. and Wijewickreme, D. (2015). Residual shear strength of fine-grained soils and soil-solid interfaces at low effective normal stresses, Canadian Geotechnical Journal, 52: 198-210.

[15] Ganesan, S., Kuo, M., and Bolton M.D. (2013). Influences on pipeline interface friction measured in direct shear tests. ASTM Geotechnical Testing Journal, 37(1), 14pp.

[16] Gibson, R., and Henkel, D. (1954). Influence of duration of tests at constant rate of strain on measured drained strength. Géotechnique, 4(1): 6–15.

[17] Hill A., White D.J., Bruton D.A.S., Langford T., Meyer V., Jewell R. and Ballard J-C. (2012). A new framework for axial pipe-soil interaction illustrated by a range of marine clay datasets, Proc. Int. Conf. on Offshore Site Investigation and Geotechnics. SUT, London.

[18] ISO (2025). ISO 19901-4: Oil and gas industries including lower carbon energy — Specific requirements for offshore structures, Part 4: Geotechnical design considerations. Edition 3, 2025.

[19] Kuo M. Y-H., Vincent C.M., Bolton M.D., Hill A. and Rattley M. (2015). A new torsional shear device for pipeline interface shear testing, Proc. of the 3rd International Symposium on Frontiers in Offshore Geotechnics, Oslo, Norway, 10-12 June 2015.

[20] Ladd, C.C. and Foott, R. (1974). New design procedure for stability of soft clays, Journal Geotechnical Engineering Division, ASCE, Vol. 100, No. GT7, pp. 763-786.

[21] Low, H.E., Ramm, M., Bransby, M.F., White, D.J., and Westgate, Z.J. (2017). Effect of through-life changes in soil strength and axial pipe-seabed resistance for HPHT pipeline design, Proc. SUT Offshore Site Investigations and Geotechnics Conf., London.

[22] Meyer, V.M., Dyvik, R. and White, D.J. (2015). Direct shear interface tests for pipe-soil interaction assessment, Frontiers in Offshore Geotechnics III, Taylor & Francis Group, London.

[23] Najjar, S.S., Gilbert, R.B., Liedtke, E.A., and McCarron, B. (2003). Tilt table test for interface shear resistance between flowlines and soils, Proc. 22nd International Conference on Offshore Mechanics and Arctic Engineering-OMAE, Vol. 3, ASME, Cancun, Mexico, pp. 859–866. doi:10.1115/OMAE2003-37499.

[24] Najjar, S.S., Gilbert, R.B., Liedtke, E.A., McCarron, B. and Young, A.G. (2007). Residual shear strength for interfaces between pipelines and clays at low effective normal stresses. ASCE Journal of Geotechnical and Geoenvironmental Engineering, Vol. 133, No. 6, pp. 695-706.

[25] Pedersen, R.C., Olsen, R.E. and Rausch, A.F. (2003). Shear and interface strength of clay at very low effective stresses. ASTM Geotechnical Testing J., 26(1):71-783.

[26] Phoon, K.K. and Kulhawy, F.W. (1999). Evaluation of geotechnical property variability, Canadian Geotechnical Journal, 36: 625-639.

[27] Potts, D. M., Dounias, G.T., and Vaughan, P.R. (1987). Finite element analysis of the direct shear box test, Geotechnique 37(1), 11-23.

[28] Sahdi, F., Tom, J.G., Watson, P., Gaudin, C. and Bransby, M.F. (2020). Effect of water entrainment on seabed soils during cyclic pipe-soil interaction, Proc. 4th International Symposium on Frontiers in Offshore Geotechnics, Austin, Texas.

[29] Ward, H. C. 1999. Rough surfaces. Edited by T. R. Thomas. London: Longman.

[30] Watson, P., Bransby, F., Delimi, Z.L., Erbrich, C., Finnie, I., Krisdani, H., Meecham, C., O'Neill, M., Randolph, M., Rattley, M, Silva, M., Stevens, B., Thomas, S., and Westgate, Z. (2019). Foundation design in offshore carbonate sediments – building on knowledge to address future challenges, Proc. XVI Panamerican Conf. Soil Mech. and Geotech. Engrg., Cancun, Mexico.

[31] Westgate, Z.J. (2022). Residual interface shear strength under low normal stress conditions, Proc. Geo-Congress, Richmond, Virginia.

[32] Westgate, Z.J. and White, D.J. (2015). Quantifying spatial variability in pipeline embedment for subsea pipeline design, Proc. Int. Conf. Offshore Mechanics and Arctic Engineering, OMAE2015-42292.

[33] Westgate, Z.J., Argiolas, R., Wallerand, R. and Ballard, J-C. (2021). Experience with interface shear box testing for axial pipe-soil interaction assessment on sand, Proc. Offshore Tech. Conf., Houston, OTC-31268.

[34] Westgate, Z.J., Randolph, M.F., White D.J. and Li, S. (2010). The influence of seastate on as-laid pipeline embedment: a case study, Applied Ocean Research, Vol. 32, No. 3, pp 321-331.

[35] Westgate, Z.J., White, D.J. and Savazzi, M. (2018). Experience with interface shear box testing for axial pipe-soil interaction assessment on soft clay. Proc. Offshore Tech. Conf., Houston, OTC-28671.

[36] White, D.J. (2014). Axial pipe-soil interaction framework. Report to Atkins and the SAFEBUCK Joint Industry Project Phase III/GEO. UWA Geo Report 13684v2, 176 pp.

[37] White, D.J. and Randolph, M.F. (2007). Seabed characterisation and models for pipeline-soil interaction, Journal of Offshore and Polar Engineering, Vol. 17, No. 3, pp. 193-204.

[38] White, D.J., Westgate, Z., Ballard, J-C., de Brier, C., and Bransby, M.F. (2015). Best practice geotechnical characterization and pipe-soil interaction analysis for HPHT flowline design. Proc. Offshore Technology Conf., Houston. OTC 26026-MS.

[39] White, D.J., Campbell M., Boylan N. and Bransby M.F. (2012). A new framework for axial pipe-soil resistance: illustrated by shearbox tests on carbonate soils, Proc. 8th Intl Conf on Offshore Site Investigation and Geotechnics. London: Society for Underwater Technology.

[40] White, D.J., Clukey E.C., Randolph M.F., Boylan N.P., Bransby M.F., Zakeri A., Hill A.J., Jaeck C. (2017). The state of knowledge of pipe-soil interaction for on-bottom pipeline design. OTC 27623, Proc. Offshore Technology Conference, Houston.